THE $^1D_2 \leftarrow {}^1A_1$ ELECTRONIC TRANSITION

OF

SELENIUM DIOXIDE

THE $^1B_2 \leftarrow {}^1A_1$ ELECTRONIC TRANSITION OF SELENIUM DIOXIDE

by

PATRICK ROBERT McLEAN, B.Sc., M.Sc.

A Thesis

Submitted to the Faculty of Graduate Studies

in Partial Fulfillment of the Requirements

for the Degree

Doctor of Philosophy

McMaster University

October, 1972

DOCTOR OF PHILOSOPHY (1972)
(Chemistry)

McMASTER UNIVERSITY
Hamilton, Ontario

TITLE: The $^1B_2 \leftarrow {}^1A_1$ Electronic Transition of Selenium Dioxide

AUTHOR: Patrick Robert McLean, B.Sc., M.Sc.

SUPERVISOR: Professor G. W. King

NUMBER OF PAGES:

SCOPE AND CONTENTS:

The B ← X system of selenium dioxide was studied in absorption in the gas phase and has been assigned to the electronic transition $^1B_2 \leftarrow \tilde{X}, {}^1A_1$. A complete vibrational analysis of the electronic transition is presented. The geometry of the excited state has been determined completely from rotational analysis of the 1_0^3 vibronic band and further confirmed by Franck-Condon calculations. The previously unknown ground state fundamentals ν_1'' and ν_2'' have been determined along with the three fundamentals of the $^1B_2$ excited state. It is proposed that selenium dioxide has an asymmetric structure with unequal bond lengths in certain vibronic levels of the excited state involving ν_3' as a result of a double-minimum potential along the Q_3' co-ordinate.

To

My Mother and Father

Bobby and Cathy

ACKNOWLEDGEMENTS

I would like to thank Dr. G.W. King for suggesting the SeO_2 problem and for many valuable discussions during the preparation of the thesis.

I am indebted to my colleagues, Mr. M. Danyluk, Mr. E. Farnworth, Mr. E. Finn, Mrs. D. Grange, Mr. F. Greening, Dr. K.G. Kidd, Mr. R. Lemanczyk, Mr. R. Meatherall, Mr. A. Van Putten and Mr. C.R. Subramaniam for both their friendship and assistance. My thanks also to Dr. D.C. Moule for the use of his Ebert spectrograph and his willing assistance and hospitality while at Brock University.

I am grateful to the Ontario government for a Fellowship (1969) and to the National Research Council of Canada for Scholarships (1970-72).

Miss Susan Hawley (typing) and Mr. Dennis McEntee (printing), thank you, you both did a beautiful job.

To Mr. Greg McLean, I am especially grateful for the professional and arduous task of drawing most of the Figures in the thesis.

Anne, thank you for "The Summer of 72" - it was great!

Finally, B.104 - You I shall never forget!

TABLE OF CONTENTS

LIST OF TABLES

LIST OF FIGURES

CHAPTER ONE

INTRODUCTION

1.1. Electronic, Vibrational and Rotational Motion of Molecules

Molecular spectroscopy is the study of the quantized electronic, vibrational and rotational motion of a molecule through its interaction with electromagnetic radiation. The complexity of most spectroscopic problems would be overwhelming were it not for the large inequality in mass between the electrons and nuclei in a molecule. Quantum mechanically this allows the nuclear and electronic motions to be considered largely independent of one another and the overall rovibronic (rotational-vibrational-electronic) wave function ψ_{evr} to be written as a product of an electronic part, vibrational part and rotational part.

$$\psi_{evr} = \psi_e \psi_{vib} \psi_{rot} = \psi_e \psi_{nuc} \tag{1.1}$$

The factorization of the wave function into components due to electronic and nuclear motion is called the Born-Oppenheimer approximation[1].

In the zeroth-order Born Oppenheimer approximation, the time independent Schrodinger equation for the electronic and nuclear motion may be written,

$$H_e(r,Q_o)\psi_e(r,Q_o) = E_e(Q_o)\psi_e(r,Q_o) \tag{1.2}$$

$$[H_N(Q) + E_e(Q)]\psi_N(Q) = E_N\psi_N(Q) \tag{1.3}$$

where the Hamiltonian for the electronic and nuclear motion is given by

$$H_e(r,Q_o) = -\sum_i \frac{\hbar^2}{2m_e}\nabla_i^2 - \sum_{i,\mu}\frac{Z_\mu e^2}{r_{i\mu}} + \sum_{i>j}\frac{e^2}{r_{ij}} \tag{1.4}$$

$$H_N(Q) = -\sum_\mu \frac{\hbar^2}{2M_\mu}\nabla_\mu^2 + \sum_{\mu>\nu}\frac{Z_\mu Z_\nu e^2}{r_{\mu\nu}} \tag{1.5}$$

The terms on the right hand side of Equation (1.4) refer respectively to the kinetic energy of the individual electrons, attractive force of the ith electron for the αth nucleus and an electron-electron repulsion term; while the nuclear Hamiltonian H_N in Equation (1.5) contains respectively a nuclear kinetic energy and repulsion term and

r is the electronic co-ordinates;

Q the nuclear displacement co-ordinates;

h is Planck's constant divided by 2π;

m_i and m_α are the mass of the ith electron and the αth nucleus;

∇^2 is the Laplacian operator;

Z_α is the atomic number of the αth nucleus;

e is the charge of the electron; and

r_{ij} is the distance between particle i and j.

The solution of Equations (1.2) and (1.3) yield the electronic and nuclear energy levels and wave functions. It is transitions between the above energy levels which are of fundamental interest to the molecular spectroscopist.

1.2. Transition Probabilities

According to the Bohr theory[2], a transition from one stationary state in the molecule to another may occur with the quantized absorption or emission of radiation of wave number σ given by

$$\sigma = \frac{E_m}{hc} - \frac{E_n}{hc} \qquad E_m > E_n \tag{1.6}$$

The transition probability that an oscillating electromagnetic field induces such a transition in a molecule, from state m to state n was first determined by Einstein[3] and is given by

$$B_{mn} = \frac{2\pi}{h^2} |N|^2 \tag{1.7}$$

where B_{mn} is the Einstein probability coefficient, $M = \langle \psi_m | \vec{r} | \psi_n \rangle$, the transition moment and $|M|^2$ is the transition probability between state m and n, $\vec{r}$ is the electric dipole operator.

1.3. Selection Rules

In order that an electric dipole transition occur between the states ψ_m and ψ_n, the following integral must be non-zero,

$$\langle \psi_m | \vec{r} | \psi_n \rangle \neq 0 \qquad (1.8)$$

In the language of group theory[o], the above integral will be non-zero only if the direct product of the representations of ψ_m, r and ψ_n contain the totally symmetric representation.

$$\Gamma\psi_m \times \Gamma r \times \Gamma\psi_n = \Gamma A_1 \qquad (1.9)$$

The application of the above selection rule to specific, electronic, vibrational and rotational transitions in SeO_2 is examined more fully in the subsequent chapters where the analysis of each is discussed in detail.

The remainder of the present chapter shall concern itself with the experimental aspects of the present work as well as a brief description of previous spectroscopic studies involving SeO_2.

1.4. Preparation of Isotopic Selenium Dioxide

Isotopically pure Se^{78} (93.3%) and Se^{80} (93.6%) and O_2^{18} (99.9%) were obtained from Union Carbide (Oak Ridge Laboratories). The three isotopic molecules $Se^{78}O_2^{16}$, $Se^{78}O_2^{18}$ and $Se^{80}O_2^{18}$ were prepared by adding a stoichiometric amount of oxygen to 300 mg of selenium isotope contained in a 50 cm all-quartz

---

[o] An introductory knowledge of group theory is assumed throughout the thesis. Accounts of the application of group theory to molecular spectroscopic problems is given by King[4], Cotton[5] or Hochstrasser[6].

cell. The cell was wound with 0.5 ohm/ft. nichrome wire, wrapped with asbestos paper and heated electrically to 350°C. The oxidation was assumed to be complete after several hours.

In order to prevent condensation of selenium on the windows, a copper envelope was extended two inches beyond the windows at each end of the cell.

The entire spectrum of the B system could be obtained with SeO_2 pressures which varied from 0.5 mm to 10 mm. The temperature ranged from 120°C to 200°C. In order to photograph the much weaker C System to the red of the B System, it was necessary to heat the cell to around 350°C. At this temperature all of the SeO_2 is in the gas phase.

In order to minimize the decomposition of SeO_2 into $Se + O_2$, an additional 100 mm of oxygen gas was added to the cell. Spectra taken both in the presence as well as the absence of the additional oxygen, when compared, showed no visible affect of pressure broadening of the rotational fine structure.

The only other oxide of selenium is SeO_3. It presented no problem to the present investigation of SeO_2 since SeO_3 decomposes into SeO_2 on heating.

1.5. Previous Spectroscopic Studies of SeO_2

At least five electronic transitions have been observed in the gas phase spectrum of SeO_2 in the spectral region between 2000 Å - 6000 Å [7-11]. Three of these transitions have been observed in absorption in the region 2070-2210 Å, 2500-3400 Å, and 3500-4000 Å and have been designated the A, B and C Systems respectively.

Haranath and Sivaramamurty[12] also observed two systems in emission with origins at 3110.9 Å and 3119.9 Å. The present investigation is concerned with the B System of SeO_2.

1.6. Gas Phase Emission Spectrum of SeO_2

Haranath and Sivaramamurty[12] observed an emission spectrum extending from 2700-4700 Å. The bands below 3200 Å were assigned as belonging to the B ← X system of SeO_2 previously reported by Duchesné and Rosen[8] under low resolution. The bands between 3200-4700 Å could not be associated with the C ← X system observed by Rosen[7] and were assigned as belonging to two new systems, involving transitions from the upper state ν_2' levels to the ground state ν_1'' levels. The observed frequencies are given in Table 1.1.

Table 1.1

Observed frequencies from emission work reported by Haranath and Sivaramamurty[12]

	Origin	ν_1'' of Lower State	ν_2' of Excited State
System I	32145 cm^{-1}	910.5 cm^{-1}	182 cm^{-1}
System II	32052 cm^{-1}	911.5 cm^{-1}	182 cm^{-1}

However, this emission work is of little use in the present study, because very few of the band frequencies reported by Haranath and Sivaramamurty agree with the frequencies measured here, even in the origin region where isotopic shifts should be small. Haranath and Sivaramamurty used selenium dioxide containing natural selenium and therefore would have observed bands due to both $Se^{70}O_2^{16}$ and $Se^{00}O_2^{16}$, but the absorption bands of these separate isotopic species show very little agreement with the reported emission bands in regions where the absorption and emission spectra overlap. An analysis of the emission spectra of the different isotopes under much higher resolution would be necessary for a satisfactory interpretation to be made. All that can be said is that Haranath and Sivaramamurty's two "electronic

origins" lie within ~ 100 cm^{-1} of the origin given here for the B system in absorption.

Their analysis postulates two separate electronic transitions with origins only 93 cm^{-1} apart. Although such a coincidence cannot be ruled out completely, it is highly unlikely that such systems are not related in some way. A possible alternate interpretation for the two emission systems observed by Haranath and Sivaramamurty is given below, on the assumption that they have indeed correctly identified emission due to SeO_2.

From the hot band spectrum in the present investigation of the B System of SeO_2, the ground state stretching frequency ν_1'' is unambiguously determined to be 923 cm^{-1}. This is in excellent agreement with the value of 922.0 determined by Cesaro et. al.[14-15] from recent low temperature infrared studies of SeO_2 in an argon matrix.

The origin band for the B ← X electronic transition in the present work is found with a high degree of certainty (from isotopic shifts as well as the analysis of the hot band spectrum) to lie at 31955.0 cm^{-1}.

In view of the proximity of the origin of the B ← X system to the origin of the two emission systems, one is tempted to think that the lower electronic state observed by Haranath and Sivaramamurty is in fact the ground electronic state. The anomaly, however, arises that the upper state of the B ← X transition observed in absorption cannot be associated with either of the above two emission systems.

In order to rationalize this seemingly uncomplainable contradiction the following alternate interpretation of Haranath and Sivaramamurty's emission work is offered. From the analysis of the hot band spectrum in the present investigation of the B ← X system, the ground state totally symmetric stretching frequency $\nu_1'' = 923$ cm^{-1}. The frequency of the second overtone, $3\nu_1''$, is observed

to be 912 cm^{-1}. The anharmonicity in ν_1'' is, therefore, about 5.5 cm^{-1} per quantum excited. In the previous gas phase analysis of the B ← X System Duchesne and Rosen[8] misinterpreted the interval $(\nu_1' + \nu_2') = 910$ cm^{-1} as a sequence interval involving ν_1''. The interval between the last observed emission bands at 32145 and 32052 cm^{-1} reported by Haranath and Sivaramamurty was observed to be 911 cm^{-1}.

It is possible that the bands observed by Haranath and Sivaramamurty at 32145 cm^{-1} and 32052 cm^{-1} do not terminate at the vibrationless level of the ground state but rather at the $3\nu_1''$ level. This interpretation then extends the origin for the emission systems some $3\nu_1'' \approx 2753$ cm^{-1} to the blue of the previously assigned origins. This explanation is, therefore, consistent with the ground state being the lower state to which the emission occurs, and removes the possibility that the upper state of the B System ($^1B_2$) is the emitting state, which is in agreement with Haranath and Sivaramamurty's observation.

The fact that the above two emission systems have not as yet been observed in absorption could, therefore, be attributed to the strongly overlapping B ← X electronic transition which is approaching its intensity maximum in the region where the present interpretation suggests the origin for the emission systems should appear in absorption.

Reinvestigation of the emission work using isotopic $Se^{78}O_2^{16}$ and $Se^{78}O_2^{18}$ would unambiguously ascertain the validity of the present interpretation since the ν_1'' levels are isotopically split by approximately 50 cm^{-1} per quanta excited, as is observed in the present analysis of the B ← X System of SeO_2.

The remaining yet unexplained presence of two low lying excited electronic states separated by less than 100 cm^{-1} can possibly be accounted for in the following way.

The present work involving the $^1B_2 \leftarrow {}^1A_1$ electronic transition of SeO_2 suggests strong evidence for the presence of a double-minimum potential well in the antisymmetric stretching co-ordinate Q_3' of the $^1B_2$ excited electronic state. The $0^+ - 0^-$ splitting is observed to be 78 cm^{-1}.

An alternate explanation for the two emission systems separated by only 100 cm^{-1} is the hypothesis of only one system containing two progressions originating on the levels $(0^+ + n\nu_2')$ and $(0^- + n\nu_2')$, $n = 0, 1, .., 4$, the $0^+ - 0^-$ splitting being of the order of 100 cm^{-1}. There is of course no basis for assuming the above explanation is correct, aside from the fact that apparently $\nu_2' = 182$ cm^{-1} for both systems. However, in view of the difference in $\nu_2' = 260$ cm^{-1} observed in the present analysis of the $\tilde{A} \leftarrow X$ system of SeO_2 with $\nu_2' = 182$ cm^{-1} observed in emission by Haranath and Sivaramamurty, it appears unlikely that the $^1B_2$ electronic state can be associated with either of the above two emission systems if their experimental frequencies are correct. A detailed discussion of the electronic states of SeO_2 is deferred to Chapter Two.

1.7. Previous Gas Phase Investigations of the B System of SeO_2 in Absorption

The $B \leftarrow X$ system of SeO_2 has been studied under low resolution by several workers: Cheong Shin-Piau[9] (1938), Asundi et. al.[10] (1937) and, more recently, by Duchesne and Rosen[8] (1941).

Duchesne and Rosen were the first researchers to study the B System of SeO_2 in the light of the Herzberg-Teller[17] selection rules. Many of the gross experimental features and observations in their work are identical to the present investigation, although of course they worked with the natural selenium dioxide. The most notable feature is the presence of long progressions involving the upper state totally symmetric stretching frequency, $\nu_1' = 660$ cm^{-1}.

This is the only upper state frequency reported by Duchesne and Rosen[8]. This is in contrast to the present work where all three fundamentals are assigned. Duchesne and Rosen also incorrectly assigned the origin for the B ← X electronic transition at 1300 cm^{-1} to the blue of the true origin, determined from isotopic shifts in the present analysis. This erroneous assignment resulted from their incorrectly assigning the frequency interval of 910 cm^{-1} to ν_1'' when in fact the interval arises from the combination band $\nu_1' + \nu_2' = 660\ cm^{-1} + 260\ cm^{-1}$.

1.8. Infrared Studies of ScO_2

The infrared spectrum of ScO_2 has been studied by Giguère and Falk[18] in the gas phase and in rare gas matrices by Hastie et. al.[15] and just recently by Cesaro, Spoliti, Hinchcliffe and Ogden[14] in argon matrices. A summary of ground state frequencies for ScO_2 is given in Table 1.2.

Table 1.2

Ground State Fundamentals for ScO_2

Frequency	Gas Phase	Matrix
ν_1	923 cm^{-1}*	923.4 cm^{-1}
ν_2	373 cm^{-1}*	372.5 cm^{-1}
ν_3	967 cm^{-1}	967.6 cm^{-1}

*Obtained from present gas phase analysis of B System of ScO_2.

1.9. Experimental Aspects of the Present Work

Low resolution spectra of $Sc^{70}O_2^{16}$, $Sc^{70}O_2^{18}$ and $Sc^{00}O_2^{16}$ were photographed in the second order of a 1.5 meter Bausch and Lomb model II spectrograph which has a resolving power of 70,000 and a reciprocal dispersion of 7.5 Å/mm. The slit width used was 32 microns. Kodak Spectrum Analysis No. 1

film was used in all instances. The spectrum was also photographed at a slightly higher dispersion on a 1.5 meter Hilger and Watts Littrow-Mounted quartz prism spectrograph.

The high resolution photographs were obtained in the first order of a 20-foot Ebert spectrograph similar to the one described by King[19]. The dispersion and theoretical resolving power of the instrument in the first order is 0.72 Å/mm and 150,000 respectively. A slit width of 30 microns was used. A few select bands were also photographed in the second order at a resolving power of 300,000 and dispersion of 0.36 Å/mm.

Several bands of the $Se^{78}O_2^{16}$ and $Se^{80}O_2^{16}$ were photographed at still higher dispersion in the 20th order on an Ebert spectrograph located in Dr. D. C. Moule's laboratory at Brock University in St. Catharines, Ontario.*

All of the absorption spectra were obtained using a 450 watt, high pressure Xenon arc, obtained from Osram Inc., as the continuous radiation source.

1.10 Measurement and Calibration of Spectra

The comparison spectrum, which was superimposed adjacent to the absorption spectrum, was an iron arc emission spectrum from a Pfund arc in the case of the Ebert and Bausch and Lomb photographs and a neon filled hollow iron cathode discharge for the Hilger pictures and those obtained at Brock University.

The relative positions of the iron arc and selenium dioxide spectral lines were measured with a MacPherson travelling microscope having a precision of 0.0001 mm. The wavelength of the iron emission lines were taken from a

---

*I would like to express my appreciation to Dr. D. C. Moule for his willing assistance and hospitality while at Brock University.

tabulated list comprised by the spectroscopy division of the National Research Council of Canada.

The measured iron lines were then fitted to an equation of the form $Y = A_0 + A_1x + A_2x^2$ by means of a least square computer program carried out on a CDC 6400 computer. Once the constants A_0, A_1 and A_2 were determined, the wavelength of the spectral lines were obtained by substituting their positions into the above equation.

The air wavelengths were converted to vacuum wavelengths by means of a formulae derived by Edlén[20]. The vacuum wavelengths were then converted to vacuum wavenumbers.

1.11. Experimental Conditions

Selenium dioxide is a white crystalline solid which sublimes at 350°C. In order to photograph the gas phase spectrum, it was necessary to heat the cell electrically to temperatures ranging between 130°C and 200°C. Between these temperatures the vapor pressure of SeO_2 varies over the range 0.01 Torr to 10 Torr[21].

The exposure time for the high resolution Ebert photographs varied from 5 to 40 minutes with Kodak Spectrum Analysis No. 1 film.

CHAPTER TWO

ELECTRONIC STRUCTURE AND SPECTRA OF SELENIUM DIOXIDE

2.1. Introduction

In the electronic ground state, selenium dioxide is a bent symmetric AB_2 type molecule containing eighteen valence electrons in its molecular orbital framework, and as such is valence isoelectronic with O_3, SO_2 and NO_2^-. Since the present sophistication of quantitative molecular orbital calculations has not yet been extended to include third row elements such as selenium the theoretical discussion of the molecular orbitals and low lying electronic states of SeO_2 must proceed by comparison with the much studied isoelectronic SO_2 and NO_2^- molecules[22-25].

2.2. Molecular Orbital Calculations for NO_2^-

In the following section a brief summary of the one electron molecular orbitals for NO_2^- is discussed. Since the nature of the present work has been spectroscopic and has not involved any numerical molecular orbital calculations, the analytical methods used in calculations will not be discussed in the thesis.

Two things that are of prime interest in so far as the present work is concerned are:

(a) the ordering and nature of the highest filled molecular orbitals in the ground state; and

(b) the electron configurations which are expected to give rise to the first few low lying excited electronic states.

The ordering of the molecular orbitals for the nitrite ion[22] (isoelectronic with SeO_2) are given in Figure 2.1. The relative ordering of the MO's remain the same in the nitrite ion (NO_2^-), ozone (O_3) and sulfur dioxide (SO_2)[22].

It therefore seems reasonable to assume the same ordering for SeO_2. However, it is difficult to say to what extent "d" orbital participation might affect this ordering.*

Maria et. al.[22] have discussed the nature of the MO's involved in generating the low lying excited electronic states of some 18 electron molecules, isoelectronic with SeO_2. A brief summary of their results will be given below.

From Figure 2.1 it can be seen that the $1a_2(\pi)$, $4b_2(\sigma)$ and $6a_1(\sigma)$ molecular orbitals are the last three occupied MO's and the $2b_1(\pi)$ is the first unoccupied MO. The form of the above four MO's is also shown in Figure 2.1 for SeO_2 and is assumed to be the same as NO_2^-.

The $1a_2$ MO is of π nature and consists entirely of group orbitals (GO's) localized on the two end oxygen atoms. The $4b_2$ MO (σ) is also localized primarily on the oxygen atoms and consists of the inplane overlap of the selenium $4p_z$ AO with the oxygen GO's $(2p_{y_1} - 2p_{y_2})$ and $(2p_{z_1} + 2p_{z_2})$ and is antibonding in both combinations. The $6a_1$ MO is also of σ type and results from overlap of the selenium $4p_y$ AO with the oxygen GO $(2p_{y_1} + 2p_{y_2})$ and is bonding. The $2b_1$ MO is π^* in nature and results from the out of plane overlap of the selenium $4p_x$ atomic orbital with the oxygen GO $(2p_{\pi_1} + 2p_{\pi_2})$. The overlap is bonding in nature.

2.3. Molecular Orbitals of SeO_2 (Linear Conformation)

It has long been recognized that the geometric shape of a molecule may be understood by considering the nature of the molecular orbitals comprising it. Mulliken[27] in 1942 and Walsh[28] later in 1953 investigated the change in orbital

---

*Keeton and Santry[26] have recently shown the importance of 3d orbital participation in minimum basis set calculations on SO_2. In SeO_2 d orbitals will quite definitely be involved in the bonding.

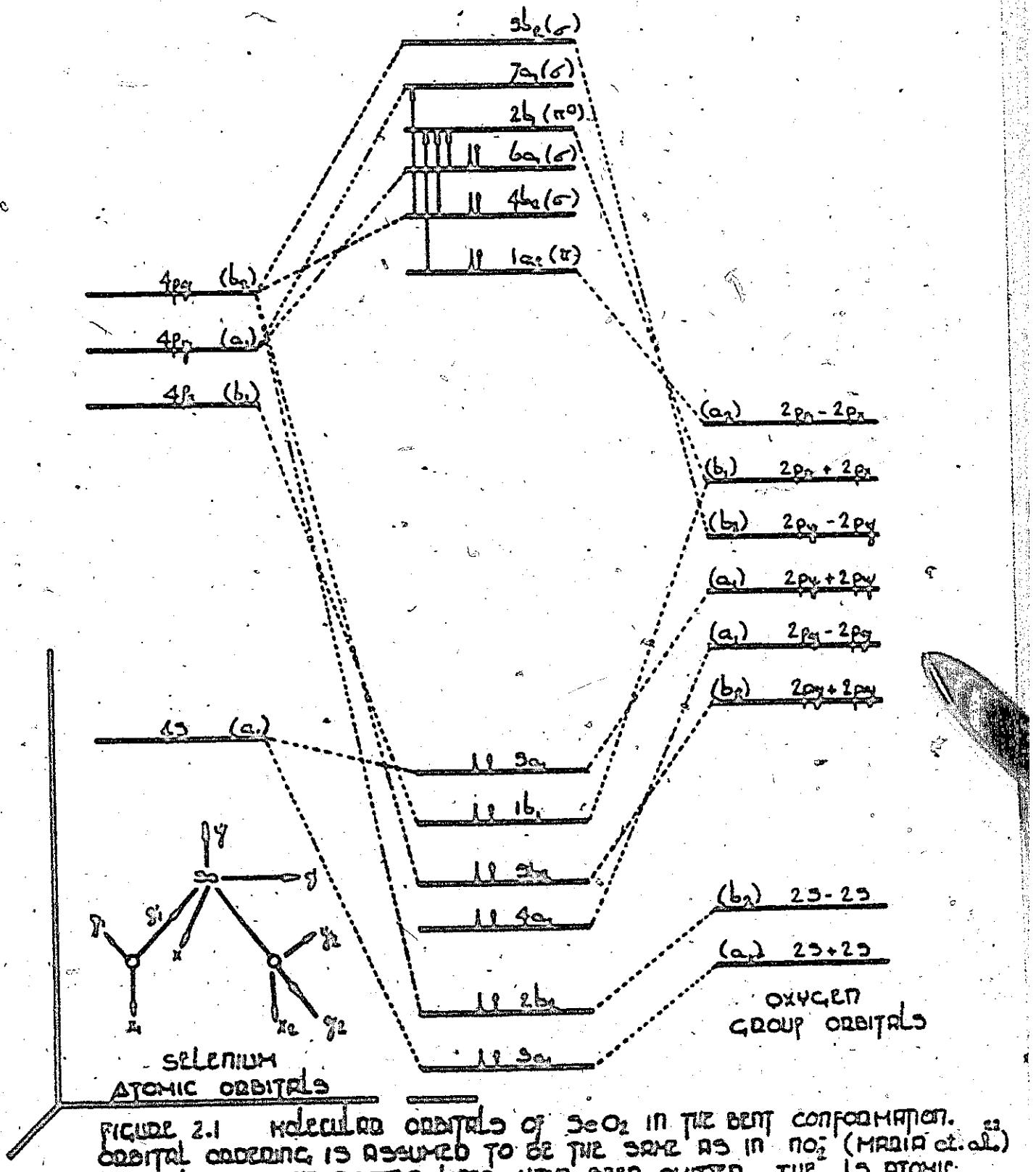

FIGURE 2.1 Molecular orbitals of SeO_2 in the bent conformation. Orbital ordering is assumed to be the same as in NO_2^- (Maria et. al.[22]) For clarity the dotted lines have been omitted. The 1s atomic orbitals have been omitted but have taken into account in the numbering of the orbitals.

energy in going from bent (90°) to a linear conformation in AB_2 type molecules. These authors have shown that a redistribution of electronic charge resulting from an electronic transition can cause a change in geometry of the molecule in the excited electronic state. Therefore, for the sake of completeness, the molecular orbitals for ScO_2 in the linear conformation are shown in Figure 2.2. The ordering of the MO's in the linear conformation is not certain. The ordering given in Figure 2.2 is the same as for CO_2 determined by Rabalais et. al.[29]

The variation in orbital energy with bond angle is given in Figure 2.3. Such a diagram is commonly referred to as a Walsh diagram[28].

It can be seen from the Walsh diagram in Figure 2.3 that the $4\sigma_g$, $3\sigma_u$, $1\pi_g$, $5\sigma_g$ and $4\sigma_u$ orbitals favor the linear conformation while $1\pi_u$-$1b_1$ and $2\pi_u$ favor the bent conformation. The addition of two electrons to the strongly bent-stabilized $6a_1$ molecular orbital is primarily responsible for the bent ground state geometry of ScO_2, while CSo_2 with 16 valence electrons remains linear with a $(1\pi_g)^4$ configuration.

2.4. Low Lying Excited States of ScO_2

According to the qualitative ordering of the one electron molecular orbitals of ScO_2 given in Figure 2.1; the ground state configuration is

$$\ldots\ldots(1a_2)^2(4b_2)^2(6a_1)^2 \qquad (2.4)$$

and, as is expected in accordance with Walsh's rules, the molecule is bent, having a $^1A_1$ ground electronic state.*

The low lying excited electron configurations and the electronic states

---

*The basic group theoretical methods involved in determining the symmetry and multiplicity of electronic states resulting from electron configurations has been assumed throughout this thesis. A complete discussion of group theory and its application to molecular spectroscopy can be found in either of Herzberg[30], King[4], or Hochstrasser[5].

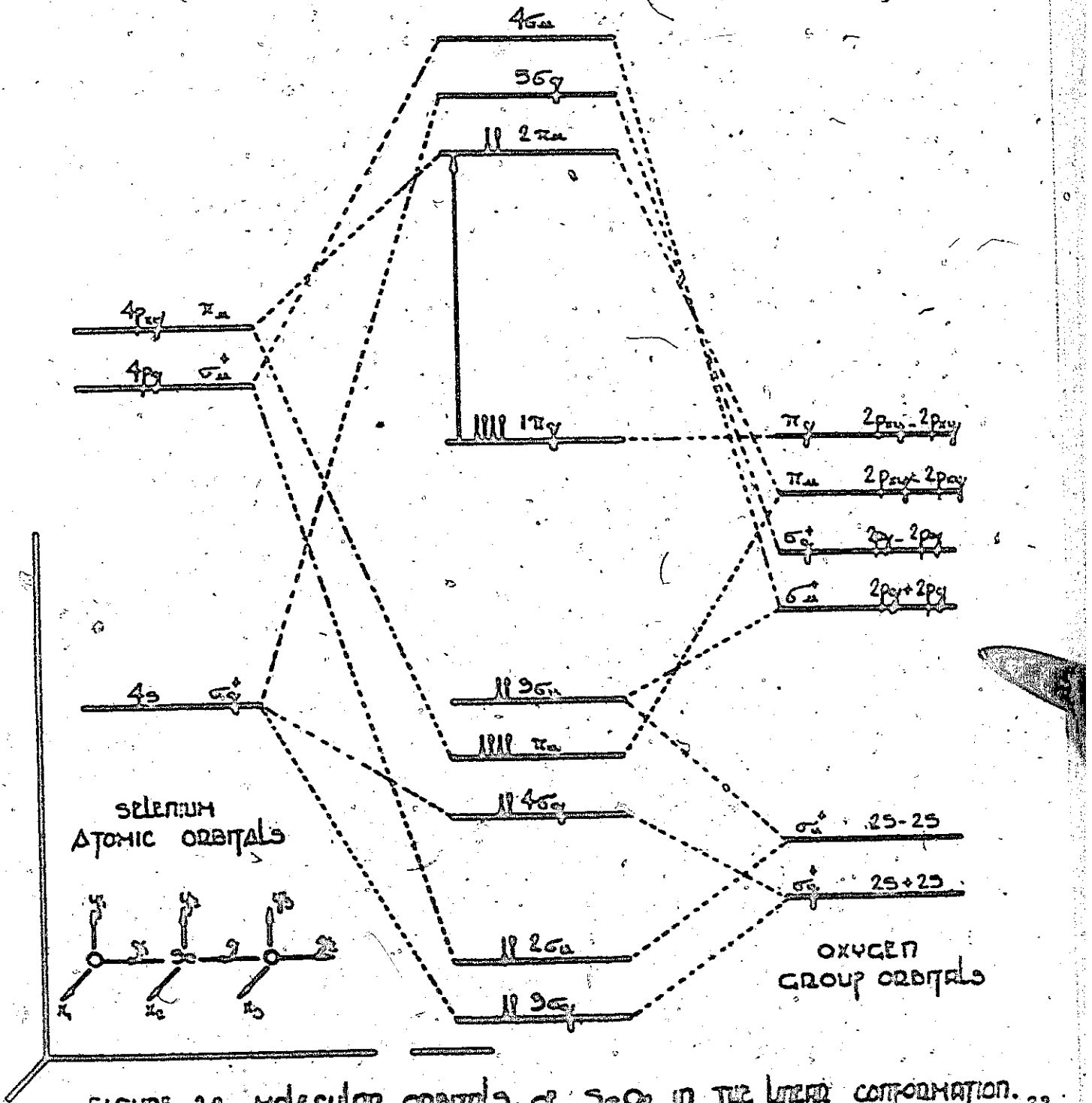

FIGURE 2.2 Molecular orbitals of SeO_2 in the linear conformation. Orbital ordering is assumed to be the same as CO_2 (Brodalais et. al.[32]). For clarity some of the dotted lines have been omitted. The 1s orbitals a and b have been omitted but have been taken into account in the numbering of the orbitals.

arising from each of these, in approximate order of increasing energy are given below[31]:

$$.....(1a_2)^2(4b_2)^2(6a_1)^1(2b_1)^1 \qquad {}^{1,3}B_1 \qquad (2.5)$$

$$.....(1a_2)^2(4b_2)^2(6a_1)^0(2b_1)^2 \qquad {}^{1}A_1 \qquad (2.6)$$

$$.....(1a_2)^2(4b_2)^1(6a_1)^2(2b_1)^1 \qquad {}^{1,3}A_2 \qquad (2.7)$$

$$.....(1a_2)^2(4b_2)^1(6a_1)^1(2b_1)^2 \qquad {}^{1,3}B_2 \qquad (2.8)$$

$$.....(1a_2)^1(4b_2)^2(6a_1)^2(2b_1)^1 \qquad {}^{1,3}B_2 \qquad (2.9)$$

$$.....(1a_2)^1(4b_2)^2(6a_1)^1(2b_2)^2 \qquad {}^{1,3}A_2 \qquad (2.10)$$

Under C_{2v} symmetry, the three components of the dipole moment operator transform as A_1, B_1 and B_2. Therefore, transitions from the totally symmetric ground state to $^{1,3}A_2$ states (2.7 and 2.10) are, within the Born-Oppenheimer approximation forbidden and could appear only weakly through a vibronic mechanism[32]. Transitions to $^1A_1$ (2.6) and $^1B_2$ (2.8) are allowed but should be weak since double electron excitation is involved[31]. The transitions $^1B_1$ (2.5) $\leftarrow \tilde{X}, ^1A_1$ and $^1B_2$ (2.9) $\leftarrow \tilde{X}, ^1A_1$ are electronically allowed and should appear in the visible or ultraviolet region of the spectrum in most 18-electron molecules. The $^1B_1 \leftarrow {}^1A_1$ transition is expected to give rise to "perpendicular" Type C bands and should be accompanied by a moderate increase in bond angle and a small increase in bond length in the excited state[31]. The $^1B_2 \leftarrow {}^1A_1$ transition, on the other hand, should give rise to "parallel" Type A bands and should be accompanied by a decrease in bond angle and an increase in bond length in the excited state[31]. The present work concerning the $^1B_2 \leftarrow \tilde{X}\ {}^1A_1$ transition in ScO_2 substantiates the above predictions for the excited $^1B_2$ state. The bond angle was found to decrease from 113.83° to 101.0° in the excited state while the bond length increased from 1.607 Å to 1.74 Å.

Drozd and Srikameswaran[40] have recently shown the intense absorption

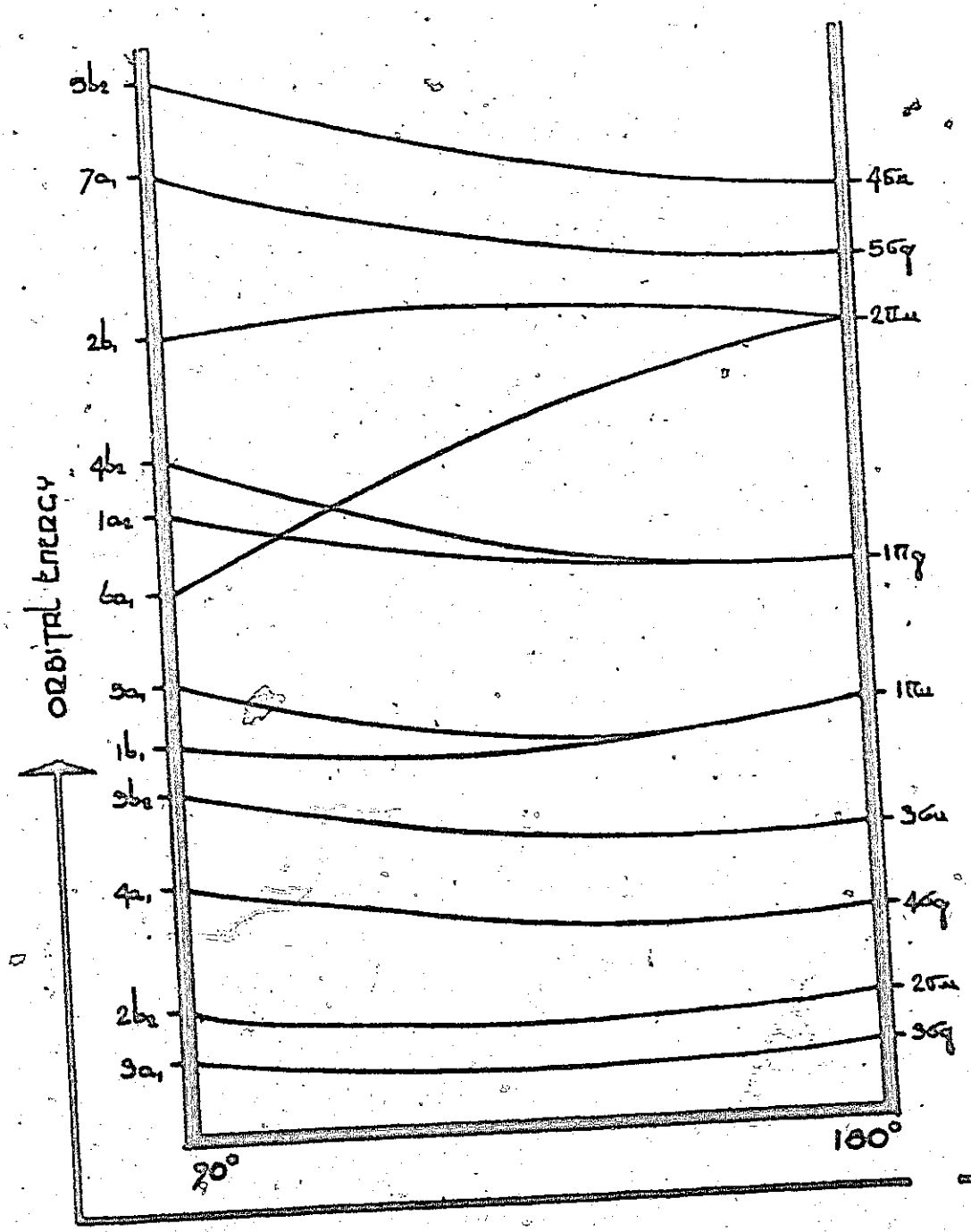

FIGURE 2.3 WALSH DIAGRAM FOR AB_2 TYPE MOLECULE. THE ORDERING OF THE ORBITALS AT RIGHT AND LEFT IS NOT UNIQUELY DETERMINED. THE 1s ORBITALS OF A AND B ARE OMITTED BUT HAVE BEEN TAKEN INTO ACCOUNT IN THE NUMBERING OF THE ORBITALS.

in SO_2 centered around 2350 Å to be due to the $^1B_2 \leftarrow \tilde{X}\ ^1A_1$ electronic transition. They also observed an increase in bond length while the bond angle decreased relative to the ground state in the $^1B_2$ excited state of SO_2. Merer[42] and more recently Brand[41] have shown the weak absorbtion in SO_2 around 3800 Å as due to the $^3B_1 \leftarrow X\ ^1A_1$ electronic transition. The spectral region around 2900 Å is thought to contain the $^1B_1 \leftarrow X\ ^1A_1$ transition, but this as yet has not been confirmed by rotation analysis.

The observed electronic transitions of SO_2 in the visible and ultraviolet region of the spectrum are in excellent agreement with the low lying excited states predicted from molecular orbital considerations.

The observed experimental data and assignments of the electronic transition for O_3, SO_2 and NO_2^- are given in Table 2.1 after Maria et. al.[22]

In SeO_2 unlike SO_2, the first observed low lying electronic transition is $^3B_2 \leftarrow \tilde{X}\ ^1A_1$, followed in energy by the $^1B_2 \leftarrow \tilde{X}\ ^1A_1$ transition.* It is probable that the expected $^1B_1$ and $^3B_1$ electronic states in SeO_2 lie to the red of the $^3B_2$ excited state. Efforts are in progress to detect transitions to these electronic states.** Weak rather continuous absorbtion is observed in the spectral region >4800 Å, and it is possible that for some reason the $^{1,3}B_1$ excited states of SeO_2 are dissociative. This is in direct contrast to SO_2 where the $^3B_1 \leftarrow X\ ^1A_1$ electronic transition is sharp and discrete[42].

Since it is possible for SeO_2 to become linear in an excited electronic state[28], it is important to know how the electronic states in each conformation correlate.

In the linear conformation, the ground state electron configuration is[28]:

---

*Present work.

**R. Weatherall, Private Communication.

Table 2.1

Experimental Data and Assignment of Electronic States for SO_2, O_3 and NO_2^-

(after Maria et. al.[22])

Molecule	Transition $^3B_1 \leftarrow {}^1A_1$	$^1B_1 \leftarrow {}^1A_1$	$^1A_2 \leftarrow {}^1A_1$	$^3B_2 \leftarrow {}^1A_1$	$^1B_2 \leftarrow {}^1A_1$
Ozone (O_3)	1.5 eV (43) $\epsilon \approx 2 \times 10^{-5}$ Gas	2.1 eV (44) ϵ_{max} 1.3 Gas	$\sim$ 3.5 eV Indistinct -	$\sim$2.2 eV (22) Estimated -	5 eV (45) ϵ_{max} 2800 Gas
Sulfur dioxide (SO_2)	3.2 eV (24,42,46,47) $\epsilon_{max} \approx 0.2$	3.7 eV (24,46,47) $\epsilon_{max} \approx 400$	$\sim$ 4.4 eV (48) Indistinct	$\sim$ 3.7 eV (22) Estimated	$\sim$ 5.3 eV (25,49)
Nitrite ion (NO_2^-)	2.8 eV (50-52) $\epsilon_{max} \sim 0.003$	3.5 eV (53) ϵ_{max} 25	$\sim$ 4.1 eV (54) $\epsilon_{max} \sim 110$ (In water)	$\sim$ 3.2 eV (55) Computational	5.9 eV (56) $\epsilon_{max} \sim 5500$

$$\ldots\ldots(1\pi_g)^4(2\pi_u)^2 \qquad {}^3\Sigma_g^-,\ {}^1\Delta_g,\ {}^1\Sigma_g^+$$

with the ${}^3\Sigma_g^-$ state lying lowest in energy, followed by the ${}^1\Delta_g$ and ${}^1\Sigma_g^+$ in agreement with Hund's rules.

The first excited state configuration is assumed to be

$$\ldots\ldots(1\pi_g)^3(2\pi_u)^3 \qquad {}^{1,3}\Delta_u,\ {}^{1,3}\Sigma_u^+,\ {}^{1,3}\Sigma_u^-$$

The manner in which the electronic states of bent (C_{2v}) and linear ($D_{\infty h}$) SeO_2 correlate with each other is shown in Figure 2.4.

Since in the present work, the molecule remains strongly bent in both electronic states, the Renner[33] effect and other phenomena relating to linear and quasi-linear[34] molecules will not be considered.

2.5. Double-Minimum Potentials in AB_2 Type Molecules

Usually the geometric structure of a bent AB_2 molecule has C_{2v} symmetry when the nuclei are in their equilibrium positions. However, there is evidence that occasionally a bent AB_2 molecule has an excited state with two equilibrium structures which deviate from C_{2v} symmetry by $\pm Q_3$ where Q_3 is a normal co-ordinate representing a small antisymmetrical displacement[35]. This means that the electronic state has a double-minimum potential in the antisymmetric vibrational co-ordinate Q_3', and that the molecule will have a stable non-symmetric structure in those vibrational levels associated with Q_3' which lie well below the peak of the barrier. The molecular symmetry will be reduced from C_{2v} to C_s and those vibronic levels below the barrier may exhibit the consequence of C_s symmetry (e.g., the $S_0^1(0^- \leftarrow 0^+)$ band should be an A-B hybrid type band). Above the barrier to inversion, the molecule freely moves from one structure to the other and the equilibrium symmetry becomes C_{2v} again.

Coon[36-38] has postulated the existence of a double-minimum potential in

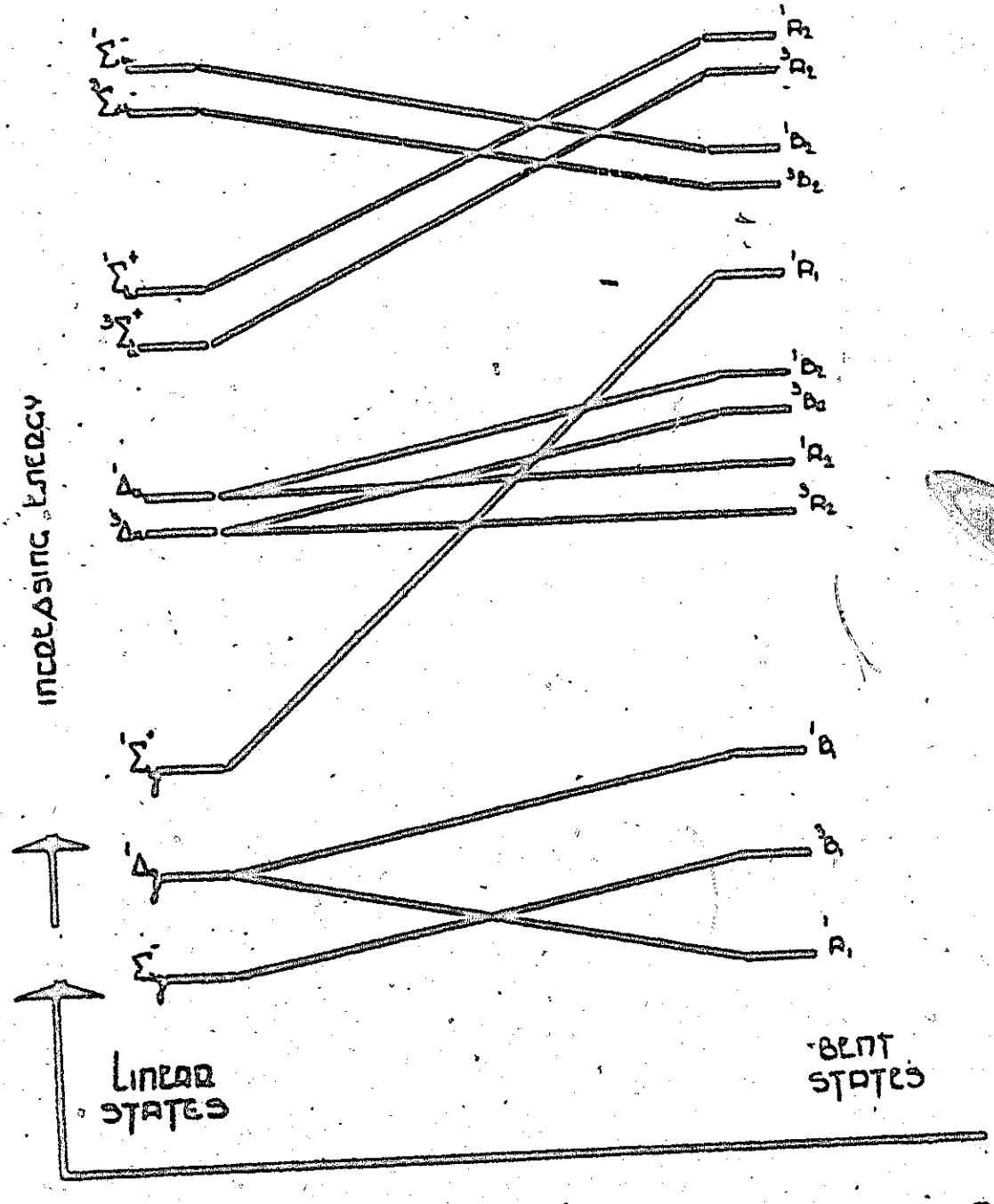

FIGURE 2.4 CORRELATION OF THE ELECTRONIC STATES OF SiO_2 IN THE LINEAR AND BENT CONFIGURATIONS. THE ORDERING OF THE HIGHER ELECTRONIC STATES IS ONLY TENTATIVE PENDING FURTHER EXPERIMENTAL WORK.

the 4758 Å electronic transition of ClO_2 as well as the 2348 Å system of SO_2 and the 2491 Å system of NO_2. The present analysis of the 3120 Å system of SeO_2 also strongly suggests the presence of a double-minimum potential well in the excited state Q_3' co-ordinate. A further discussion of double-minimum potentials is deferred to Chapter Three where the vibrational analysis is discussed in detail. The resolution of the symmetry species of C_{2v} into those of C_s are given in Table 2.2.

Table 2.2

Correlation of symmetry species of the C_{2v} point group into those of C_s symmetry

C_{2v}	C_s (σ_{yz})	
A_1	A'	y (b-axis)
A_2	A''	
B_1	A''	x (c-axis)
B_2	A'	z (a-axis)

CHAPTER THREE

VIBRATIONAL ANALYSIS OF SELENIUM DIOXIDE SPECTRUM

3.1. Description of SeO_2 Spectrum

At least five discrete electronic transitions have been observed in the gas phase spectrum of the selenium dioxide molecule in the spectral region between 2000 Å and 6000 Å [7-11]. Three of these transitions have been observed in absorbtion in the regions 2070-2210 Å, 2300-3400 Å, and 3500-5200 Å and have been designated the A, B and C systems respectively. Haranath and Sivaramamurty[12] also claim to have observed two systems in emission with origins at 3110 Å and 3119 Å. The present work is concerned primarily with the B system of selenium dioxide.

3.2. The B System of SeO_2

The B system of SeO_2 has been photographed under both high and low resolution using pure selenium and oxygen isotopes. Portions of the spectra of the $Se^{78}O_2^{16}$ and $Se^{70}O_2^{16}$ molecules are shown under low dispersion in Figure 3.1.

The most prominent features in the spectrum are long progressions with the frequency interval of approximately 660 cm^{-1}. This frequency can be assigned to ν_1', the totally symmetric stretching frequency of the excited state. Both the excited state bending frequency ν_2' = 260 cm^{-1} and the asymmetric stretching frequency of 1372 cm^{-1} ($2\nu_3'$) appear in the spectrum as false origins for totally symmetric progressions in ν_1'. All three fundamental frequencies have decreased in the excited state. The ground and excited state frequencies, along with their percentage decreases, are summarized in Table 3.1.

Many of the bands in the system are double headed and several frequency

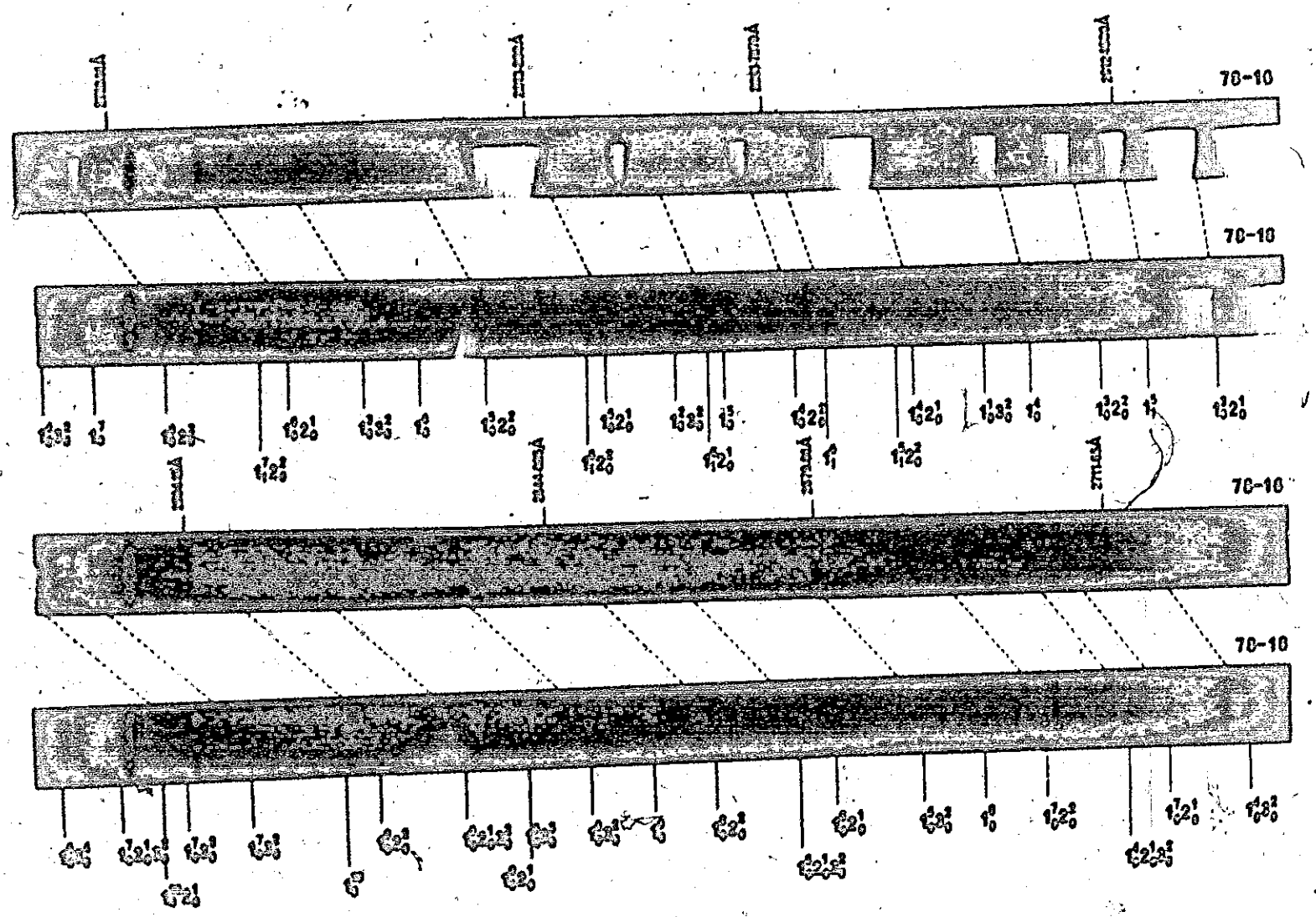

Figure 3-1 Portion of the spectrum of the $Se^{76}O_2^{16}$ and $Se^{78}O_2^{16}$ molecules associated with the $^1B_2 - {}^1A_1$ electronic transition

intervals are abnormally large. Each of these anomalies will be discussed separately, later in the chapter.

The strongest progression in the spectrum involves ν_1' and originates on the unobserved 2_0^2 level and contains twelve members. The intensity maximum occurs in the sixth member. The presence of such an extended progression in ν_1' in combination with ν_2' indicates a substantial change in both bond length and bond angle in the excited electronic state.

3.3. The Origin Band of the B System of SeO_2

The spectra of the two isotopic molecules $Se^{78}O_2^{16}$ and $Se^{78}O_2^{18}$ were photographed under high resolution and the positions of the band heads carefully determined using a travelling microscope accurate to 0.0001 centimeters. In Figure 3.2 is shown a plot of isotopic splitting against number of quanta of ν_1' excited for the two isotopic molecules $Se^{78}O_2^{16}$ and $Se^{78}O_2^{18}$. The origin band for the electronic transition has an isotopic splitting of -8.9 cm^{-1} for the $Se^{78}O_2^{16}$ and $Se^{78}O_2^{18}$ molecules, the heavier isotope band lying to the blue of the lighter one. The origin band* for the $Se^{78}O_2^{16}$ isotope occurs at 31955.0 cm^{-1}. The origin band of the $Se^{78}O_2^{16}$ and $Se^{80}O_2^{16}$ molecules have an isotopic splitting of -2.4 cm^{-1}. For the $Se^{78}O_2^{16}$ and $Se^{78}O_2^{18}$ molecules, the isotopic splitting is found to be 80 cm^{-1} per quanta of ν_1' excited, with the lighter isotope to the blue of the heavier one. A similar plot using the isotopic splittings from the $Se^{78}O_2^{16}$ and $Se^{80}O_2^{16}$ molecules gives a value of 1.46 cm^{-1} per quanta of ν_1' excited. It is possible to observe three quanta of the ground state totally symmetric stretching frequency ν_1'', as hot bands to the red of the above assigned origin band. Figure 3.2 (lower curve) shows the

*Unless otherwise stated, all frequencies used in the text refer to the $Se^{78}O_2^{16}$ isotope.

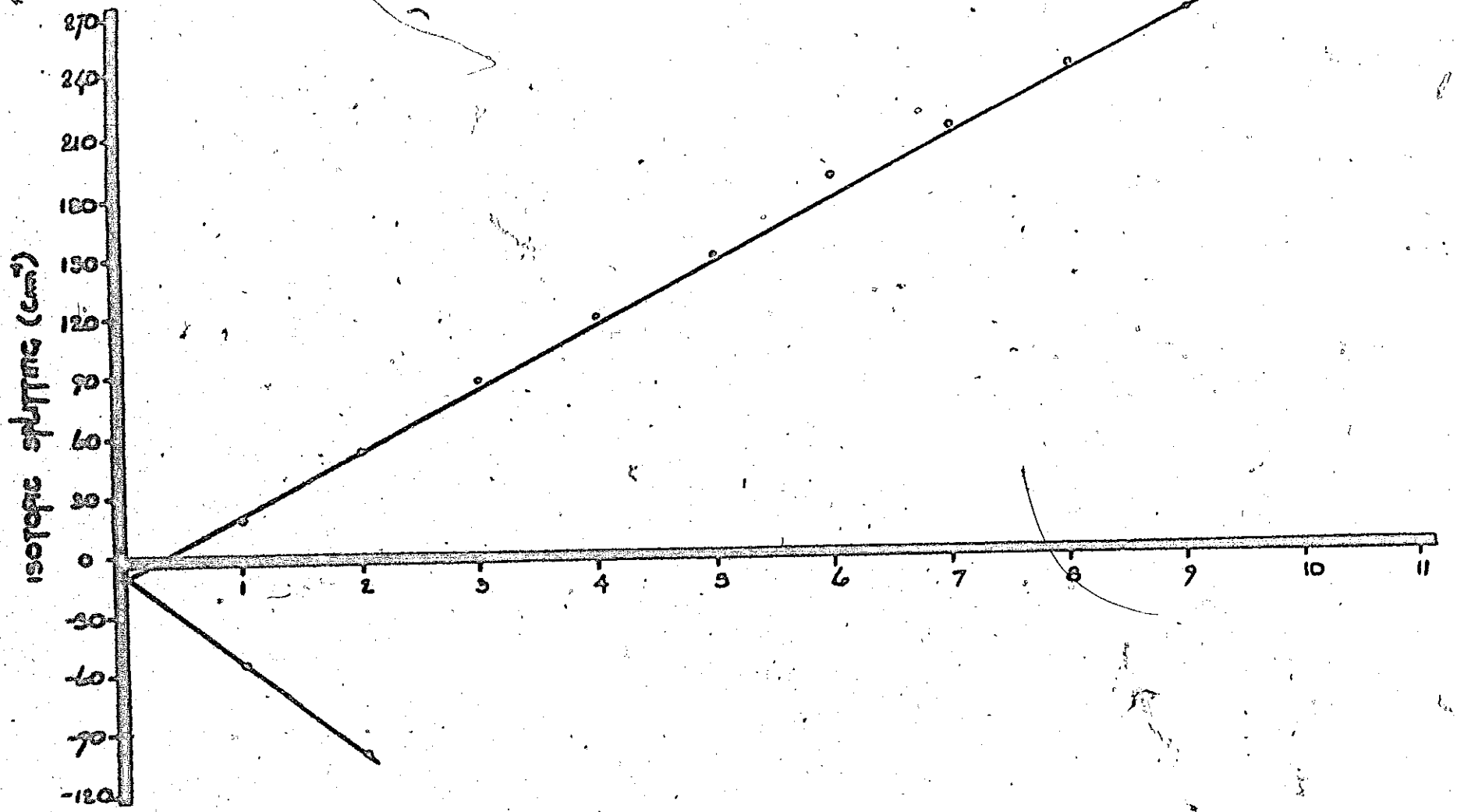

FIGURE 9.2 ISOTOPIC SPLITTING PER QUANTA OF ν_1' EXCITED IN THE 0-0 PROGRESSION (UPPER CURVE) AND ISOTOPIC SPLITTING PER QUANTA OF ν_1'' EXCITED IN THE HOT BAND SPECTRUM (LOWER CURVE). THE ISOTOPIC MOLECULES USED WERE $Se^{78}O_2^{16}$ AND $Se^{78}O_2^{18}$. A SIMILAR PLOT USING $Se^{78}O_2^{16}$ AND $Se^{80}O_2^{16}$ SHOWS AN ISOTOPIC SPLITTING OF 1.46 cm^{-1} PER QUANTA OF ν_1' EXCITED AND EXTRAPOLATES TO THE SAME ORIGIN.

corresponding plot for ν_1''. As is expected there is a reversal in the direction of the isotopic splitting in the hot band spectrum to that in the cold band spectrum. The average splitting is -47.0 cm^{-1} per quanta of ν_1'' excited with the heavier isotope now appearing to the blue of the lighter one.

The explanation for this reversal is simple, and can be understood with the aid of Figure 3.3.

3.4. Isotopic Splittings in Hot and Cold Bands of Electronic Transitions

A cold band in an electronic transition is due to a transition originating on the vibrationless level of the ground state and terminating on an excited state vibronic level, while a hot band transition originates from an excited vibronic level in the ground state and terminates on an excited state vibronic level. The transitions designated (a) in Figure 3.3 give cold bands while those designated (b) give hot bands. If, for the moment, we assume that the isotopic splitting of the vibrationless level in both the ground and excited state is too small to resolve, then for a decrease in frequency in going to the excited state as a result of a shallower potential well in this state, the levels will have a larger splitting in the ground than in the excited state. The level belonging to the lighter isotope will have a higher energy since it vibrates at a higher frequency. Since the splitting of the $\nu_1'' = 2$ isotopic levels in the ground state is larger than the $\nu_1' = 2$ splitting in the upper state, then the bands of the lighter isotope will lie to the blue of the heavier in (a) but to the red of the heavier in (b). In the present case the origin band has an isotopic splitting of -8.9 cm^{-1}, the heavier isotope origin band lying to the blue of the lighter one. This can be rationalized in the following way. Since the three fundamental frequencies decrease considerably in the excited state, therefore, the potential wells along these co-ordinates

will be shallower than the corresponding wells in the ground electronic state. Accordingly, the $v_i = 0$ vibrational levels will lie both closer together and closer to the bottom of the well in the excited state than in the ground state. The zero point energy will, therefore, be less in the excited state than in the ground state. Since the isotopic splitting of the vibrationless level is larger in the ground than in the excited state, with the lighter isotope lying at higher energy, the origin band of the heavier isotope is expected to lie to the blue of the origin band for the lighter isotope and thus a reversal in the direction of the isotopic splitting is observed. The reversal in the direction of the isotopic splitting is shown in Figure 3.3 by the set of transitions labelled (c).

3.5. Ground State Fundamentals of SeO_2

The infrared spectrum of selenium dioxide has been studied in the gas phase by Giguère and Falk[18] and in the solid phase in rare gas matrices by Hastie et. al.[15] and Cesaro et. al.[14] The gas phase work of Giguére and Falk give ν_3'' as 967 cm^{-1} in good agreement with the value of 970.2 cm^{-1} found in neon matrices by Hastie et. al. and 965 cm^{-1} reported by Cesaro et. al. The weak ν_1'' fundamental could not be definitely assigned in the gas phase because of overlap with the intense ν_3'' absorption. Duchesne and Rosen[8], however, assigned $\nu_1'' = 910$ cm^{-1} from their analysis of the B system of selenium dioxide. The present analysis of the B system indicates 923 cm^{-1} for the totally symmetric stretching frequency of the ground state. The interval of 910 cm^{-1} attributed to ν_1'' by Duchesne and Rosen was incorrectly interpreted. The isotopic analysis of SeO_2 unambiguously shows the 910 cm^{-1} interval is in fact due to the excited state combination band $\nu_1' + \nu_2'$ where $\nu_1' = 660$ cm^{-1} and $\nu_2' = 260$ cm^{-1}. Higher members of the excited state progression involving ν_1'

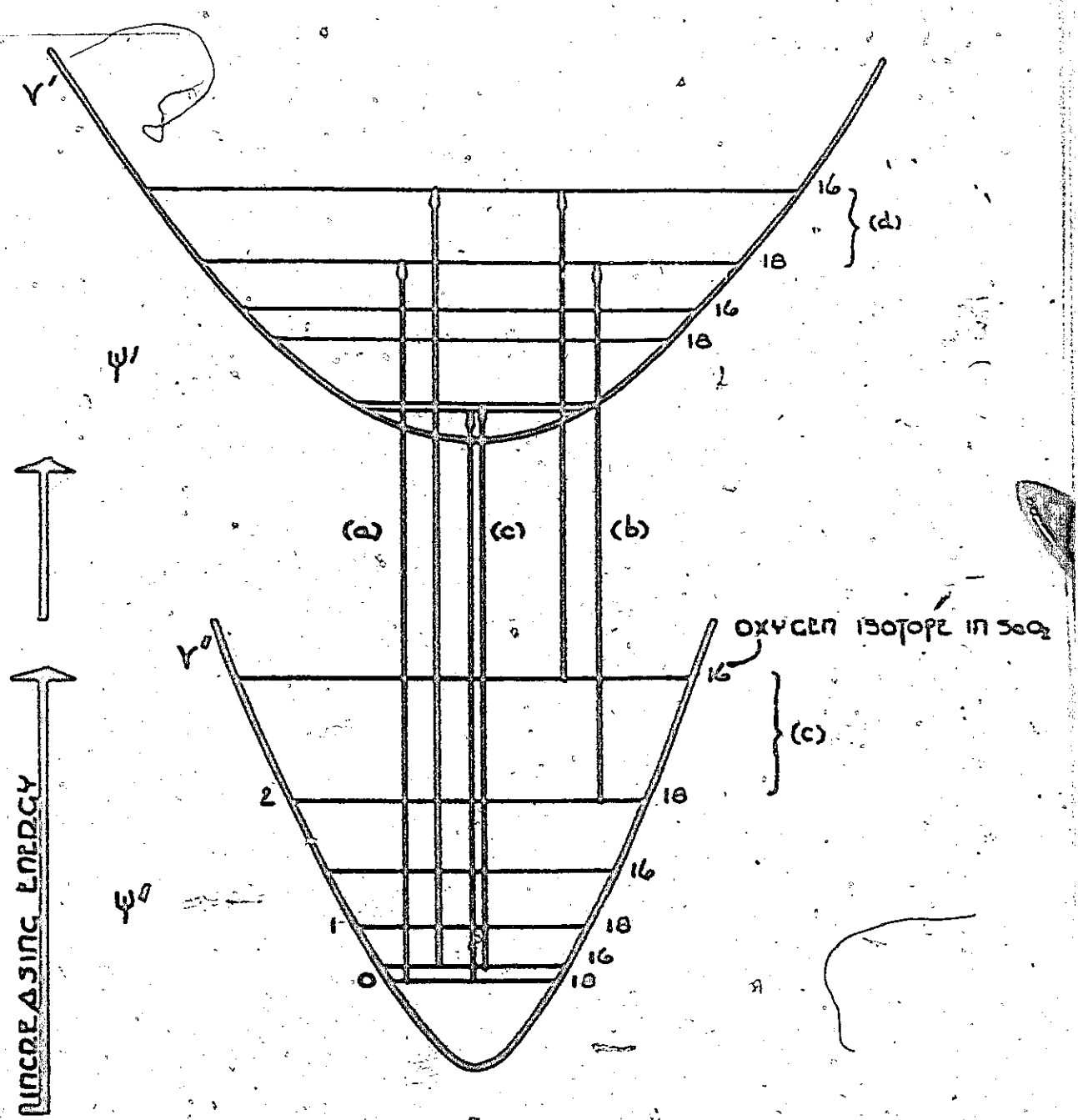

FIGURE 3.3 THE ISOTOPIC SPLITTING OF THE ν_1'' AND ν_1' LEVELS IN $Se^{78}O_2^{16}$ AND $Se^{78}O_2^{18}$. THE SPLITTING IS GREATLY EXAGGERATED. THE WELL IS FLATTER IN THE EXCITED STATE ψ' SINCE THE FREQUENCY WAS DROPPED AND THE Se - O BOND LENGTH INCREASED.

show a frequency interval of approximately 650 cm^{-1}. Hot band progressions in ν_1' originating on the 1_1^0 and 1_2^0 levels are quite weak with fewer members in the progression. Duchesne and Rosen incorrectly assigned the origin band for the transition 1375 cm^{-1} to the blue of the true origin. Prior to the present analysis the interval corresponding to ν_1'' and ν_2'' had not been observed in absorbtion in either the gas phase or in low temperature matrices. Takeo et. al.[57], from the microwave spectrum of SeO_2, have estimated $\nu_2'' = 362 \pm 14$ cm^{-1}, using Coriolis coupling constants and inertial defects. From the present work the frequency interval associated with ν_2' has been observed to be 373 cm^{-1}. This is in excellent agreement with the value of 372.5 recently determined by Cesaro et. al.[14] from studies of SeO_2 in an argon matrix.

3.6. Excited State Fundamentals of SeO_2

In the present vibrational analysis of the B system of SeO_2, all three excited state fundamentals are assigned. By far the most active frequency in the spectrum is $\nu_1' = 660$ cm^{-1} which occurs in long progressions with as many as twelve members. The bending frequency $\nu_2' = 260$ cm^{-1} appears only in combination with ν_1' and ν_3' while the asymmetric stretching frequency $2\nu_3' = 1372$ cm^{-1} appear in the spectrum both as the fundamental and in combination with ν_1' and ν_2'. The ground and excited state frequencies for the $Se^{78}O_2^{16}$ and $Se^{78}O_2^{18}$ molecules are summarized in Table 3.1.

3.7. Major Progressions in the B System of SeO_2

The majority of bands in the spectrum may be accounted for in terms of progressions in ν_1'. The following act as origins for a progression in this mode: 0_0^0, 2_0^1, 2_0^2, 3_0^2, $3_0^2 2_0^1$, 3_0^3, 3_0^6, 1_1^0, 1_2^0. The $2_0^2 1_0^n$ progression contains the strongest bands in the spectrum. The wavelengths and assignments for the above progressions are given in Appendix I of the thesis. Since there are so many

Table 3.1

Ground and Excited State Fundamentals of $Se^{78}O_2^{16}$ and $Se^{78}O_2^{18}$

Isotope†	Frequency (cm^{-1})	Ground State	Excited State	Percent Change on Excitation
$Se^{78}O_2^{16}$	ν_1 (a_1)	923 cm^{-1}	660 cm^{-1}	-28.5%
	ν_2 (a_1)	373 cm^{-1}	255 cm^{-1}	-30.3%
	ν_3 (b_2)	967 cm^{-1}	___*	-29.1%
$Se^{78}O_2^{18}$	ν_1 (a_1)	878 cm^{-1}	625 cm^{-1}	-28.9%
	ν_2 (a_1)	359 cm^{-1}	245 cm^{-1}	-31.8%
	ν_3 (b_2)	___**	___*	___

*Evidence is presented which suggests the presence of a double-minimum potential in the asymmetric vibrational co-ordinate Q_3' in the excited state of SeO_2 and, therefore, it is not possible to assign a particular frequency to ν_3'. However the interval $(0^+ - 1^+) = 2\nu_3'$ has been observed as 1372 cm^{-1}.

**Not observed.

†The fundamental frequencies of $Se^{80}O_2^{16}$ are almost identical with those of $Se^{78}O_2^{16}$ and are therefore not shown.

long progressions of bands, all of type-A and further since the combination band $\nu_1' + \nu_2' = 920$ cm^{-1} is almost identical with $\nu_1'' = 923$ cm^{-1}, there can occur quite strong Fermi resonances in the spectrum.

The three progressions in ν_1' originating on the levels 0_0^0, 2_0^1 and 2_0^2 are quite straightforward. Each contains twelve members with the sixth member being the strongest in each progression. The 2_0^1 and 2_0^2 bands, however, appear in absorbtion only in combination with ν_1'; the ν_2' fundamental is not observed. It is possible that ν_2' also appears in combination with the 3_0^1 level.* This hypothesis is discussed in greater detail later in the chapter.

The region of the 0—0 band is both very weak and badly overlapped. The considerable overlap in this region is due to the presence of combination sequence bands of the type $1_1^1 2_0^1$ and $1_1^1 2_0^2$; the first occurs at almost an identical frequency to that of the origin band.

The hot band spectrum very clearly shows the three bands 1_1^0, 1_2^0 and 1_3^0. All three bands are themselves false origins for progressions in ν_1'. Higher members in this progression further complicate the region of the origin band.

3.8. The Presence of Another Electronic Transition?

The hot band spectrum of the B system of SeO_2 was photographed under both high and low resolution and extends for 2750 cm^{-1} to the red of the origin band. The origin band for the transition occurs at 31955 cm^{-1}. The ground state fundamentals $\nu_1'' = 923$ cm^{-1} and $\nu_2'' = 373$ cm^{-1} can be unambiguously assigned. The three hot bands in the spectrum appearing at 31032 cm^{-1}, 30115 cm^{-1}, and 29201 cm^{-1}, separated by the respective intervals 923.0 cm^{-1}, 918.4 cm^{-1} and 912.0 cm^{-1} have been assigned to the 1_1^0, 1_2^0 and 1_3^0 bands respectively.

---

*There is strong evidence showing the presence of a double-minimum potential in the asymmetric stretching co-ordinate Q_3'' of the excited state. The (0°—0°) splitting is observed to be 78 cm^{-1} and can be associated with the frequency interval 3_0^1.

This assignment can be made with a high degree of certainty and is substantiated by the isotopic splitting for each band.

A puzzling thing about the above three hot bands is the fact that they appear to be doublets, each having an additional head at an average separation of 78 cm^{-1} to the blue. The calculated band contour of the 1_0^3 band in the cold spectrum shows no indication of the presence of a second head in the band 78 cm^{-1} to the blue of the first head. From the rotational analysis of the 1_0^3 band, the excited state was determined to be of B_2 symmetry, the electric dipole for the electronic transition being polarized along the a-axis (i.e., the axis parallel to the line joining the oxygen nuclei) of the molecule. The possibility that both heads separated by 78 cm^{-1} could be associated with one vibronic band was, however, still considered.

If in fact the head 78 cm^{-1} to the blue is to be associated with the same vibrational band then one of the heads° must be due to a q branch ($\Delta K = 0$) while the other is due to an s or o branch ($\Delta K = \pm 2$) in the K structure. The latter two branches are expected to be much weaker than the q branch since they acquire intensity only as a result of the asymmetry of the molecule or through a perturbation such as Coriolis coupling or centrifugal distortion.

The origin of the sub-bands ($J = 0$), in the q branch of a parallel transition of an asymmetric top, in the near prolate symmetric top approximation, is given by:

$$\nu^{sub} = \nu_0 + [(A' - \bar{B}') - (A'' - \bar{B}'')]K^2 \qquad (3.1)$$

where $\bar{B} = \frac{1}{2}(B + C)$ and the primes and double-primes refer to excited and ground state respectively.

°In this content the word "head" is meant to indicate an accumulation of very closely spaced K sub-bands.

The sub-band origins for a parallel transition in the o and s branch of the K-structure is given by

$$\nu^{sub} = \nu_o + 4(A'-\bar{B}') \pm 4(A'-\bar{B}')K + [(A'-\bar{B}') - (A''-\bar{B}'')]K^2 \qquad (3.2)$$

The value of K at the head is determined by differentiating Equation (3.2) and setting it equal to zero. The resulting equation is:

$$K_{HEAD} = \frac{\pm 2(A'-\bar{B}')}{[(A'-\bar{B}') - (A''-\bar{B}'')]} \qquad (3.3)$$

Substitution of Equation (3.3) into (3.2) gives, for the separation of the heads in the q and o branch, and the q and s branch of the K-structure:

$$\nu_o^s - \nu_q = 4(A'-\bar{B}') \frac{\pm 12(A'-\bar{B}')^2}{[(A'-\bar{B}') - (A''-\bar{B}'')]} \qquad (3.4)$$

From the microwave spectrum[57], $(A''-\bar{B}'') = 0.712\ cm^{-1}$ while from the present rotational analysis $(A'-\bar{B}') = 0.361\ cm^{-1}$. Substitution of these values into Equation (3.4) gives a head separation of $\pm 3\ cm^{-1}$. The observed separation between the two heads in the spectrum is $78\ cm^{-1}$. The hypothesis that the two heads belong to the one vibronic band is therefore rejected since the observed separation is much too large. The fact that both heads are of equal intensity is also strong evidence against both belonging to one and the same band, since the o and s branches would be expected to have considerably less intensity than the q branch.

It was therefore necessary to assign the four bands located at 32033.8 cm^{-1}, 31110.8 cm^{-1}, 30192.5 cm^{-1} and 29280.5 cm^{-1} to different vibronic transitions.

Naranath and Sivaramamurty[12] studied the gas phase emission spectrum of ScO_2 and observed a number of bands in the spectral region 4700 Å to 2750 Å.

The bands below λ 3200 Å to λ 2700 Å were assigned as belonging to the previously assigned B—X system of SeO_2 studied by Duchesne and Rosen[8] in 1941. The remaining bands were assigned by Haranath and Sivaramamurty as belonging to two new systems of selenium dioxide with origins at 32145 cm^{-1} and 32052 cm^{-1}. A summary of the vibrational constants determined by Haranath and Sivaramamurty is given in Table 3.2.

Table 3.2

Vibrational Frequencies of System-I and System-II Observed in Emission of SeO_2

	0_0^0	ν_1''	ν_2'
System-I	32145 cm^{-1}	910.5 cm^{-1}	182 cm^{-1}
System-II	32052 cm^{-1}	911.5 cm^{-1}	182 cm^{-1}

Both of the above emission systems could, if they terminate on the ground electronic state, appear in absorbtion in the same spectral region as the B System of SeO_2. An attempt was therefore made to try and observe their absorbtion spectrum in the hope of perhaps accounting for the four sequence bands discussed above.

The only conceivable assignment which could be made would be to assign the four vibronic bands located at 32033.8 cm^{-1}, 31110.8 cm^{-1}, 30192.5 cm^{-1} and 29280.5 cm^{-1} as the 0_0^0, 1_1^0, 1_2^0, and 1_3^0 of one of the two electronic states observed by Haranath and Sivaramamurty.

It was, however, not possible to observe the frequency interval of 182 cm^{-1}, anywhere in the spectrum, nor was it possible to assign any new frequency interval resulting from the presence of a close lying second electronic transition.

Since there are no excited state frequencies observed, along with the fact that the presence of a second electronic transition, only 78 cm^{-1} away, is difficult to account for theoretically, the hypothesis of a second electronic transition was rejected. In the emission work of Haranath and Sivaramamurty both transitions were found to have the same intensity. It would be difficult to explain why only one of the two emission systems should appear in absorbtion if both were transitions terminating in emission on the ground state. The four vibronic bands mentioned above, though still unexplained, were assumed to be sequence bands associated in some way with the B System of SeO_2.

The possibility that the above vibronic bands were due to an impurity molecule such as Se_2 was excluded since the bands showed an O^{18} isotopic shift when the $Se^{78}O_2^{18}$ spectrum was photographed. Since isotopic selenium was used, the only other realistic impurity which was considered was SeO. Along with the fact that the observed frequencies of the bands are different to those of SeO observed by Shin-Piaw[58], the rotational structure appears much too complex to be associated with a diatomic molecule.

The isotopic splitting of all bands was found to be almost linear with displacement from the origin, regardless of the nature of the band. Since the four sets of bands were separated by only 78 cm^{-1}, both members of each set showed approximatoly the same isotopic shift; so the isotopic molecule gave no new information, other than the bands do in fact belong to SeO_2.

3.9. The Cold Spectrum of the B System of SeO_2

All of the bands in the cold spectrum can be accounted for by progressions in the excited state totally symmetric stretching frequency $\nu_1' = 660\ cm^{-1}$. Two interesting features are present in the spectrum.

1. There is an abnormally high intensity associated with the 3_0^2 transition

(see below).

2. Many, but not all, of the bands are double-headed.

3.10. Progressions in Anti-Symmetric Vibrations

According to the simple classical principle of Franck[59], the geometric conformation of the nuclei and their relative velocities does not change during an electronic transition. Therefore, the instantaneous symmetry of the equilibrium position of the nuclei is the same in both combining electronic states. The classical principles of Franck were later developed quantum mechanically by Condon; the combined treatment is now most often referred to as the Franck-Condon principle.

If a non-totally symmetric vibration is excited during an electronic transition (and once again it is assumed that the instantaneous symmetry of the excited state is the same as that of the ground oléctronic state) then this requires that the potential surfaces for all non-totally symmetric vibrations have their origins directly above one another. The potential well along Q_3, the asymmetric stretching normal co-ordinate is shown in Figure 3.4 for two combining electronic states (the double-minimum character is ignored in this section). The centers of the two wells must be directly above one another since any displacement along Q_3 in the excited state relative to that of the ground state will correspond to an equilibrium asymmetric structure in the excited state. This would then violate the initial assumption that the symmetry of the molecule remain unchanged during an electronic transition. Therefore, within the Franck-Condon approximation, the transition probability between two electronic states is proportional to the square of the matrix element

$$\langle \phi' v' | \hat{r} | \phi'' v'' \rangle \qquad (3.5)$$

where ψ and ϕ are the electronic and vibrational wavefunctions respectively and $\vec{r}$ is the electric dipole operator. The primes refer to the upper state while the double primes refer to the lower state.

Within the Born-Oppenheimer[1] approximation the nuclear and electronic motion may be considered independent and Equation (3.5) reduces to

$$\langle\psi'|r|\psi''\rangle\langle\phi'|\phi''\rangle \tag{3.6}$$

In order for an electronic transition to occur, Equation (3.6) must be non-zero. The transition probability will be different from zero only if the integrand of Equation (3.6) is totally symmetric.

The first integral of Equation (3.6), $\langle\psi'|r|\psi''\rangle$, is the transition moment and is non-zero only if the direct product of the representations to which the electronic wavefunctions belong transform as one of the components of the electric dipole operator r, which transforms like the translations T_x, T_y, and T_z. We, therefore, have the following selection rule:

$$\Gamma\psi' \times \Gamma\psi'' = \Gamma T_i \qquad i = x, y, z \tag{3.7}$$

The second integral of Equation (3.6), $\langle\phi'|\phi''\rangle$, is called the Franck-Condon overlap integral and is non-zero only if the following selection rule is satisfied:

$$\Gamma\phi' \times \Gamma\phi'' = \Gamma A_1 \tag{3.8}$$

If we assume transitions from the ground state occur from the vibrationless level, then $\Gamma\phi'' = A_1$ and, therefore, according to the Franck-Condon principle, within the Born-Oppenheimer approximation, the following vibrations may be excited:

1. Totally symmetric vibrations may change by any number of quanta.
2. Antisymmetric vibrations must change by an even number, $\Delta v = 0,2,4,\ldots$, where v is the vibrational quantum number.

If the symmetry is different in both states then only those vibrations will be excited which preserve the symmetry elements common to both states.

Therefore, according to the Franck-Condon principle, the 0—0, 1—1, ..., v—v transitions will be intense, with the higher members becoming progressively weaker due to their decreased Boltzmann factor.

Sponer and Teller[60] have shown, for purely harmonic vibrations, that the ratio of the intensity of the 0—0 band, to that of all the other members in a progression involving an asymmetric vibration Q, is given by

$$\frac{(\nu'\nu'')^{1/2}}{\frac{1}{2}(\nu'+\nu'')} = \frac{\text{intensity of band 0—0 in Q}}{\text{intensity of all bands 0—v in Q}} \qquad v = 0,2,4,\ldots \qquad (3.9)$$

where ν' and ν'' are the frequencies in the two combining electronic states. This means that even in the extreme case when the vibrational frequencies in the upper and lower state change by 50%, the intensity of the 0—0 band amounts to 94.4 percent of the total intensity and only 5.6 percent is left for transitions from $v'' = 0$ to $v' \neq 0$ levels. Hence the 3_0^2, 3_0^4 and higher bands should be very weak and in all probability not be observed in the spectrum.

It is possible to rationalize the above results in the following manner. Since the potential wells for asymmetric vibrations belonging to different electronic states must be directly above one another, as shown in Figure 3.4, then transitions of the type 0—0, 1—1, etc., will have a larger Franck-Condon factor than transitions of the type 0—2 or 0—4. The actual intensity of any one band is proportional to

$$\int |\phi'_{vib}\phi''_{vib}d\tau_{nucl}|^2 \qquad (3.10)$$

where ϕ' and ϕ'' are the vibrational wavefunctions of the combining states and the integration is over the nuclear co-ordinates. Each combining electronic state contains its own unique set of ortho-normal vibrational wavefunctions.

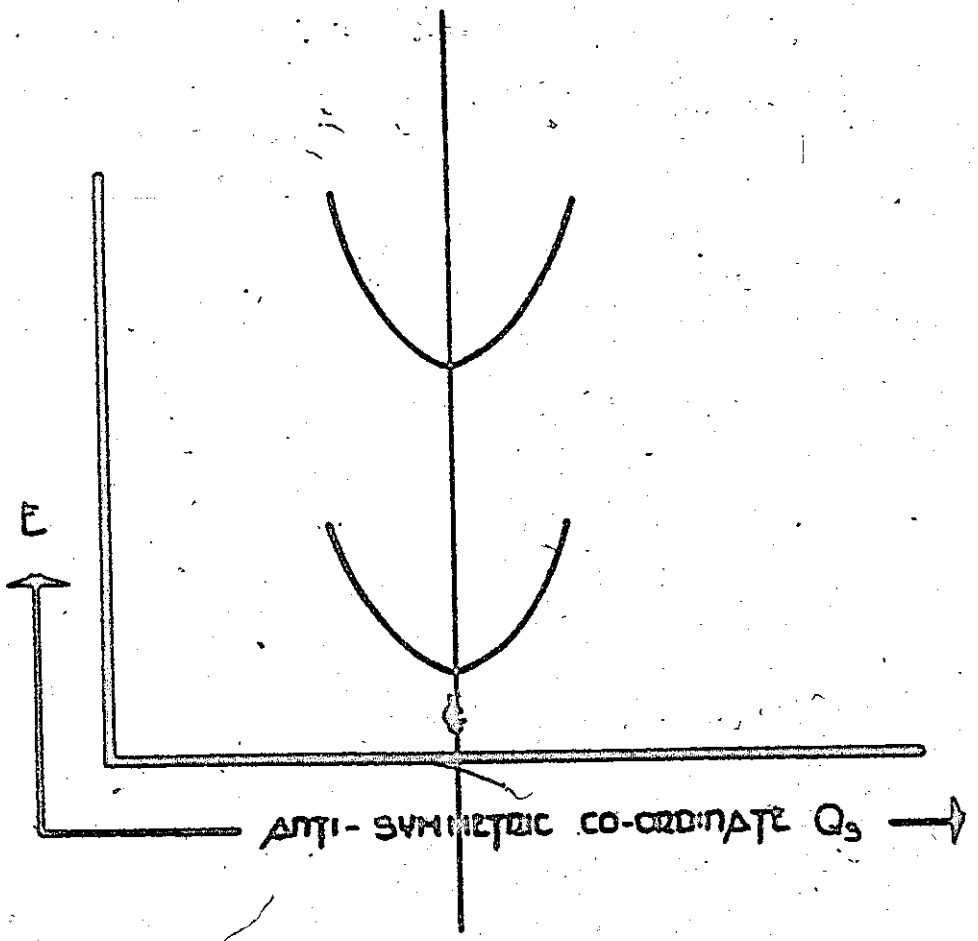

FIGURE 3.4 PLOT OF POTENTIAL ENERGY VERSES THE ANTISYMMETRIC NORMAL CO-ORDINATE Q_3 FOR TWO COMBINING ELECTRONIC STATES. SINCE THE SYMMETRY MUST, ACCORDING TO THE FRANCK-CONDON PRINCIPLE BE THE SAME IN BOTH STATES, THE POTENTIAL WELLS ALONG Q_3 MUST DIRECTLY BE ONE ABOVE ONE ANOTHER.

In a symmetric triatomic molecule such as SeO_2, the only asymmetric vibration is ν_3, the antisymmetrical stretching frequency. Therefore, for an electronic transition in SeO_2 involving ν_3, in the limit that $\nu_3' = \nu_3''$, then the complete set of vibrational wavefunctions in both combining states are identical and transitions between levels whose vibrational quantum numbers differ, are forbidden by the orthogonality of the wavefunctions. Small differences in ν_3' and ν_3'' remove the orthogonality and transitions to higher vibronic levels may occur, but will be weak.

In the present analysis of the D system of selenium dioxide the intensity ratio of the 0—0 band to the 3_0^2 band is approximately 0.2, or the 3_0^2 band is five times stronger than the 0—0 band. This is inconsistent with the above discussion concerning the expected intensity of the 3_0^2 band. There are two ways in which the 3_0^2 band can acquire intensity. Since the above arguments are based on the assumption of purely harmonic vibrations, therefore the inclusion of cubic and quartic terms in the potential energy render the vibrations anharmonic and the above arguments are no longer true.

Coon and his co-workers[36,61] have suggested the possibility of the existence of a double-minimum potential in the anti-symmetrical vibrational co-ordinate of an excited state of CsO_2 as a possible explanation for the abnormally high intensity of the 3_0^2 band in the CsO_2 spectrum. There is also strong evidence for the existence of a double-minimum in the antisymmetric co-ordinate of the 2348 Å transition of SO_2 [37,62,63], as well as the 2491 Å band system of the ND molecule[38]. The present work indicates strong evidence* for a double-minimum potential in the Q_3' co-ordinate of the 3125 Å system of SeO_2. It

*The experimental observation of the 3_0^1 vibronic band (transition from the vibrationless level of the ground state to the 0$^-$ level of Q_3' in the excited state) appears to be at present the only existing experimental evidence for the presence of a double-minimum potential in the antisymmetric stretching co-ordinate of a symmetric bent AB_2 type molecule.

appears as if there may be some common mechanism among seventeen, eighteen and nineteen electron bent symmetric triatomic molecules through which the 3_0^2 transition gains intensity. Mulliken[64] has suggested that a double-minimum potential might occur if an electron occupies a $2b_1$ molecular orbital. The antibonding effect of this orbital is expected to be smaller for an unsymmetrical structure than for a symmetric one.

It will now be shown how, in the present analysis, the assumption of a double-minimum potential in the excited state asymmetric vibrational co-ordinate Q_3', accounts for the four as yet unexplainable sequence bands mentioned above, as well as the abnormally high intensity of the $2\nu_3'$ transition.

3.11. A Double-Minimum In the Excited State Asymmetric Stretching Co-ordinate of SeO_2

As a result of the abnormally high intensity of the 3_0^2 band, which could not be explained in terms of a harmonic potential in Q_3', it has been necessary to assume that there is a double-minimum potential with respect to the anti-symmetric stretching co-ordinates of the excited state. J. B. Coon[35] has constructed a three parameter double-minimum potential function in a convenient form for general application, and tabulated the energy levels. The methods outlined by Coon have been applied in the present analysis to the SeO_2 molecule.

The double-minimum potential function used is of the form

$$V(Q) = \frac{1}{2}\lambda Q^2 + Q \exp(-a^2Q^2) \quad , \qquad (3.11)$$

where Q is a mass-weighted co-ordinate defined by $2T = \dot{Q}^2$. In order to apply the method outlined by Coon[35], it is necessary to experimentally determine at least three levels in the progression involving the asymmetric vibration. In the present calculation the frequency intervals between 0_0^0 (0^+), 3_0^1 (0^-) and

3_0^2 (1^+) bands were used.

The $3\nu_3'$ vibronic band is also observed and is a false origin for a totally symmetric progression involving ν_1'. The $4\nu_3'$ vibronic band is not observed; however, the higher members in the progression $3_0^b 1_0^n$ are observed. The lower members of both the $3_0^3 1_0^n$ and $3_0^b 1_0^n$ progressions are expected to be weak due to a small Franck-Condon factor. In addition these bands lie in the same region as many of the intense members of the strong 1_0^n, $1_0^n 2_0^1$ and $1_0^n 2_0^2$ progressions. The intense bands in these progressions are probably mainly responsible for the lower members of the $3_0^3 1_0^n$ and $3_0^4 1_0^n$ progressions not being observed in the spectrum. Extrapolation of the higher members in the $3_0^4 1_0^n$ progression to the origin (3_0^b), further allowed the $4\nu_3'$ band position to be determined. The extrapolated value for the $4\nu_3'$ (2^+) interval is 3084 cm^{-1} with the $4\nu_3'$ vibronic band lying approximately at $0_0^0 + 3084 = 35039$ cm^{-1}. The actual calculations and a fuller description of the double-minimum parameters are given in Appendix II of the thesis. Only a brief summary of the results will be given here.

The 0_0^0, 3_0^1, 3_0^2, 3_0^3 and 3_0^b vibronic bands appear in the spectrum of the $Se^{78}O_2^{16}$ molecule at 31955.0 cm^{-1}, 32033 cm^{-1}, 33327 cm^{-1}, 34026.5 cm^{-1} and 35039 cm^{-1} (estimated) respectively. The interval $\nu_3' = G(0^-) - G(0^+)$ is 78.9 cm^{-1} while the $2\nu_3' = G(1^+) - G(0^+)$ interval is observed to be 1372 cm^{-1}. The $3\nu_3' = G(1^-) - G(0^+)$ is observed as 2071.5 cm^{-1} and the extrapolated value of $4\nu_3' = 3084$ cm^{-1}. The interval $4\nu_3' - 2\nu_3' = G(2^+) - G(1^+)$ is calculated to be 1712 cm^{-1}.

The energy levels for the first four levels of the double-minimum well have been calculated for $\rho = 0.6$, 0.9, 1.2 and 1.5 for the isotopic molecules $Se^{70}O_2^{16}$, $Se^{70}O_2^{18}$ and $Se^{80}O_2^{16}$ and are tabulated in Table 3.3. The corresponding B values and barrier heights are given in Table 3.4. The parameter ρ determines

the shape of the potential function. For low ρ values the outer walls of the potential rise more steeply than the walls of the barrier. For $\rho = 1.5$ the minima are parabolic, while for larger values of ρ the walls of the barrier rise more steeply than the outer walls of the potential. In the present application to the excited state of SeO_2, $\rho = 0.6$ was found to give the best fit. The effect of the parameter ρ on the shape of the double-minimum potential is shown in Figure 3.5.

The barrier height separating the two minima is calculated to be 1986.5 cm^{-1} for $\rho = 0.6$ and the $(0^+ - 0^-)$ separation is 79.2 cm^{-1}. Coon[61] has calculated the $(0^+ - 0^-)$ interval to be 69 cm^{-1} in CO_2 and 103 cm^{-1} in the 2491 Å absorbtion system of the NO_2 molecule[38]. The double-minimum potential in the asymmetric vibrational mode of the $^1B_2$ excited state of SeO_2 is shown in Figure 3.6 for $\rho = 0.6$.

The calculated and observed energy levels of the double-minimum well along Q_3' appears to be best for $\rho = 0.6$. The calculated value for the $3\nu_3'$ (1^-) level of 2063.6 cm^{-1} is in excellent agreement with the observed value of 2071.5 cm^{-1}. The calculated value for $4\nu_3'$ (2^+) is poorer. The poorer agreement for the $4\nu_3'$ level may possibly be due to an anharmonicity in the double-minimum well. The potential used by Coon[35] reduces to a harmonic potential for large values of ν_3'; therefore, the calculated level will be in error if any anharmonicity is present. It is difficult to know at what value of ν_3' in the double-minimum well does anharmonicity become important.

The barrier height (B_{ν_0}) and the shape of the potential surface (ρ) are assumed to be invariant to isotopic substitution. Comparison of the barrier height in all three isotopes for $\rho = 0.6$ shows that the agreement is excellent for $Se^{78}O_2^{16}$ and $Se^{80}O_2^{16}$ and within 5% for the $Se^{78}O_2^{18}$ isotope. While the interconversion from one structure to another primarily occurs

Table 3.3

Calculated Energy Levels of the Double-Minimum Potential Well for the Asymmetric Stretching Co-ordinate Q_3' of the $^1B_2$ Excited State of $Se^{78}O_2^{16}$, $Se^{78}O_2^{18}$ and $Se^{80}O_2^{16}$ in cm^{-1} for the Shape Parameter $\rho = 0.6, 0.9, 1.2$ and 1.5

Selenium Isotope	v_i	ρ 0.6	0.9	1.2	1.5	Observed
$Se^{78}O_2^{16}$	0 (0^+)	0.0	0.0	0.0	0.0	0.0
	1 (0^-)	79.2	78.85	77.4	79.13	78.9
	2 (1^+)	1372.3	1372.2	1372.6	1372.6	1372.6
	3 (1^-)	2063.6	2013.4	1962.2	1905.6	2071.5
	4 (2^+)	3177.2	3084.8	2993.8	2898.84	3084.0*
$Se^{80}O_2^{16}$	0 (0^+)	0.0	0.0	0.0	0.0	0.0
	1 (0^-)	78.4	80.99	82.8	78.23	77.9
	2 (1^+)	1368.5	1368.2	1368.7	1368.7	1368.5
	3 (1^-)	2062.9	2046.9	1954.1	1897.9	2067.2
	4 (2^+)	3163.5	3137.8	2981.1	2887.7	3080.0*
$Se^{78}O_2^{18}$	0 (0^+)	0.0	0.0	0.0	0.0	0.0
	1 (0^-)	78.5	79.06	82.77	69.56	78.5
	2 (1^+)	1309.52	1309.55	1309.55	1318.74	1309.52
	3 (1^-)	1978.5	1933.29	1881.86	1827.96	1938.27
	4 (2^+)	3046.45	2960.58	2868.58	2777.96	2905.0*

*$4\nu_3'$ (2^+) is estimated from extrapolation of $S_0^1D_0^1$ progression.

Table 3.4

Calculated B Values and Barrier Heights B_{ν_o} (cm^{-1})

for the Asymmetric Stretching Co-ordinate Q_3' of the $^1B_2$ Excited State

of $Se^{78}O_2^{16}$, $Se^{78}O_2^{18}$ and $Se^{80}O_2^{16}$ for the Shape Parameter

ρ = 0.6, 0.9, 1.2 and 1.5

Selenium Isotope	ρ	0.6	0.9	1.2	1.5
$Se^{78}O_2^{16}$	B	1.0637	1.3557	1.6305	1.9094
	ν_o	1867.6	1402.3	1252.94	1099.68
	B_{ν_o}	1986.57	2009.55	2042.91	2099.72
$Se^{80}O_2^{16}$	B	1.0663	1.35906	1.6346	1.9142
	ν_o	1861.67	1494.38	1248.86	1095.98
	B_{ν_o}	1985.1	2030.95	2041.38	2097.93
$Se^{78}O_2^{18}$	B	1.05309	1.34075	1.6135	1.8875
	ν_o	1784.57	1416.95	1197.73	1051.3
	B_{ν_o}	1879.1	1899.77	1932.53	1984.3

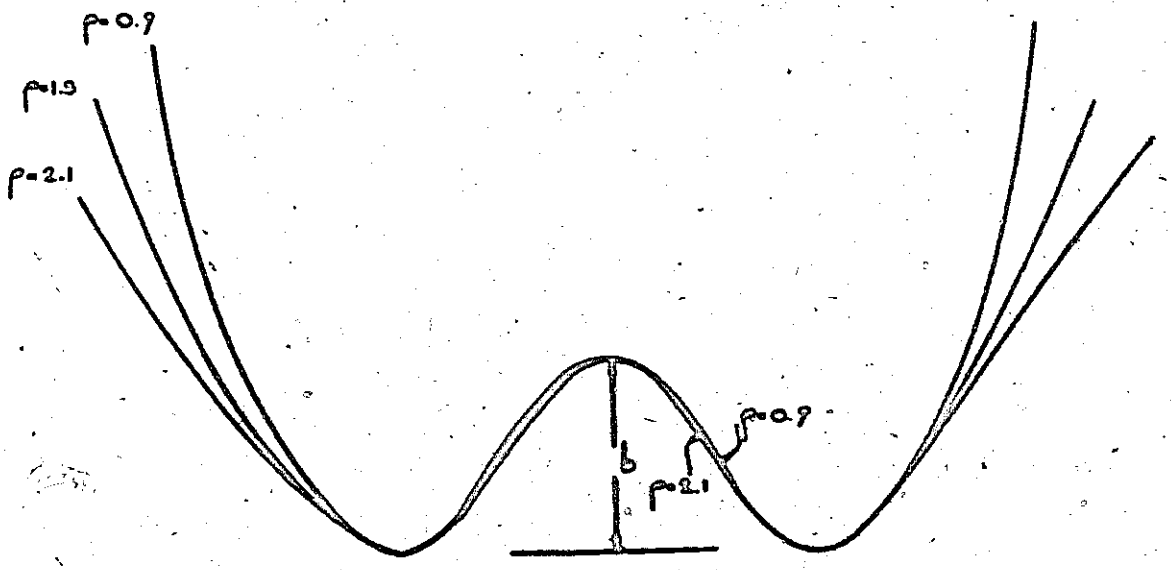

FIGURE 9.5 THE EFFECT OF THE PARAMETER ρ ON THE SHAPE OF THE DOUBLE-MINIMUM POTENTIAL, AFTER COOP. FOR ρ=1.9 THE MINIMA ARE PARABOLIC.

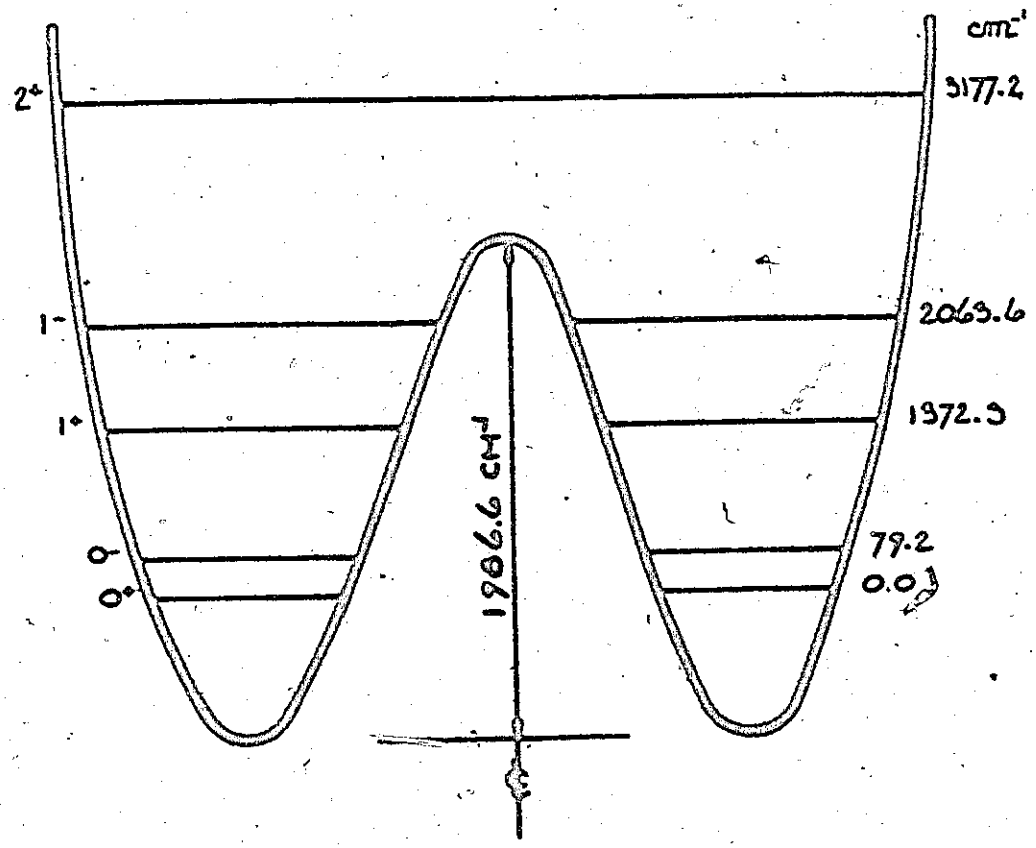

FIGURE 3.6 THE DOUBLE MINIMUM - POTENTIAL IN THE ANTISYMMETRIC STRETCHING CO-ORDINATE OF THE $^1B_2$ EXCITED STATE OF $Se^{70}O_2^{16}$. THE VALUE OF $\zeta(0^+)$ = 897 CM^{-1}. AND THE BARRIER HEIGHT IS 1906.6 CM^{-1}.

along Q_3' there are small changes along Q_1' and Q_2' as well. Small differences in the barrier height are therefore expected since the normal co-ordinates are slightly different for all three isotopes and may be involved to different extents in each isotope in the motion which converts one isodynamic structure of selenium dioxide into the other.

The selenium dioxide molecule is the first molecule in which it has been possible to experimentally observe transitions to the 3_0^1 (0^-) and 3_0^3 (1^-) levels. It is felt that this observation is strong evidence for the existence of a double-minimum potential in the Q_3' co-ordinate of SeO_2. The 78 cm^{-1} interval between the 1_2^0 - $1_2^0 3_0^1$ and 1_3^0 - $1_3^0 3_0^1$ bands of the $Se^{78}O_2^{16}$ molecule is shown in Figure 3.7.

Both the 3_0^1 and 3_0^3 vibronic bands have a noticeably different band profile from all other bands in the spectrum. The transition to the level $\nu_3' = 1$ originating on the four levels 0_0^0, 1_1^0, 1_2^0 and 1_3^0 in all cases show a very sharp line-like head which is the most prominent feature of the band. The sub-band structure (K-structure) is very irregular and it is difficult to unambiguously assign the various sub-bands. This is in direct contrast to all of the other bands in the spectrum where the quadratic nature of the sub-bands is quite distinct, and as many as fifteen sub-bands can be easily assigned. The rotational structure of the $1_0^2 3_0^1$ vibronic band is discussed in detail in Chapter Four.

The 3_0^3 vibronic band is also quite different in band profile to the other vibronic bands in the spectrum. The band contains fewer sub-bands and unlike all of the other bands in the spectrum which are strongly red degraded, the 3_0^3 vibronic band lacks a head.

The 3_0^3 and $3_0^2 1_0^1$ bands are expected to be almost co-incident. Due to the extended Franck-Condon maximum in the excited state ν_1' progression (sixth

member), the $3_0^2 1_0^1$ band is not likely to be observed and the observed headless band is probably the pure 3_0^3 band.

Since the 3_0^3 band is expected to be a B-type band whereas the $3_0^2 1_0^1$ band is A-type, then no Fermi resonance can occur between the upper levels of those transitions, and the headless feature of the 3_0^3 band cannot be attributed to a Fermi resonance since both levels must be of the same symmetry for such a perturbation to occur.

The band profile could however be altered due to a Coriolis-type perturbation involving the 3_0^3 and the $3_0^2 1_0^1$ levels. The selection rule for Coriolis-type perturbations between vibronic levels has been given by Jahn[70]. An interaction can occur only if the direct product for the irreducible representations to which the two vibrational wavefunctions belong transform, or has a component that transforms like a rotation. Since the direct product

$$\Gamma 3_0^3 \times \Gamma 3_0^2 1_0^1 = B_2 \times A_1 = B_2 \qquad (3.12)$$

then a Coriolis perturbation can occur between these levels as a result of rotation about the c-axis of the molecule, perpendicular to the molecular plane. It is difficult to know to what extent Coriolis perturbations have altered the rotational structure of the 3_0^3 vibronic band. It is doubtful that the Coriolis perturbation alone is responsible for the headless feature of the band.

The asymmetric stretching vibration of ScO_2 is an in-plane vibration of B_2 symmetry and therefore odd quanta of this vibration are forbidden in the zeroth order Born-Oppenheimer approximation and should not appear in the spectrum. The 3_0^1 (ν_3') and 3_0^3 ($3\nu_3'$) bands however appear in the spectrum and are reasonably strong bands.

The antisymmetric stretching co-ordinate of the excited $^1B_2$ electronic

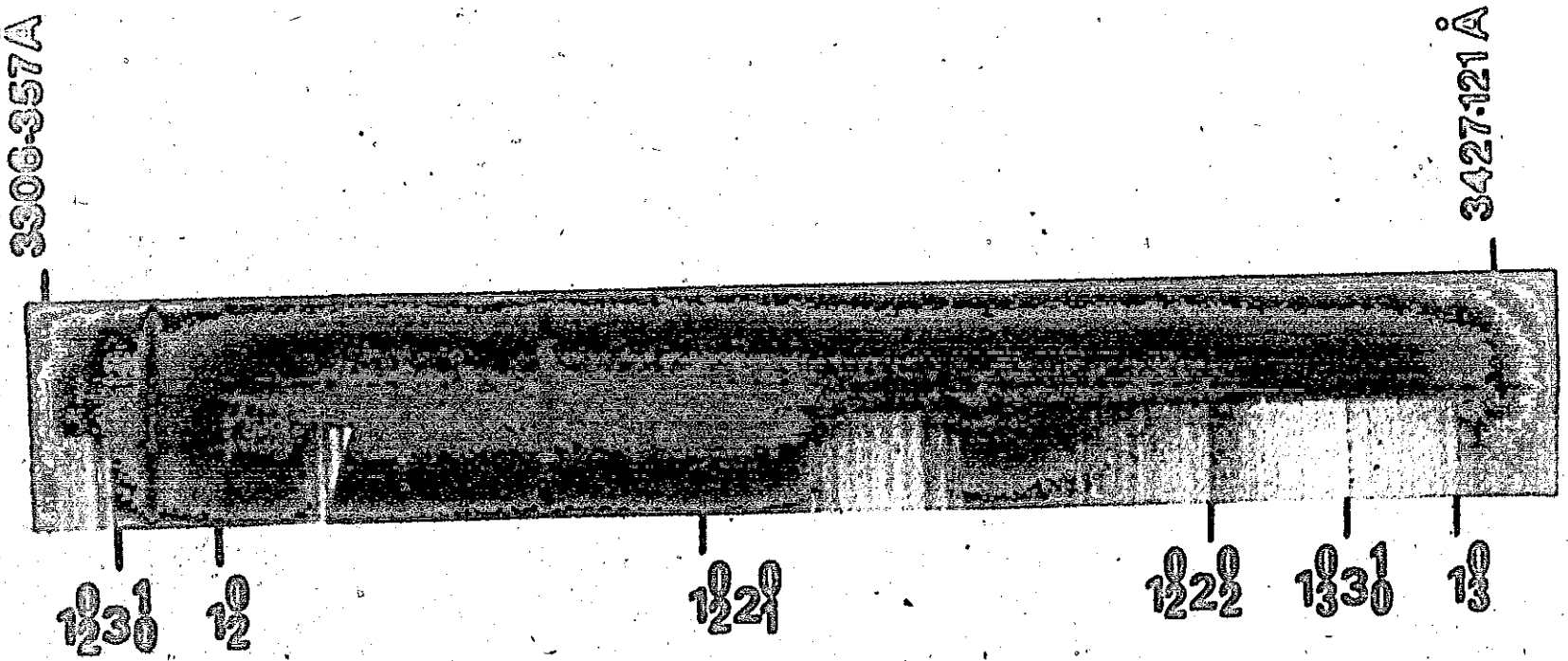

Figure 3·7

2nd order Bausch & Lomb photograph of the 1_2^0 and 1_3^0 bands of $Se^{78}O_2^{16}$ showing the $1_2^0 3_0^1$ and $1_3^0 3_0^1$ bands 78cm^{-1} to the blue. The $1_2^0 2_1^1$ and $1_2^0 2_2^2$ vibronic bands are also shown.

state is believed to have a double-minimum potential well, the barrier to inversion being $\sim 2000\ cm^{-1}$ ($\rho = 0.6$). The $\nu_3' = 1$ (0^-) level is very close to the bottom of the well ($78\ cm^{-1}$) and therefore when the SeO_2 molecule is in this vibronic level it will tunnel from one asymmetric structure to the other with only low probability. In fact, when the molecule is in the 3_0^1 (0^-) vibronic level, it effectively has an equilibrium asymmetric structure with one bond length longer than the other. The symmetry of the molecule is therefore reduced from C_{2v} to C_s. Under C_s symmetry both the A_1 and B_2 vibrations become A' and transitions from the vibrationless level in the ground state to the 0^+ and 0^- levels of Q_3' in the excited state are allowed and expected to have comparable intensity. Transitions to both the 0^+ and 0^- levels of the excited state are experimentally observed with almost identical intensity.

The 3_0^1 vibronic band is also allowed under C_{2v} symmetry when in a higher approximation it is considered how nuclear displacements affect the interactions between electronic states. Herzberg and Teller[17] have shown that when vibronic coupling is important the electronic and vibrational motions cannot be considered independent and the vibronic transition moment which now must be non-zero takes the form

$$\langle \phi'(r,Q)\phi'(Q) | \hat{r} | \phi''(r,Q)\phi''(Q) \rangle \neq 0 \qquad (3.13)$$

where the product $\phi(r,Q)\phi(Q)$ is the vibronic wave function and r and Q are the electronic and nuclear co-ordinates respectively. $\hat{r}$ is the electric dipole operator.

In order for the integral of Equation (3.13) to be non-zero, the following direct product must be totally symmetric

$$\Gamma\phi'\phi' \times \Gamma r \times \Gamma\phi''\phi'' = \Gamma A_1 \qquad (3.14)$$

Since the ground state is totally symmetric and the excited state has been shown to be electronically of B_2 symmetry,* then (3.14) becomes

$$B_2 \times B_2 \times \Gamma r \times A_1 \times A_1 = A_1 \qquad (3.15)$$

and Equation (3.15) will be non-zero if there is a component of the dipole operator $\vec{r}$ which transforms as A_1. Since the component of $\vec{r}$ along the b-axis passing through the selenium atom is of A_1 symmetry, then Equation (3.15) is non-zero and the 3_0^1 transition is therefore vibronically allowed; the intensity is said to be "stolen" or "borrowed" from an allowed $^1A_1 \leftarrow {}^1A_1X$ electronic transition with the 3_0^1 band then having the polarization of the transition from which the intensity derives. Therefore the 3_0^1 band is expected to be a perpendicular type-B band in C_{2v} symmetry approximation.

If the intensity derives from a change in selection rules resulting from a reduction in symmetry ($C_{2v} \rightarrow C_s$) rather than through a vibronic mechanism, then the 3_0^1 band is expected to be an A-B hybrid type band consisting of a superposition of a parallel type-A and perpendicular type-B band. The intensity of each band type will be determined by the direction of the electric dipole with respect to the a and b axes of the molecule. The rotational structure of the 3_0^1 band will be discussed later in Chapter Four.

The 3_0^3 (1^-) level lies above the barrier to inversion and therefore when the molecule is in the 3_0^3 vibronic level it can classically move freely from one asymmetric structure to the other. The equilibrium structure is symmetric and the electronic and vibrational wave functions must be classified under C_{2v} symmetry. The only mechanism by which the 3_0^3 band can then acquire intensity is the vibronic one, and the band is expected to be B-type. All

*A rotational analysis of the 1_0^3 vibronic band has shown this band to be A-type and therefore the excited electronic state to be of B_2 symmetry.

that can be said with regards to the experimentally observed 3_0^3 band is that it is headless and in no way resembles the band profile of A-type bands which have a head and are strongly red degraded. If the intensity of the 3_0^3 transition is borrowed from another allowed electronic transition, then one might expect to see an intensity alternation between the even and odd numbers of the 3_0^n progression. This is not apparent and is perhaps due to overlap with adjacent bands.

The interval of 78 cm^{-1} which has been assigned to the (0^+-0^-) splitting was also tried as an assignment for the (0^+-1^+) splitting, it being concurrently assumed that the (0^+-0^-) splitting was too small to be resolved experimentally. The above assumption results in an extremely high barrier (a consequence of the small (0^+-0^-) splitting). An extremely high barrier height would be inconsistent with the observed spectrum since the perturbation is obvious, as manifested in the abnormally high intensity of the 3_0^2 and 3_0^8 vibronic bands. For this reason the assignment of the 78 cm^{-1} interval to the (0^+-1^+) splitting was rejected.

The presence of a double minimum potential, with the relatively low barrier height of 2000 cm^{-1} in the asymmetric stretching vibrational coordinate of the excited state of SeO_2 suggests that the molecule is non-rigid in the excited state and as such should be classified according to a non-rigid point group. A brief discussion of isodynamic operations, and the Schrodinger super group with respect to SeO_2 is given below. For an excellent account of non-rigid point groups, the reader is referred to articles by Altman[65] and Longuet-Higgins[66] where the basic principles are presented and applied to several non-rigid molecules.

3.12. Non-Rigid Molecules, Point Groups and the Schrodinger Supergroup.

Non-rigid molecules are those for which there are several equilibrium

configurations that cannot be transformed one into another by a Schrodinger group operation (reflection or rotation) but have, nevertheless, identical energies. Such configurations are called isodynamic configurations, and the operations that transform one isodynamic structure into another are called isodynamic operations[65]. They are not symmetry operations, but rather motions (translations or rotations) of an atom or group of atoms with respect to the rest of the molecule. Isodynamic operations involve the displacement of material points, and are denoted by a superscript I added to the conventional symmetry operations.

The symmetry groups of non-rigid molecules possess, therefore, two subgroups: one is that of all the symmetry operations of the Schrodinger group (rotations and reflections) and the other is the Isodynamic group, containing all of the isodynamic operations belonging to the molecule.

Therefore for non-rigid molecules the familiar interpretation of symmetry operations breaks down and an entirely new system of operations is necessary. They are constructed as follows[65]: E, E* and P are respectively the identity operation, the inversion of all particle positions and a permutation of the position and spins of identical nuclei. P* is the product E*P = PE*. Any of these operations is feasible when it can be achieved without passing over an insurmountable energy barrier. The molecular symmetry group is then the set of: all feasible P (including E), and all feasible P*.

The two isodynamic structures of ScO_2 of importance in the present analysis result from the asymmetric vibrational motion of the molecule in the $^1B_2$ excited state, and are shown in Figure 3.8.

The two isodynamic structures in Figure 3.8 occur in the ScO_2 molecule as a result of the asymmetric vibrational motion shown below in Figure 3.9.

In going from structure (a) to (b) in Figure 3.8, the Sc atom moves

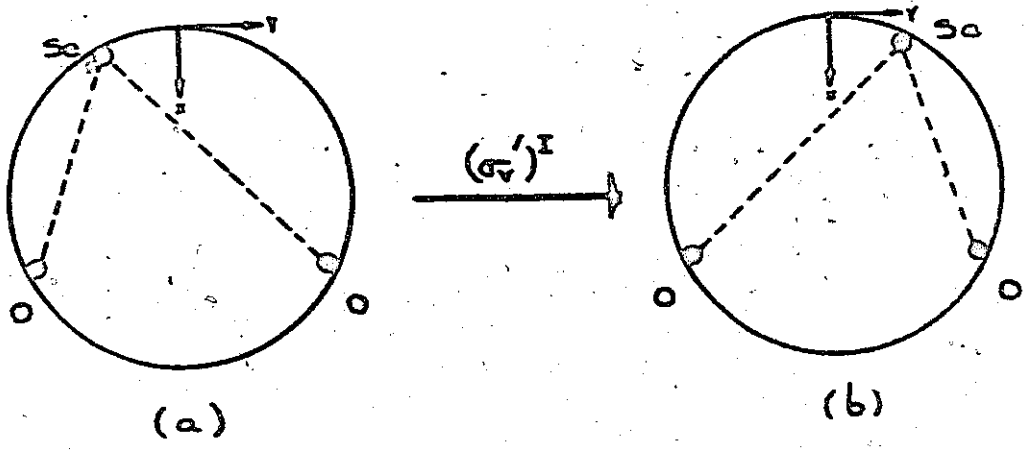

FIGURE 9.8 THE ISODYNAMIC OPERATION $(\sigma_v')^x$, WHICH IS A DISPLACEMENT OF THE Se ATOM PERPENDICULARLY TO THE x y PLANE, INTO ITS REFLECTED POSITION WITH RESPECT TO IT. THE y AXIS IS DIRECTED PERPENDICULAR TO THE PLANE OF THE PAPER. (AFTER ALTMANN[69])

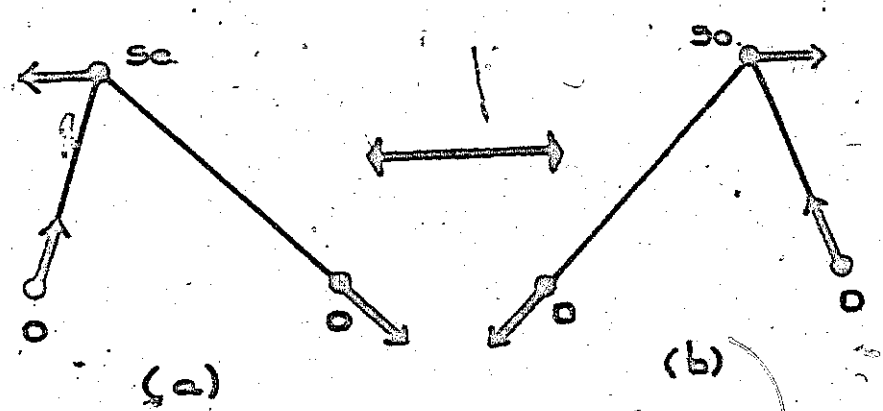

FIGURE 9.9 ASYMMETRICAL VIBRATIONAL MOTION OF SeO_2.

across a potential well with a minimum where it crosses the x axis. The splitting of the levels in the double-minimum potential well depends on the magnitude of the perturbation matrix element $\int \phi_a H' \phi_b d\tau$ where the perturbation term H' is small if the depth of the well is large. An alternate way of viewing the perturbation is in terms of the barrier height separating the two isodynamic structures. The lower the barrier height the stronger the perturbation and consequently the greater will be the splitting of the levels in the well. The isodynamic operation $(\sigma_v')^I$ may be thought therefore as a tunnelling through the potential barrier separating the two configurations of Figure 3.8.

3.13. Quasilinear Molecules

Quasilinearity has been treated theoretically by Thorson and Nakagawa[67] in an explanation of the infrared spectrum of disiloxane and in triatomic molecules by Dixon[68] and Johns[69]. The mathematical treatment of these authors involves the solution of the two-dimensional harmonic oscillator which is perturbed by a potential hump. The effect of the perturbation is that, for the lower vibrational levels, the molecule is stable in the bent conformation while in the higher vibrational levels the molecule is stable in the linear conformation. Both Johns and Dixon considered only the vibrational motion involving ν_2 in a quasilinear electronic state. Quasilinearity as described above is then only important in linear to bent or bent to linear transitions involving long progressions of the upper state bending frequency ν_2'.

In the present analysis of the ScO_2 molecule, the prominent frequency in the spectrum is the upper state symmetric stretching frequency while ν_2' appears only in combination with ν_1' and ν_3'. However, the molecule becomes more bent in the excited state° at equilibrium, with a bond angle of $2\alpha = 101°$ as

---

°Present rotational analysis of the 1_0^3 vibronic band.

compared to be value of $2\alpha = 113.8°$ observed in the ground state[57]. For this reason quasilinearity was not considered important in the present work.

3.14. Summary of Gross Features in Vibrational Analysis of B System

The missing piece to the puzzle in the present analysis was the assignment of the 32033.8 cm^{-1} band to the 3_0^1 transition. The observed intensities of both the 0_0^0 and 3_0^1 band are about the same, as is expected since in C_s symmetry (equilibrium symmetry of the excited state in this vibronic level), both the 0_0^0 and 3_0^1 (0^-) levels are of A' symmetry and thus transitions from the vibrationless level of the ground state are electronically allowed to each of these vibronic levels of the excited state. Transitions from ground state v_1'' levels to v_3' levels of the excited state are shown in Figure 3.10. The vibrational and vibronic symmetry of the levels is also shown.

Progressions in both the excited state symmetric and antisymmetric stretching frequencies appear in the spectrum. The longest progressions involve v_1' and contain as many as thirteen members. A progression of four members involving v_3' is observed. The anomalous intensity of the higher members in the v_3' progression results from the presence of a double-minimum potential well along Q_3'. The excited state bending frequency v_2' appears in the spectrum only in combination with v_1' and v_3'. There was considered, however, an alternate assignment to the one presented in the present analysis which involves the assignment of a v_2' progression containing six members. Both assignments will be discussed briefly.

In the present analysis $v_1' = 660$ cm^{-1} and $v_2' = 260$ cm^{-1} while $v_1'' = 923$ cm^{-1}. Therefore, on the basis of an observed 260 cm^{-1} interval between successive bands, it is very difficult to distinguish between a nv_2'

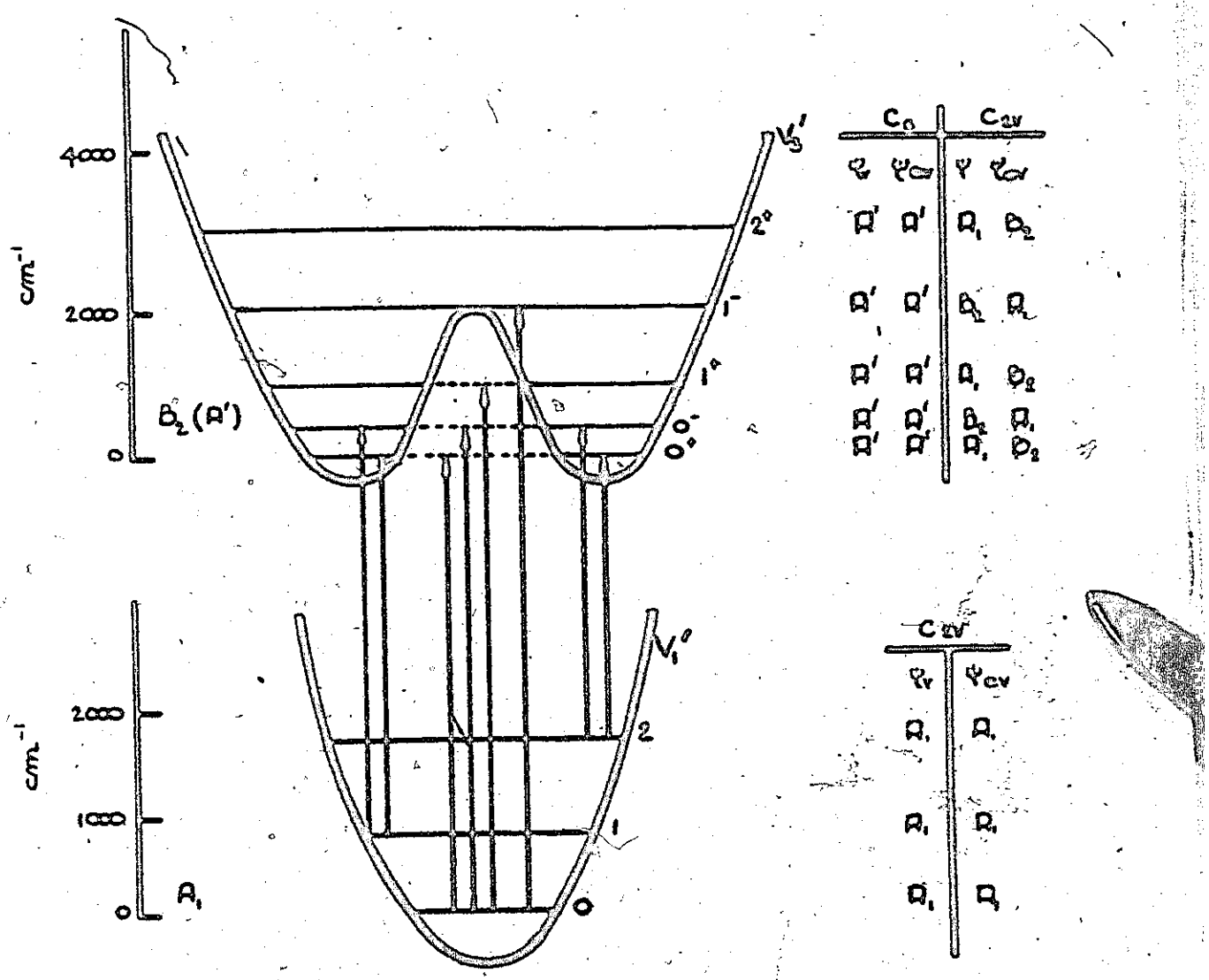

FIGURE 3.10 TRANSITIONS FROM THE GROUND STATE TOTALLY SYMMETRIC VIBRATIONAL LEVELS v_1^0 TO THE EXCITED STATE ASYMMETRIC VIBRATIONAL LEVELS v_3'. THE TRANSITIONS SHOWN ARE OBSERVED EXPERIMENTALLY.

progression and a group of sequence bands of the type 1_n^n = n(923-660) = n260.

In the spectrum of the $So^{78}O_2^{16}$ isotope, eight vibronic bands are observed with the energies shown below. The two possible assignments considered are also shown.

Position	Δ	Assignment 1	Assignment 2
33594.5 cm^{-1}		$3_0^2 2_0^1$	$2_0^6 3_0^1$
	267 cm^{-1}		
33327.6 cm^{-1}		3_0^2	$2_0^5 3_0^1$
	261.4 cm^{-1}		
33066.2 cm^{-1}		$3_0^2 1_1^1$	$2_0^4 3_0^1$
	264.9 cm^{-1}		
32801.3 cm^{-1}		$3_0^2 1_2^2$	$2_0^3 3_0^1$
	262.1 cm^{-1}		
32539.2 cm^{-1}		$3_0^2 1_3^3$	$2_0^2 3_0^1$
	262.1 cm^{-1}		
32277.1 cm^{-1}		$3_0^2 1_4^4$	$2_0^1 3_0^1$
	243.2 cm^{-1}		
32033.9 cm^{-1}		3_0^1	3_0^1
	78.9 cm^{-1}		
31955.0 cm^{-1}		0_0^0	0_0^0

Assignment Two above has the following serious difficulty. The higher members in the ν_2' progression show a reasonably constant interval of approximately 262 cm^{-1}. However the interval between the 2_0^1 and the 0_0^0 band is not 262 cm^{-1} but rather 322 cm^{-1}. To account for this abnormally high interval it could be postulated that perhaps the above progression in ν_2' was in fact a progression in combination with one quanta of ν_3', i.e., $2_0^n 3_0^1$, n = 0,1,...,6. However, the interval between the origin band and the $2_0^1 3_0^1$ band is not 262 + 78 = 340 cm^{-1} but only 322 cm^{-1}. The barrier height to inversion along Q_3' between the two asymmetric structures is expected to be a function of the bond angle 2α, and consequently the $(0^+ - 0^-)$ splitting is a function of the bond angle. The hypothesis was then made that in fact the interval of 322 cm^{-1} could be associated with the combination band $2_0^1 3_0^1$ = 262 + 60 = 322 cm^{-1}. The interaction between Q_2' and Q_3' was considered responsible for reducing the

(0^+-0^-) splitting in Q' from 78 cm^{-1} to 60 cm^{-1}. If in fact this hypothesis is correct, then a very serious problem results. Why does the (0^+-0^-) interval remain constant when additional quanta of ν_2' are excited? Since excitation of successive quanta of ν_2' increases the angular displacement of the oxygen atoms, it seems unreasonable to assume that Q_3' should be sensitive to the first quantum of ν_2' excited yet almost completely insensitive to excitation of additional quanta of ν_2'. For this reason Assignment Two was discarded.

Assignment One removes the above problem. The band located at 33327.6 cm^{-1} is assigned to the 3_0^2 transition. This assignment is also strongly suggested by the fact that there is a strong ν_1' progression which extrapolates to this band as a false origin, i.e., $3_0^2 1_0^n$ progression. It is otherwise impossible to satisfactorily assign a false origin for this progression. The vibronic band located at 33594.5 is then easily assigned as $3_0^2 2_0^1$.

The four bands to the red of the 3_0^2 band located at 33066.2 cm^{-1}, 32801.3 cm^{-1}, 32539.2 cm^{-1} and 32277.1 cm^{-1} are assigned to the four sequence bands $3_0^2 1_1^1$, $3_0^2 1_2^2$, $3_0^2 1_3^3$ and $3_0^2 1_4^4$ respectively. This seems a reasonable assignment since ν_1 is by far the most active frequency in both the hot and the cold spectrum. In addition the three sequence bands 1_1^1, 1_2^2 and 1_3^3 appear strongly in the spectrum. The 1_4^4 band may appear weakly but lies in a region that is both weak and strongly overlapped by the So_2 spectrum.

The 3_0^4 transition is not observed but is thought to occur around 35039 cm^{-1} from extrapolation of the $1_0^n 3_0^4$ progression to its origin. It was not possible to observe the 3_0^5, 3_0^6 or higher members in the ν_3' progression. This is probably a result of the intense members of the 1_0^n, $1_0^n 2_0^1$ and $1_0^n 2_0^2$ progression which fall in the same region as where the 3_0^5 and 3_0^6 bands are expected to appear.

The $^1D_2 \leftarrow {}^1A_1\bar{X}$ electronic transition extends from approximately 29000

cm^{-1} to 45000 cm^{-1}, the origin for the transition occurring at 31955 cm^{-1}. The bands in the region of the origin band are weak and badly overlapped. Vibronic bands appearing in the region 35500 cm^{-1} to 33900 cm^{-1} are sharp and red degraded. The sub-bands (K-structure) are sharp and distinct.

Bands to the blue of 35500 cm^{-1} become progressively more diffuse with the distinct rotational fine structure now becoming smeared and the individual sub-bands no longer distinguishable. It appears as if the $^1B_2$ excited state of SeO_2 is being predissociated in the region to the blue of 36000 cm^{-1} by another electronic state. It is also possible that the $^1B_2$ electronic state is itself becoming dissociative to the blue of 36000 cm^{-1} thus accounting for the diffuse bands in this region.

The most striking features of the hot spectrum (to the red of the origin band) are the sets of paired sequence bands 1_1^0, $1_1^0 3_0^1$; 1_2^0, $1_2^0 3_0^1$; and 1_3^0, $1_3^0 3_0^1$. The intensity of members in the same set are about equal. Two quanta of the ground state bending vibration $\nu_2'' = 372$ cm^{-1} are also observed in the hot spectrum and originate on the 0_0^0, 1_1^0, 1_2^0 and 1_3^0 vibronic levels. Regions of the hot band spectrum are weak and badly overlapped due to the co-incidal overlap of these bands with members of excited state ν_1' progression originating on the 1_1^0, 1_2^0 and 1_3^0 vibronic levels.

3.15. Fluctuations in Excited State ν_1' Progressions

The most prominent frequency in the spectrum is the excited state totally symmetric stretching frequency $\nu_1' = 660$ cm^{-1} and appears most strongly in the three progressions 1_0^n, $1_0^n 2_0^1$ and $1_0^n 2_0^2$. The ν_1' interval of 660 cm^{-1} appears to randomly fluctuate ± 10 cm^{-1} in all three progressions.

Since $\nu_1' = 660$ cm^{-1}, $\nu_2' = 260$ cm^{-1} and $\nu_1'' = 928$ cm^{-1}, therefore $\nu_1' + \nu_2' = \nu_1''$ and the nth member of the 1_0^n progression can be in Fermi resonance

with the (n + 1)th member of the $1_1^n 2_0^1$ progression. Similarly the nth member of the $1_0^n 2_0^1$ progression can interact strongly with the (n + 1)th member of the $1_1^n 2_0^2$ progression. Also the nth member of the 1_0^n progression is expected to fall very close to the (n + 2)th member of the $1_2^n 2_0^2$ progression.

Many of the bands in the 1_0^n, $1_0^n 2_0^1$ and $1_0^n 2_0^2$ progressions appear to be double-headed. The two heads however belong to separate vibronic bands resulting from the coincidental overlap of members in other progressions as a result of the fact that $\nu_1' + \nu_2' \sim \nu_1''$.

The rotational fine structure (K-structure) of all the resolvable bands in the 1_0^n, $1_0^n 2_0^1$ and $1_0^n 2_0^2$ progressions was also measured and the head to origin distance compared. This separation was found to randomly fluctuate. Since it is the frequencies of the heads of the bands which were used in the vibrational analysis, then the small changes (2-3 cm^{-1}) in the head to origin separation might well also be partly responsible for the small fluctuation in the ν_1' interval observed in these progressions.

3.16. An Anomalously Large Frequency Difference

The two vibronic bands located at 35010.3 cm^{-1} and 34306.5 cm^{-1} have a separation of 703.9 cm^{-1} and have been assigned to the 1_1^6 and 1_1^5 transitions. The observed interval is considerably larger than the expected interval of 660 cm^{-1}. The assignment is based on the fact that the earlier members in the 1_1^n progression are also observed but with the correct interval of ~660 cm^{-1}. Since the strongest members in the 1_0^n progression are the 5th and 6th, the two corresponding sequence bands 1_1^5 and 1_1^6 are expected to appear and most probably be the strongest members in the 1_1^n progression. The separation between these two bands is abnormally large in all three isotopic molecules studied and therefore cannot be attributed to a perturbation of the Fermi

resonance type.

Since the intensity of both bands is comparable to that of the intense members in the 1_0^n progression, it is unlikely that they could originate from higher ground state levels than in the present assignment.

An alternate assignment for the 1_1^5 band is $3_0^3 2_0^1$; however, this band would then be expected to be a B-type band. The observed band is unfortunately identical in structure to the 1_0^3 band which rotational band contour analysis has conclusively shown to be A-type. An alternate assignment for these bands consistent with their observed intensity is not obvious.

CHAPTER FOUR

ROTATIONAL ANALYSIS OF SELENIUM DIOXIDE

4.1. Moments of Inertia

The moments of inertia of a rigid molecule about each of the three axes passing through the center of mass are defined by

$$\begin{aligned} I_x &= \sum_i m_i(y_i^2 + z_i^2) \\ I_y &= \sum_i m_i(x_i^2 + z_i^2) \\ I_z &= \sum_i m_i(x_i^2 + z_i^2) \end{aligned} \tag{4.1}$$

where (x_i, y_i, z_i) are the co-ordinates of the ith atom with mass m_i.

If we define the products of inertia by the equations

$$\begin{aligned} I_{xy} &= \sum_i m_i x_i y_i \\ I_{yz} &= \sum_i m_i y_i z_i \\ I_{xz} &= \sum_i m_i x_i z_i \end{aligned} \tag{4.2}$$

with $I_{xy} = I_{yx}$, etc., then the equation

$$I_x X^2 + I_y Y^2 + I_z Z^2 - 2I_{xy}XY - 2I_{yz}YZ - 2I_{xz}ZX = 1 \tag{4.3}$$

represents a quadratic surface, called the momental ellipsoid. The ellipsoid itself has three axes, a, b and c, called the principal axes of the momental ellipsoid. In terms of these axes the ellipsoid is given by

$$I_a a^2 + I_b b^2 + I_c c^2 = 1 \tag{4.4}$$

in which the products of inertia have vanished. The three principal axes are chosen such that the moments of inertia about them have the order of magnitude $I_c > I_b > I_a$.

The moments of inertia in the principal axes system in which the products of inertia are zero are obtained by solving the determinental equation[80]

$$\begin{vmatrix} I_{xx}-\lambda & -I_{xy} & -I_{xz} \\ -I_{xy} & I_{yy}-\lambda & -I_{yz} \\ -I_{xz} & -I_{yz} & I_{zz}-\lambda \end{vmatrix} = 0 \qquad (4.5)$$

We, therefore, wish to find the transformation matrix $\underline{S}$ relating the arbitrary axes (x, yz) and the principal axes (a, bc). The transformation matrix $\underline{S}$ can then be used to diagonalize the matrix X, formed from the co-efficients in Equation (4.5), by means of the similarity transformation $\underline{S}^{-1}\underline{X}\underline{S} = \underline{\Lambda}$. The diagonal matrix $\underline{\Lambda}$ will have the form

$$\begin{pmatrix} I_a & & \\ & I_b & \\ & & I_c \end{pmatrix} \qquad (4.6)$$

and contains as its elements the required co-efficients in Equation (4.4).

Molecules are calssified according to the relative magnitude of their principal moments of inertia in the following way:

i) $I_a = I_b = I_c$ - spherical top

ii) $I_a = 0 \quad I_b = I_c$ - linear (symmetric top)

iii) $I_a < I_b = I_c$ - prolate symmetric top

iv) $I_a = I_b > I_c$ - oblate symmetric top

v) $I_a < I_b < I_c$ - asymmetric top

ScO_2, shown in Figure 4.1, is a bent triatomic molecule with all three moments of inertia different, and as such is classified as an asymmetric top molecule.

There is, however, a particular value of the angle $2\alpha = 2\alpha_S$, given by

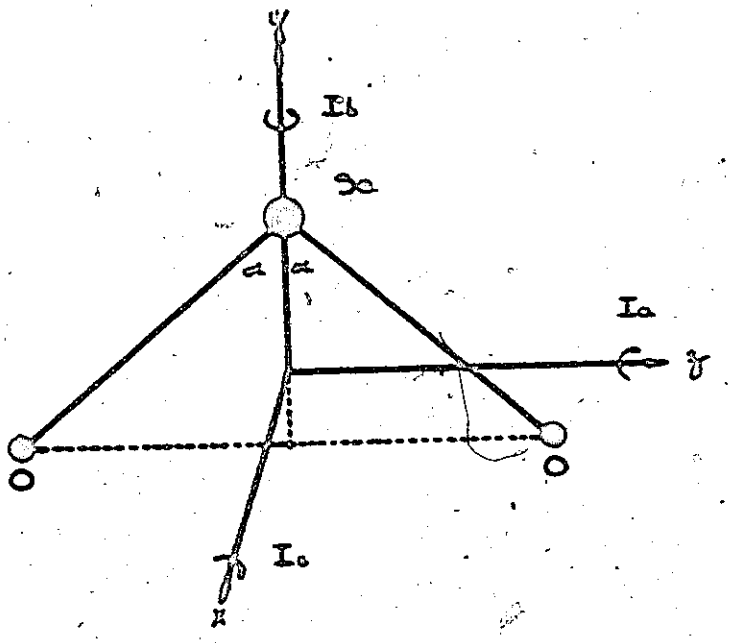

FIGURE 4.1 SO_2 molecule, showing the directions of the principal moments of inertia.

Equation 4.7 for which $I_a = I_b = \frac{1}{2} I_c$, in which case the molecule is an accidental oblate symmetric top and as such will display all of the physical features of a true symmetric top molecule[81].

$$\tan \alpha_S = \sqrt{\frac{M_{Se}}{M_{Se} + 2m_o}} \qquad (4.7)$$

A value of $2\alpha_S = 84.8°$ is the angle for which the ScO_2 molecule is an accidental oblate symmetric top. From recent microwave studies of SeO_2 by Takeo et. al.[57], the ground state bond angle was determined to be $2\alpha = 113°50'$.

The degree of asymmetry of an asymmetric top molecule is commonly determined by a dimensionless parameter κ (Kappa) given by[4]

$$\kappa = \frac{2B - A - C}{A - C} \qquad -1 \leq \kappa \leq +1 \qquad (4.8)$$

which in the prolate limit (B = C) has the limiting value -1, while in the oblate symmetry top limit (A = B), $\kappa = +1$. In the ground state of ScO_2 $\kappa = -0.81$, which is sufficiently close to -1, that ScO_2 might be expected to behave as a near prolate symmetric top. From the present rotational analysis of the B system of ScO_2 the excited state bond angle has been found to have the value $2\alpha = 101°$. The molecule is, therefore, a stronger asymmetric top ($\alpha = -0.536$) in the excited state, than in the ground electronic state.

4.2. Rotational Structure of Parallel and Perpendicular Electronic Transitions

The rotational energy levels of a prolate symmetric top are given by[4]

$$F_v(J,K) = B_v J(J+1) + (A_v - B_v)K^2 \qquad (4.9)$$

where J is the total angular momentum and K the component of the total angular

momentum about the top axis. $A_v = h^2/2I_a$ and $B_v = h^2/2I_b$ are the rotational constants of the vth vibrational level in cm^{-1}.

The selection rules governing the allowed rotational transitions accompanying a vibronic transition are determined by the polarization of the electronic transition. If the change of the dipole moment of the electronic transition is parallel to the top axis (parallel band), we have the following selection rules[82] for the quantum numbers J and K,

$$\begin{aligned} &\Delta K = 0, \quad \Delta J = 0, \pm 1 \quad \text{if } K \neq 0 \\ &\Delta K = 0, \quad \Delta J = \pm 1 \quad \text{if } K = 0 \end{aligned} \tag{4.10}$$

and if the transition is porpendicular to the top axis (porpendicular band) we have

$$\Delta K = \pm 1, \quad \Delta J = 0, \pm 1 \tag{4.11}$$

The top axis in SeO_2 is the a-axis in Figure 4.1. The symmetry in the C_{2v} point group and classification of the possible electronic transitions as to parallel or porpendicular is given in Table 4.1. The co-ordinate system used for the polarizations given is that shown in Figure 4.1.

Table 4.1

Symmetry Classification of Electronic Transitions in SeO_2 According to the C_{2v} Point Group

Symmetry of Excited State	Polarization of Transition	Designation
A_1	y	porpendicular
A_2	forbidden	-
B_1	z	porpendicular
B_2	x	parallel

For an asymmetric top the quantum number K is not strictly defined but for a molecule such as SeO_2 which is nearly a prolate symmetric top, we may expect the selection rules $\Delta K_p = 0$ and $\Delta K_p = \pm 1$ to apply to parallel and perpendicular transitions respectively. K_p then gives the component of the total angular momentum along the "pseudo" unique axis of the near prolate symmetric top. For parallel bands[82] it follows from Equation (4.9) that

$$\nu = \nu_o + \bar{B}'J'(J'+1) - \bar{B}''J''(J''+1) + [(A'-\bar{B}') - (A''-\bar{B}'')]K_p^2 \qquad (4.12)$$

while for perpendicular transitions

$$\nu = \nu_o + \bar{B}'J'(J'+1) - \bar{B}''J''(J''+1) \pm (A'-\bar{B}')K_p + [(A'-\bar{B}') - (A''-\bar{B}'')]K_p^2 \qquad (4.13)$$

where the primes and double primes refer to the excited and ground state respectively, K_p is the ground state value, and $\bar{B} = \frac{1}{2}(B+C)$.

The formulae for a perpendicular transition given by Equation (4.13) is to be used with the (+) sign in the linear term for an r branch ($\Delta K_p = +1$) and with a (-) sign for a p branch ($\Delta K_p = -1$). However, both the r and p branch together may be represented by a single equation of the form[83]

$$\nu = \nu_o + \bar{B}'J'(J'+1) - \bar{B}''J''(J''+1) + \tfrac{1}{2}[(A'-\bar{B}') - (A''-\bar{B}'')] + [(A'-\bar{B}') + (A''-\bar{B}'')]k + [(A'-\bar{B}') - (A''-\bar{B}'')]k^2 \qquad (4.14)$$

where k is a convenient index number with the value $k = K_p + \frac{1}{2}$ for the r branch ($\Delta K_p = +1$) and $k = -K_p + \frac{1}{2}$ for the p branch ($\Delta K_p = -1$).

We may speak of K-structure and J-structure when discussing the rotational fine structure of vibronic bands. It is convenient to think of K and J structure in terms of sub-bands. A sub-band in the K structure corresponds to the set of rotational transitions for a fixed K_p'' and ΔK_p but differing values of J'' and ΔJ in Equations (4.12), (4.13) and (4.14). Each sub-band (constant K_p) is then expected to contain a P, Q and R branch

corresponding to $J = -1, 0, +1$, respectively. The total rotational fine structure of a vibronic band is then the sum of all the sub-bands of differing K_p. Usually the distance between lines is much smaller in the J-structure than in the K-structure and we may therefore regard the set of transitions with $J = 0$, $K_p = 0, 1, 2, \ldots, n$ in Equations (4.12), (4.13) and (4.14) as giving the positions of sub-band origins in the vibronic band.

From Equations (4.12), (4.13) and (4.14), levels which differ only in the sign of K_p have the same energy and are therefore degenerate. In passing from a symmetric to an asymmetric top, the molecule no longer possesses a unique axis (i.e., an axis about which a component of angular momentum is conserved). The K degeneracy is removed (K-type doubling) and for each value of J there are $2J+1$ different energy levels. The quantum number K is no longer defined for an asymmetric top. The $2J+1$ components for each value of J are for convenience designated by a subscript τ added to J such that τ takes the values

$$\tau = -J, -J+1, -J+2, \ldots, +J \qquad (4.15)$$

Unlike symmetric top molecules, the energy levels of an asymmetric top molecule cannot be represented by a single quantitative formulae. For a discussion of the energy levels of asymmetric tops, the reader is referred to Herzberg[82].

4.3. Rotational Selection Rules for Asymmetric Top Molecules

When the molecule is a strongly asymmetric top, the selection rule $\Delta K = 0, \pm 1$ is no longer valid since K is no longer a good quantum number. Rather we must now apply the general selection rules for K_a and K_c developed by Cross, Hainer and King[99]. K_a and K_c are the quantum numbers for rotation about the a and c axes in the limiting cases of prolate and oblate symmetric tops respectively. The correlation of the asymmetric top rotational levels

with those of the prolate and oblate symmetric top limits is shown in Figure 4.2. For K_a and K_c we have the following selection rules[90].

If the transition moment is in the a-axis

$$\Delta K_a = 0, \pm 2, \ldots \qquad \Delta K_c = \pm 1, \pm 3, \ldots \tag{4.16}$$

if the transition moment is in the b-axis

$$\Delta K_a = \pm 1, \pm 3, \ldots \qquad \Delta K_c = \pm 1, \pm 3, \ldots \tag{4.17}$$

and if the transition moment is in the c-axis

$$\Delta K_a = \pm 1, \pm 3, \ldots \qquad \Delta K_c = 0, \pm 2, \ldots \tag{4.18}$$

An alternate way of stating these selection rules is in terms of the parity of the rotational levels. Only the following transitions may occur[82].

If the transition moment is in the a-axis

$$++ \leftrightarrow -+ \quad \text{and} \quad +- \leftrightarrow -- \tag{4.19}$$

if the transition moment is in the b-axis

$$++ \leftrightarrow -- \quad \text{and} \quad +- \leftrightarrow -+ \tag{4.20}$$

and if the transition moment is in the c-axis

$$++ \leftrightarrow +- \quad \text{and} \quad -+ \leftrightarrow -- \tag{4.21}$$

In order to designate the various branches for the rotational structure of an asymmetric top, we require two superscripts to be added to the usual P, Q, R symbols (which give the ΔJ value for the transition). The first of these superscripts indicates ΔK_a, the second the ΔK_c value. The $B \leftarrow X$ transition of ScO_2 is shown in the present work to be a parallel transition with the transition moment polarized along the a-axis of the molecule. The excited electronic state is therefore of D_2 symmetry. In accordance with the selection rules given by Equations (4.16) and (4.19) the following branches may occur in an A-type band of an asymmetric top such as ScO_2.

$$qr_R,\ qt_R,\ qp_R,\ qn_R,\ {}^{s,r}R,\ {}^{o,r}R,\ \ldots\ldots \qquad (4.22)$$

with similar Q and P branches.

The principal sub-branches of the asymmetric rotor are those for which both ΔK_a and ΔK_c change by 0 or ±1, since they become the p, q and r branches in both the prolate and oblate symmetric limiting cases[90]. Branches which correspond to forbidden transitions in the limiting prolate and oblate symmetric tops will not be considered in this discussion. The reader is referred to Cross, Hainer and King[90] for further discussion of these forbidden branches.

In the general case of the asymmetric rotor for a transition parallel to the a-axis, $\Delta K_a = 0, \pm 2, \pm 4$, etc. and $\Delta K_c = \pm 1, \pm 3$, etc. However, not all combinations of ΔK_a and ΔK_c are possible because the sum $K_a + K_c$ for each combining level is either equal to J or J+1. The permitted values of $\Delta(K_a + K_c)$ are given in Table 4.2.

Table 4.2

Permitted Changes in $\Delta(K_a + K_c) = \Delta K_a + \Delta K_c$ for Asymmetric Top Molecules for P, Q and R branches of the Rotational Structure (after Cross, Hainer, and King[90])

Parity of Initial Level	P	Q	R
even	-1,0	0,1	1,2
odd	-1,-2	0,-1	1,0

The symmetry of the rotational levels shown in Figure 4.2 have been determined with respect to both the rotational sub-group (C_2) after Dennison[88] and the full molecular symmetry group (C_{2v}) after Mecke[91].

Since rotation of SeO_2 by 180° about any of the three principal axes of the momental ellipsoid leads to an orientation which has the same probability as the original orientation then the rotational wavefunction can only be multiplied by +1 or by -1 when any of the operations C_2^a, C_2^b, C_2^c are carried out.

Since C_2^b is always the product of C_2^c and C_2^a, it is sufficient to designate the four symmetry species as ++, +-, -+, and --, where the first sign refers to the behaviour with respect to C_2^c and the second with respect to C_2^a.

Dennison[88] has shown that the highest level J_{+J} for each set of a given J is + with respect to C_2^c, the next two -, the two next are + and so on. The lowest level J_{-J} of each set is + with respect to C_2^a, the next two higher ones are -, the next two + and so on. Figure 4.2 show the result for J = 0 to J = 3 for SeO_2.

The symmetry of rotational wave functions with respect to the full molecular point group were determined using the methods outlined by Hougen[91] where reflection at a plane of symmetry is equivalent to a two-fold rotation about an axis perpendicular to that plane. The results are summarized in Table 4.3.

Table 4.3

Classification of Asymmetric Rotational Levels According to C_{2v} Point Group

$C_2^c(x)$	$C_2^a(z)$	$C_2^b(y)$	$\sigma_{yz}(C_2^c)$	$\sigma_{xy}(C_2^a)$	Symmetry
+	+	+	+	+	A_1
+	-	-	+	-	B_2
-	+	-	-	+	B_1
-	-	+	-	-	A_2

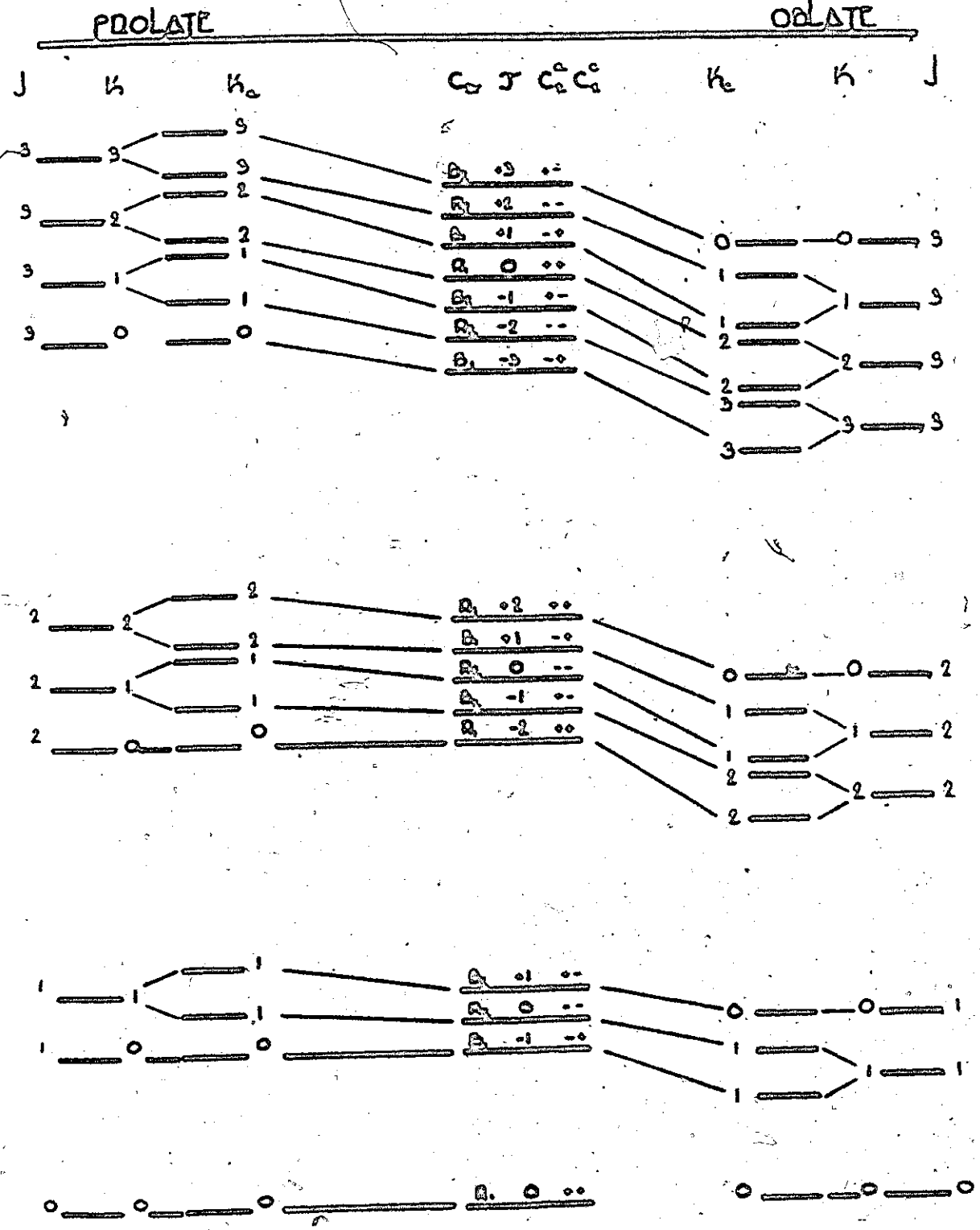

FIGURE 4.2 CORRELATION OF ASYMMETRIC TOP WITH PROLATE AND OBLATE SYMMETRIC TOP ROTATIONAL LEVELS. THE SYMMETRY OF THE ASYMMETRIC ROTATION FUNCTIONS HAVE BEEN DETERMINED WITH RESPECT TO THE C_{2v} POINT GROUP AFTER HOUGEN[7].

The rovibronic symmetry of a particular level is then easily determined from the symmetry of the direct product

$$\Gamma\psi_{VIB} \times \Gamma\psi_{ROT} \times \Gamma\psi_{EL} = \Gamma\psi_{ROVIBRONIC} \tag{4.23}$$

The general selection rule for an electric dipole transition between two rovibronic states of species Γ' and Γ'' is given by[90]

$$\Gamma' \times \Gamma'' = \Gamma_{T_i} \times \Gamma_{R_i} \tag{4.24}$$

Therefore, in order for a rovibronic transition to be dipole allowed the symmetry of the direct product of the combining states must be the same as the symmetry of a component of the direct product of a translation T_i and the corresponding rotation R_i about the same axis, where i = x, y, z determines the polarization of the transition. For molecules of C_{2v} symmetry (SeO_2) the three direct products $\Gamma_{T_i} \times \Gamma_{R_i} = A_2$. Therefore, the general rovibronic selection rule of Equation (4.24) becomes

$$\Gamma' \times \Gamma'' = A_2 \tag{4.25}$$

where Γ' and Γ'' are the rovibronic symmetry of the upper and lower state respectively.

4.4. Nuclear Statistical Weights for SeO_2

The nuclear statistical weights for each rotational level of SeO_2 are easily determined by considering the total wave function ψ_{TOT} given by

$$\psi_{TOT} = \psi_{el}\psi_{vib}\psi_{rot}\psi_{n.s.} \tag{4.26}$$

where ψ_{el}, ψ_{vib}, ψ_{rot}, and $\psi_{n.s.}$ are the electronic, vibrational, rotational and nuclear spin wave functions respectively. Consider the behaviour of each wave function with respect to C_2^b (interchange of identical nuclei). Since the nuclear spin of O^{16} is zero, $\psi_{n.s.}$ must be symmetric and therefore trans-

form as A_1. Since the nuclei have integral spin (zero in this case), they obey Bose-Einstein statistics and Ψ_{TOT} must be symmetric with respect to the interchange. Therefore, it follows that the rovibronic wave function $\psi_{el}\psi_{vib}\psi_{rot}$ must be of A symmetry.

The ground electronic state of SeO_2 is known to be of A_1 symmetry[57] while the upper state in the B ← X electronic transition has been shown to be of B_2 symmetry from the present work. Therefore, only the A levels of SeO_2 are populated in the ground state and transitions may occur to only the B levels of the $^1B_2$ excited state.

4.5. Intensity of Rotational Transitions

The intensity of a rotational transition in absorption is proportional to the product[82]

$$I(J,K) = CA_{KJ}\nu g_{KJ} e^{-F(K,J)hc/kT} \tag{4.27}$$

where C is a constant independent of K and J but depending on the vibrational transition and which may be determined if the absolute intensity of the absorption lines has been measured[87]. g_{JK} and F(K,J) are respectively the statistical weight and term value of the lower state and A_{KJ} is proportional to the square of the transition moment $R_{xf}^2 + R_{yf}^2 + R_{zf}^2$ summed over all orientations of J[82]. For a parallel transition of a symmetric top ($\Delta K = 0$) Dennison[88] has shown that A_{KJ} is

$$\text{for } \Delta J = +1: \quad A_{KJ} = \frac{(J+1)^2 - K^2}{(J+1)(2J+1)} \tag{4.28}$$

$$\text{for } \Delta J = 0: \quad A_{KJ} = \frac{K^2}{J(J+1)} \tag{4.29}$$

$$\text{for } \Delta J = -1: \quad A_{KJ} = \frac{J^2 - K^2}{J(2J+1)} \tag{4.30}$$

The statistical weights g_{KJ} are $2J+1$ for $K = 0$ and $2(2J+1)$ for $K \neq 0$.

The relative intensity of the P, Q and R branch in a symmetric top molecule has been determined by Teller[89] as a function of I_A/I_B and is shown in Figure 4.3. The relative intensity distribution within the P and R branches of a sub-band is essentially determined by the population of the lower levels irrespective of K; the total relative intensity of the P and R branch being determined by the number of molecules in a level with a given J value (summed over all K values)[82].

The intensity of lines in the Q branch is zero for $K = 0$ and increases rapidly with $K > 0$, but decreases rapidly with increasing J.

The ratio $I_a/I_b = 3.3$ for SeO_2. Therefore the intensity of the Q branch is expected to be larger than the intensity of the P and R branches. Since the band is strongly red degraded, the R branch should form a head and probably be the most prominent feature in the spectrum. The Q branch lines should also be prominent in the spectrum with the P branch possibly being too weak to observe above the background.

4.6. Rotational Analysis of 1_0^3 Vibronic Band

The ground state rotational constants for SeO_2 have been determined by Takeo, Hirota and Morino[57] from microwave studies. An appropriate set of rotational constants was obtained for the excited state in the following way. The origin of the K_p sub-band ($J = 0$ in Equations (4.12), (4.13) and (4.14)) minus the origin of the K_p+1 sub-band is given by

$$[(A'-\bar{B}') - (A''-\bar{B}'')](K_p - (K_p+1)^2) = -[(A'-\bar{B}') - (A''-\bar{B}'')]2K_p+1 \qquad (4.31)$$

Therefore a plot of the first difference in the K structure verses K_p should give a straight line with slope $-2[(A'-\bar{B}') - (A''-\bar{B}'')]$. The ground

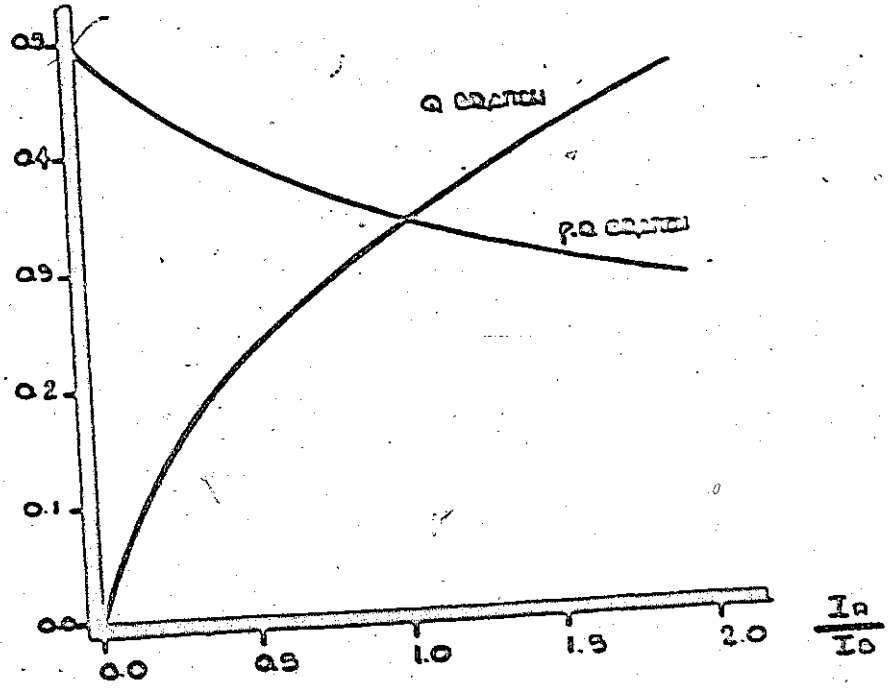

FIGURE 4.3 RELATIVE INTENSITY OF P, Q AND R BRANCH AS A FUNCTION OF I_a IN A PARALLEL BAND OF A SYMMETRIC TOP.

state constants are known, therefore it is possible to determine the excited state difference $A'-\bar{B}'$. Figure 4.4 shows a plot of $\Delta\nu$ verses K_p for the 1_0^5 vibronic band of $Se^{78}O_2^{16}$. The slope is found to equal -0.71875 which gives $A'-\bar{B}' = 0.36339\ cm^{-1}$ for the excited state.

The sub-band heads (^QR heads) were also fitted by least squares to Equations (4.12) and (4.14) which are both quadratic equations. The value of $A'-\bar{B}'$ obtained from the quadratic coefficient is $0.36046\ cm^{-1}$ which is in good agreement with the value of $A'-\bar{B}' = 0.36339\ cm^{-1}$ obtained from the verses K_p plot.

The linear coefficient in Equation (4.13) changes with the K_p numbering of the sub-bands while the quadratic coefficient is independent of the K_p numbering. The correct K_p numbering for a perpendicular band gives $A_1 = \pm(A'-\bar{B}')$ while for a parallel band $A_1 = 0$ (i.e., Equation (4.13) reduces to Equation (4.12)). The calculated K_p numbering for a parallel and perpendicular transition for the 1_0^3 band of $Se^{70}O_2^{16}$ is given in Table 4.4. The first few sub-bands corresponding to low K_p values were omitted in the above least square fit since for low (J,K) the molecule is only poorly approximated as a near prolate symmetric top. The corresponding plot of $\Delta\nu$ against K_p, along with the K_p numbering for assumed parallel and perpendicular bands for the $Se^{78}O_2^{18}$ and $Se^{80}O_2^{16}$ molecules are given in Appendix III.

From the least square procedure outlined above, it was possible to determine the K_p'' numbering for the sub-bands. It was, however, not possible to distinguish between a parallel and perpendicular transition since the K_p numberings determined in each case were very similar. However, the number of sub-bands which appear in the spectrum between the head and the sub-band located at $33876.903\ cm^{-1}$ was closer to six rather than eight. For this reason

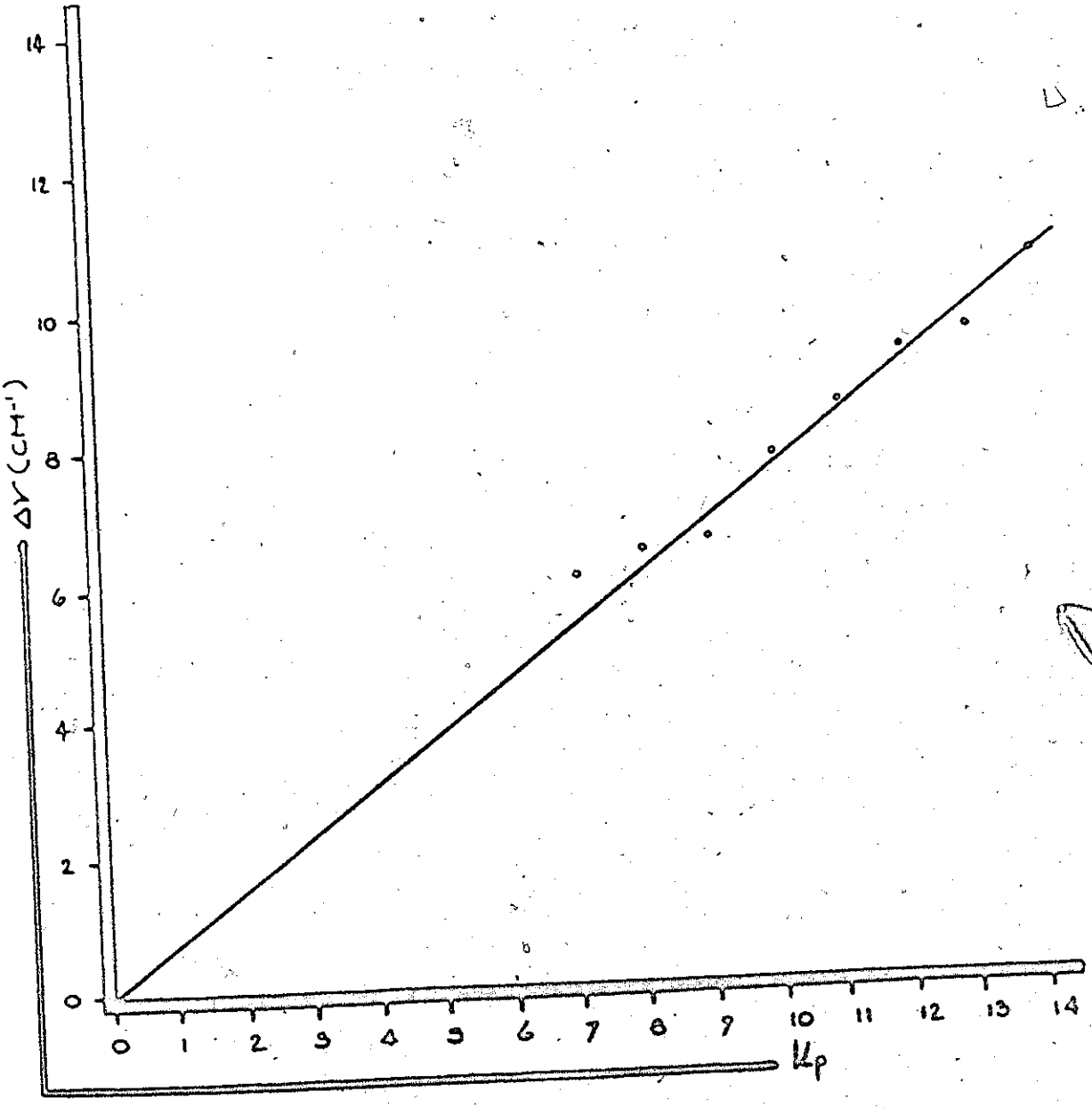

FIGURE 4.4 PLOT OF Q BRANCH HEAD SEPARATION (ΔV) AGAINST Kp FOR THE 1_0^3 VIBRONIC BAND OF $S_0^{32}O_2^{16}$. FROM A LEAST SQUARE FIT OF THE ABOVE POINTS THE INTERCEPT IS FOUND TO BE -0.042.

Table 4.4

K_p Numbering for Sub-Band Origins of 1_0^3 Vibronic Band of $Se^{78}O_2^{16}$ Assuming a Parallel Band*

K_p''	ν (Experimental) cm^{-1}	ν (Calculated) cm^{-1}	Deviation (cm^{-1})
7	33876.903	33876.701	-0.201
8	33870.817	33871.022	0.205
9	33864.355	33864.638	0.283
10	33857.765	33857.550	-0.21
11	33849.902	33849.757	-0.14
12	33841.290	33841.259	-0.03
13	33831.884	33832.057	0.17
14	33822.285	33822.150	-0.13
15	33811.477	33811.539	0.06

*From a similar least square analysis assuming a perpendicular band, the sub-band at 33876.903 cm^{-1} is assigned to the value $K_p'' = 9$.

a parallel transition is favored over a perpendicular one.

In order to determine the polarization of the transition and consequently the symmetry of the excited electronic state, a rotational analysis was carried out by the band contour method. The analysis was performed using a computer program written by Pierre [unpublished; see (7)]. The program calculates the frequency and intensity of individual rotational lines in asymmetric top approximation. The line intensities are then distributed according to a Gaussian function. The nuclear statistical weights for individual rotational lines are entered as input data in the program. The contours calculated for a particular vibronic band are then compared with a microdensitometer tracing of the same band.* If the contour and trace do not match then the rotational constants are systematically varied until both are the same. Contours for both parallel and perpendicular transitions were calculated. The perpendicular contours in no way resembled the experimental profile of the band, while parallel contours resembled the experimental trace both in head position and intensity distribution. The calculated and observed contours for a transition polarized parallel to the top axis are shown in Figure 4.5 for the 1_0^3 vibronic band. The excited state rotational constants for $Se^{78}O_2^{16}$ which give the contour in Figure 4.5 are: A = 0.60657 cm^{-1}, B = 0.29221 cm^{-1} and C = 0.19721 cm^{-1}. The moments of inertia for SeO_2 are related to the bond length and bond angle (see Figure 4.1) according to the following simple relations[86]

$$I_x = \mu r^2 \cos^2 \alpha \tag{4.32}$$

$$I_y = 2\mu r^2 \sin^2 \alpha \tag{4.33}$$

---

*I would like to thank Dr. Glenn Kidd for writing the plot sub-routine used in the present band contour work.

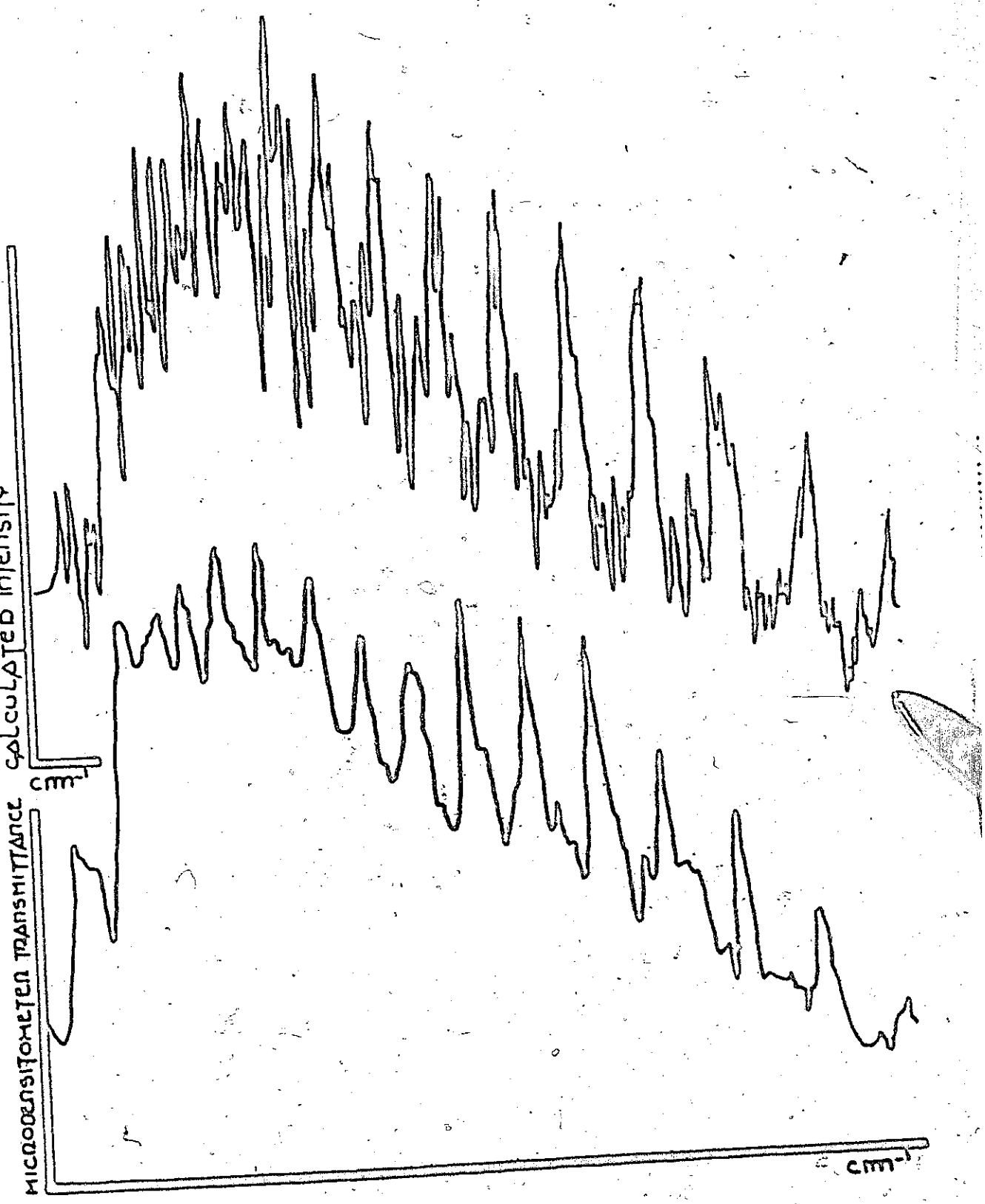

FIGURE 4.6 OBSERVED (LOWER) AND CALCULATED (UPPER) CONTOUR FOR THE 1_0^9 VIBRONIC BAND OF $^{32}SO^{16}O$.

$$I_z = I_x + I_y = 2m(\mu_3/\mu)r^2\sin^2\alpha \qquad (4.34)$$

where $\mu = 2mM/(2m + M)$ (4.35)

$$\mu_3 = \mu[1 + (\mu/2m)\cot^2\alpha] \qquad (4.36)$$

and M and m are the selenium and oxygen masses respectively. An excited state bond length of 1.74 Å and bond angle $2\alpha = 101.0°$ was calculated from the moments of inertia determined by the band contour method. The value of $A'-\bar{B}' = 0.36186\ cm^{-1}$ determined from the band contour, is in good agreement with the value $0.36046\ cm^{-1}$ obtained from the average of the second difference in the K-structure using the least square method discussed earlier.

The excited state geometry determined above for $Se^{78}O_2^{16}$ was then used with the aid of Equations (4.32) to (4.36) to calculate the rotational constants corresponding to this geometry for the isotopic molecules $Se^{78}O_2^{18}$ and $Se^{80}O_2^{16}$. The observed and calculated contour for $Se^{80}O_2^{16}$ is shown in Figure 4.6. The agreement between the observed and calculated contours for the $Se^{78}O_2^{18}$ isotope was much poorer. The tabulated rotational constants for all three isotopic molecules are given in Table 4.5.

Table 4.5

Rotational Constants of $Se^{78}O_2^{16}$, $Se^{78}O_2^{18}$ and $Se^{80}O_2^{16}$ Molecules Corresponding to the $^1B_2$ Excited State Geometry with Symmetric Bond Lengths of 1.74 Å and Bond Angle $2\alpha = 101.0°$

	$Se^{78}O_2^{16}$	$Se^{78}O_2^{18}$	$Se^{80}O_2^{16}$
A	$0.60557\ cm^{-1}$	$0.60508\ cm^{-1}$	$0.60215\ cm^{-1}$
B	$0.29221\ cm^{-1}$	$0.29127\ cm^{-1}$	$0.29221\ cm^{-1}$
C	$0.19721\ cm^{-1}$	$0.19671\ cm^{-1}$	$0.19574\ cm^{-1}$

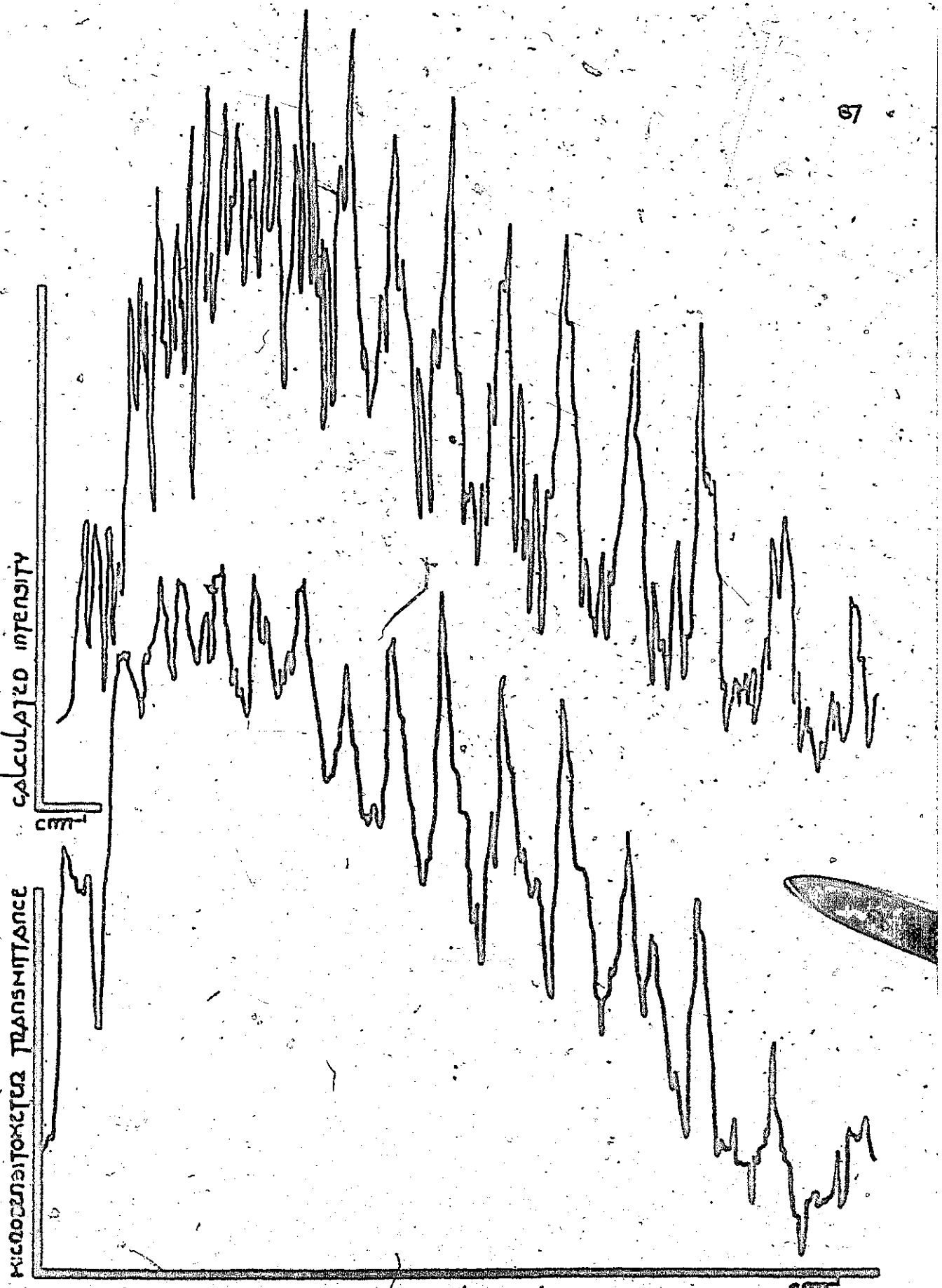

FIGURE 4.5 OBSERVED (LOWER) AND CALCULATED (UPPER) CONTOUR FOR THE 1_0^3 VIBRONIC BAND OF $Se_2^{80}Se^{82}$.

4.7. Prominent Features of 1_0^3 Vibronic Band

The 1_0^3 vibronic band is A-type and thus corresponds to a $^1B_2 \leftarrow {}^1A_1$ vibronic transition with the electric dipole polarized parallel to the top axis. Since only totally symmetric vibrations are excited in this transition, the electronic transition itself is therefore $^1B_2 \leftarrow {}^1A_1$. The 1_0^3 band is red degraded forming two principal heads separated by approximately 7 cm^{-1}. The more intense of these lies to the red forming the high frequency limit of the ^{qr}R-sub-branches (^qR sub-branch in the prolate symmetric top limit).

The weaker head to the blue corresponds to the forbidden ($\Delta K_a = +2$) symmetric rotor sub-branch ^{sr}R. This is the same type of head formation recently observed by Brand and Shrikameswaran[92] in the 0_0^0 band of the $^1B_2 \leftarrow {}^1A_1$ electronic transition of the sulfur dioxide. The most prominent feature in sub-bands of high K is the ^qR branch head and to a less extent initial lines of the ^qQ branch. A first order Ebert photograph of the 1_0^3 vibronic band of $Se^{78}O_2^{16}$ is shown in Figure 4.7.

4.8. Rotational Structure of $1_2^0 3_0^1$ Vibronic Band

The vibrational analysis has led to strong evidence for the presence of a double-minimum potential well along Q_3' in the excited $^1B_2$ electronic state of selenium dioxide. The transition from the vibrationless level of the ground state to the 0^- level of Q_3' in the excited state has been assigned. This transition is labelled the 3_0^1 vibronic band, at 32073.8 cm^{-1}.

As discussed earlier in Chapter Three this band is expected to be of B_2 symmetry (C_{2v} classification) or an AB-Type hybrid band (C_s classification).

An extensive attempt was made to analyse the $1_2^0 3_0^1$ band by the band contour method. Unfortunately it was not possible to fit the observed contour to calculated A, B or AB hybrid bands. The difficulty in obtaining a good fit

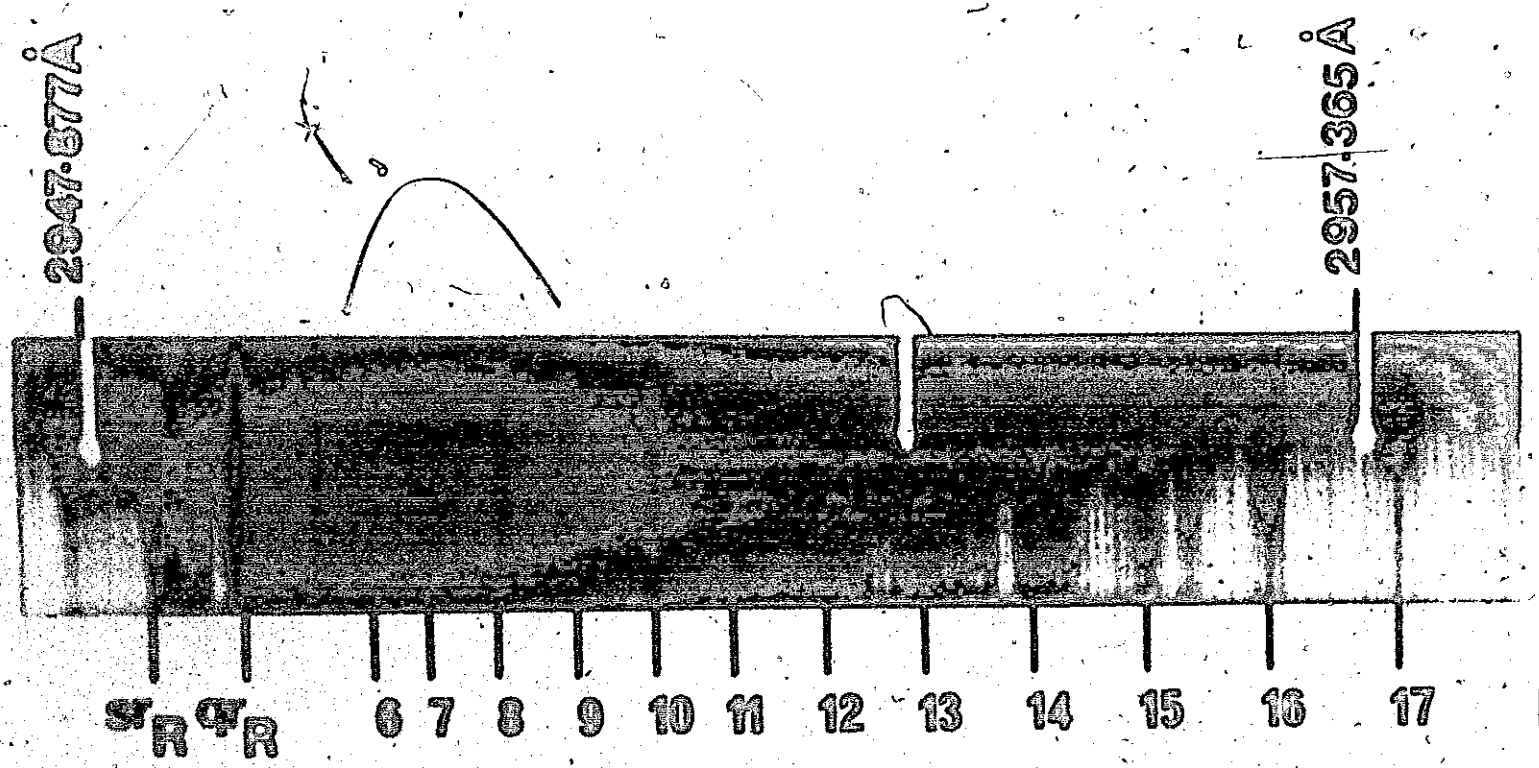

Figure 4.7

First order Ebert photograph of 1^3_0 vibronic band of $Se^{78}O_2^{16}$.

results from the fact that if the band is an AB-hybrid then the observed heads within the band will be most often due to coincidental overlap of the superimposed parallel A-type band and perpendicular B-type. The profile of the 3_0^1 band (the $1_2^0 3_0^1$ band was actually used in the analysis since it is free of overlapping sequence bands) is very distinctly different from the observed "pure" A-type bands. A first order Ebert photograph of the $1_2^0 3_0^1$ band obtained at McMaster University and a 20th order Ebert photograph taken in Dr. D. C. Moule's laboratory at Brock University in St. Catharines, Ontario, are shown in Figure 4.8. It is unfortunate that it was not possible to analyse this band in detail since the determination of its band type would provide confirmation of the vibrational analysis given in the present work. Certainly, Figure 4.8 shows that the band type must be quite different from the observed type A bands (see Figure 4.7).

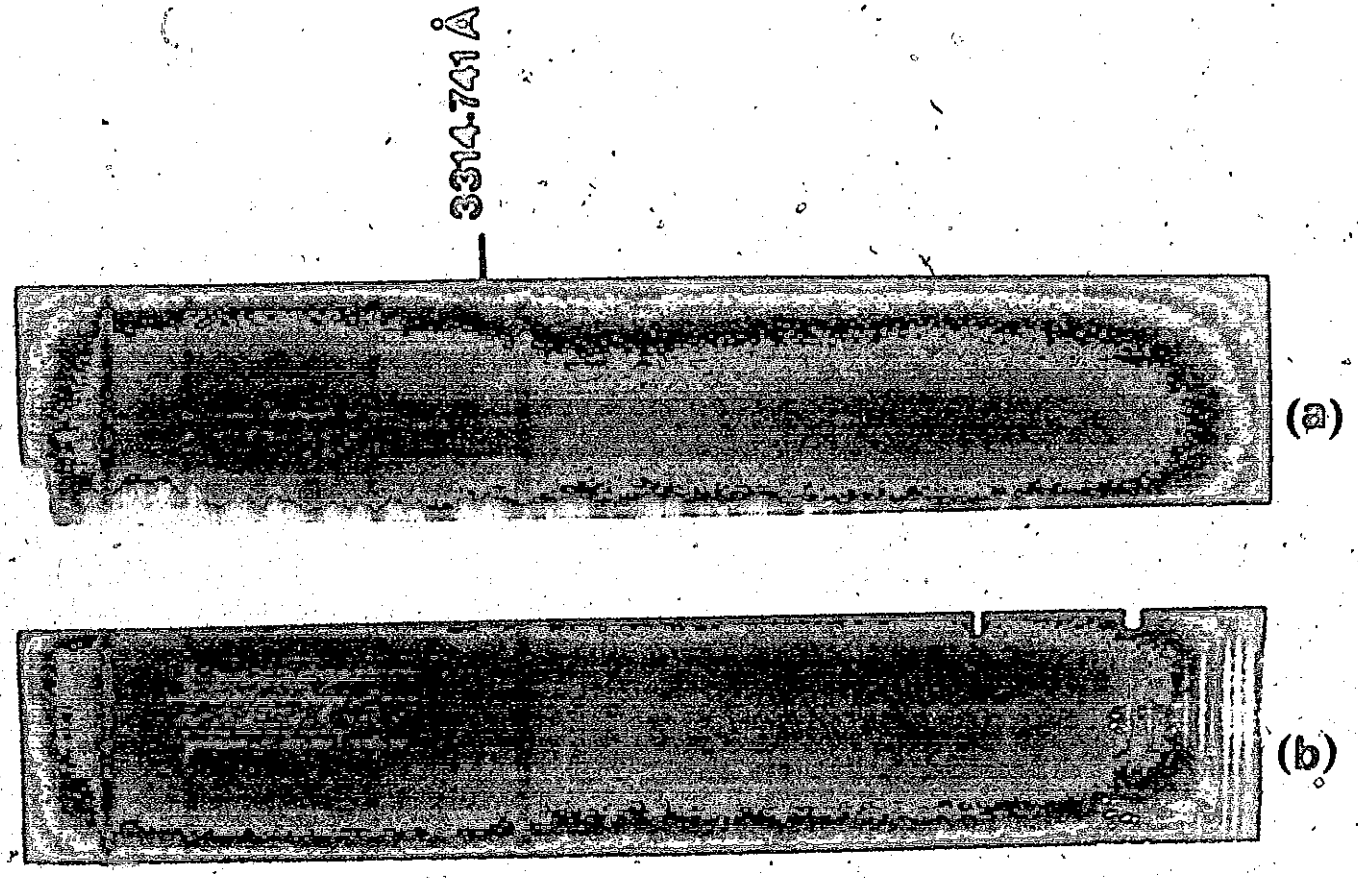

Figure 4.8

First order (a) and 20th order (b) Ebert photograph of $1_2^0 3_0^1$ vibronic band of $Se^{78}O_2^{16}$.

CHAPTER FIVE

FRANCK-CONDON CALCULATIONS

5.1. Introduction

In the present work the Franck-Condon principle was used to determine completely the structure of the $^1B_2$ electronic state of selenium dioxide. The methods outlined by Coon et. al.[71] were applied and the results are discussed. In order to perform the above calculation it was necessary to have made a normal co-ordinate analyses, or have at least an approximate set of normal co-ordinates for the excited state. The results of the normal co-ordinate analyses are discussed along with a brief description of the methods used in the normal co-ordinate analysis. The Franck-Condon calculations require only Q_1' and Q_2'. Q_3' was also calculated, although in practice the molecule has a double-minimum potential along Q_3'. It was necessary to assume a symmetric harmonic model for Q_3'. Also the value $\nu_3' = 686\ cm^{-1}$ was obtained by taking one half of the observed $2\nu_3' = 1372\ cm^{-1}$.

5.2. Normal Co-ordinate Analysis (Ground Electronic State)

The normal co-ordinates for selenium dioxide were obtained using a Urey-Bradley[72,73] force field and a general quadratic force field as an approximation to the potential function for the molecule. The computer program for the former was set up in a method similar to that described by Overend and Scherer[74], and the final normal co-ordinates obtained by the Wilson F-G method[75]. A brief description of the procedure is outlined below.

In the Urey-Bradley[76] force field we take account of bond-stretching force constants K, angle bending force constants H and repulsive force constants F. However, the non-bonding interaction between the oxygen nuclei

is not independent of Δr_i and $\Delta\phi$ and consequently is a redundant co-ordinate and must therefore be removed. The redundant co-ordinate arises due to the fact that we have four co-ordinates Δr_1, Δr_2, $\Delta\phi$ and Δq (see Fig. 5.1) but only three vibrational degrees of freedom. In general the number of adopted co-ordinates should equal the number of vibrational degrees of freedom.

The non-bonding distance q (Fig. 5.1) is given by the cosine law as

$$q^2 = r_1^2 + r_2^2 - 2r_1r_2\cos\phi \tag{5.1}$$

and the redundant condition is[77]

$$\Delta q = s\Delta r_1 + s\Delta r_2 + t(r_o\Delta\phi) + [t^2(\Delta r_1)^2 + t^2(\Delta r_2)^2 - s^2(r_o\Delta\phi)^2 - 2t^2(\Delta r_1)(\Delta r_2) + 2ts(\Delta r_1)(r_o\Delta\phi) + 2ts(\Delta r_2)(r_o\Delta\phi)]/2q_o \tag{5.2}$$

where s and t are given by

$$s = r_o(1 - \cos\phi_o)/q_o \tag{5.3}$$

$$t = r_o(\sin\phi_o)/q_o \tag{5.4}$$

Substitution of Equation (5.2) for Δq gives the Urey-Bradley potential energy for SeO_2 as[77]

$$V = \tfrac{1}{2}(K + s^2F + t^2F')(\Delta r_1)^2 + \tfrac{1}{2}(K + s^2F + t^2F')(\Delta r_2)^2 + \tfrac{1}{2}(H + t^2F - s^2F')(r_o\Delta\phi)^2 + (s^2F - t^2F')(\Delta r_1)(\Delta r_2) + ts(F + F')(\Delta r_1)(r_o\Delta\phi) + ts(F + F')(\Delta r_2)(r_o\Delta\phi) \tag{5.5}$$

The value of F and F' are dependent and usually assumed to be related in the following way.

$$F' = -0.1\,F \tag{5.6}$$

The potential energy, expressed in internal co-ordinates, is given by

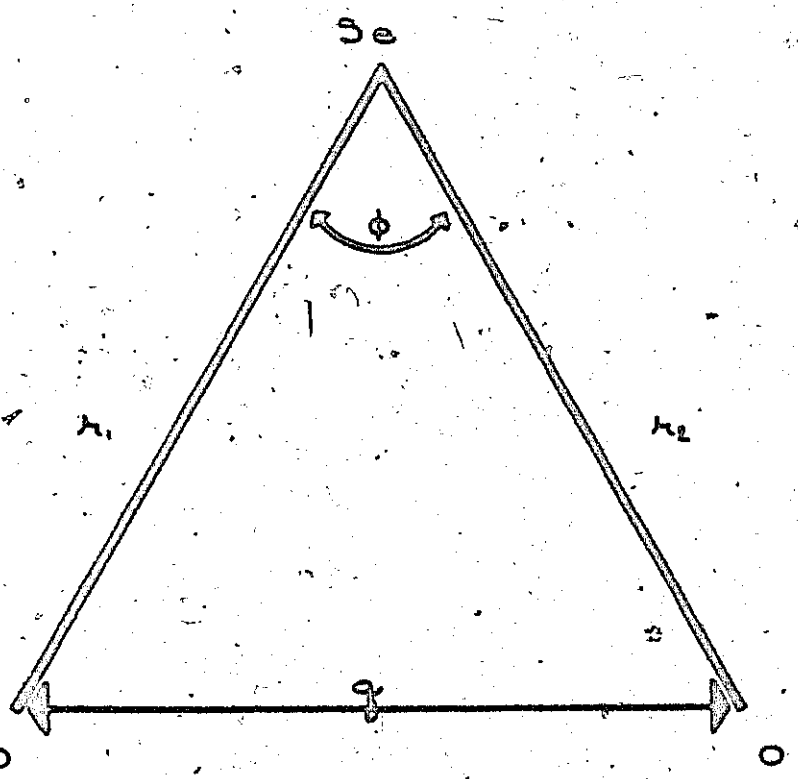

FIGURE 5.1 GEOMETRY OF SeO_2 MOLECULE

$$V = \frac{1}{2} f_{11}(\Delta r_1)^2 + \frac{1}{2} f_{22}(\Delta r_2)^2 + \frac{1}{2} f_{33}(r_o \Delta\phi)^2 + f_{12}(\Delta r_1)(\Delta r_2) + f_{13}(\Delta r_1)(r_o \Delta\phi) + f_{23}(\Delta r_2)(r_o \Delta\phi) \quad (5.7)$$

which when expressed in matrix notation is

$$V = \frac{1}{2}[\Delta r_1, \Delta r_2, r_o \Delta\phi] \begin{bmatrix} f_{11} & f_{12} & f_{13} \\ f_{21} & f_{22} & f_{23} \\ f_{31} & f_{32} & f_{33} \end{bmatrix} \begin{bmatrix} \Delta r_1 \\ \Delta r_2 \\ r_o \Delta\phi \end{bmatrix} \quad (5.8)$$

The individual elements f_{ij} of the F matrix are linear functions of the Urey-Bradley force constants ϕ_k of Equation (5.5);

$$F_j^i = \sum_k a_{jk}^i \phi_k \quad (5.9)$$

the coefficients a_{jk}^i being determined by the molecular geometry[74]. The transformation of the potential energy from Urey-Bradley space to internal co-ordinate space is effected by a transformation matrix Z.

5.3. Construction of the Z Matrix

We are seeking a transformation matrix Z of the form

$$F = Z\Phi \quad (5.10)$$

The elements of the F matrix are ordered in the following way:

$$F = \begin{bmatrix} f_1 & f_2 & f_4 \\ & f_3 & f_5 \\ & & f_6 \end{bmatrix} \quad (5.11)$$

the matrix being symmetric about the main diagonal.

The individual elements of the Z matrix are, therefore, easily obtained by equating coefficients of Equation (5.5) with those of Equation (5.7). The Z matrix elements are given in Table 5.1.

Table 5.1

Z Matrix Elements for SeO_2

	K	H	F+F'
$(\Delta r_1)^2$	1.0	0	0.86325
$(\Delta r_1)(\Delta r_2)$	0	0	0.98912
$(\Delta r_2)^2$	1.0	0	0.86325
$(\Delta r_1)(r_o \Delta\phi)$	0	0	0.68714
$(\Delta r_2)(r_o \Delta\phi)$	0	0	0.68714
$(r_o \Delta\phi)$	0	1.0	0.72199

5.4. G Matrix for SeO_2

In terms of mass weighted cartesian co-ordinates, η_i, the kinetic energy T, in matrix notation is given by,

$$2T = \dot{\eta}^t \dot{\eta} \qquad (5.12)$$

where $\dot{\eta}^t$ and $\dot{\eta}$ are a row and column vector respectively. The kinetic energy then takes the simple form of a sum of square terms when expressed in mass-weighted cartesian co-ordinates.

The potential energy is, however, expressed in internal co-ordinates. Therefore, the mass-weighted cartesian co-ordinates are transformed to internal co-ordinates r_i by a transformation matrix D.

$$R = D\eta \qquad (5.13)$$

However, since there are only 3N-6 internal co-ordinates but 3N mass-weighted cartesian co-ordinates, D is a non-square matrix with 3N-6 rows and 3N columns. Since D is a non-square matrix, it cannot be inverted to give the matrix R which we seek.

Wilson[75] has shown, however, that the kinetic energy is given by

$$2T = \dot{R}^t G^{-1} \dot{R} \qquad (5.14)$$

where $DD^t = G$ is a square matrix of dimension 3N-6 and thus possesses an inverse.

The G matrix elements are determined from the molecular geometry and are tabulated in Table 5.2. The G matrix is symmetric about the main diagonal.

Table 5.2

G Matrix Elements for SeO_2 in Internal Co-ordinates (after Shimanouchi[77])

	Δr_1	Δr_2	$r_o\Delta\phi$
Δr_1	$\mu_{Se} + \mu_O$		
Δr_2	$(t^2-s^2)\mu_{Se}$	$\mu_{Se} + \mu_O$	
$r_o\Delta\phi$	$-2ts\mu_{Se}$	$-2ts\mu_{Se}$	$4s^2\mu_{Se} + 2\mu_O$

The normal co-ordinates Q are related to the internal co-ordinates R by the transformation matrix L

$$R = LQ \qquad (5.15)$$

where L is chosen such that the kinetic and potential energy have a diagonal form when expressed in terms of the normal co-ordinates.

$$2V = Q^t L^t F L Q = Q^t \Lambda Q \qquad (5.16)$$

$$2T = \dot{Q}^t L^t G^{-1} L \dot{Q} = \dot{Q}^t E \dot{Q} \qquad (5.17)$$

where Λ is a diagonal matrix whose diagonal elements will be the quantity $\lambda_k = 4\pi^2 c^2 \nu_k^2$ and E is the unit matrix. Therefore,

$$L^t F L = \Lambda \quad \text{and} \quad L^t G^{-1} L = E \qquad (5.18)$$

In the Wilson formalism the secular equation takes the form

$$|GF - E\lambda| = 0 \tag{5.19}$$

The GF matrix is diagonalized by $L^{-1}GFL = \Lambda$ or $GFL = L\Lambda$ where Λ is the diagonal matrix consisting of the eigenvalues and L consists of the corresponding eigenvectors.

5.5. Calculation of Urey-Bradley Force Constants from Observed Frequencies

In the present analyses a trial set of Urey-Bradley force constants $\{\phi\}$ were assumed, and the elements of the F matrix calculated according to Equation (5.10). The GF matrix was then formed and subsequently diagonalized yielding a set of calculated eigenvalues $\lambda_i = 4\pi^2c^2\nu_i^2$ which could then be compared with the observed eigenvalues λ_i^o obtained from the experimentally observed frequencies. A Jacobian subroutine was used to obtain a corrected set of Urey-Bradley force constants such that the difference $(\lambda_i^o - \lambda_i^c) = 0$. The elements of the Jacobian matrix J_{ik}^{ϕ} are given by

$$J_{ik}^{\phi} = \partial\lambda_i/\partial\phi_k \tag{5.20}$$

The construction of the Jacobian is identical with that outlined by Subramanian[78] and will not be duplicated here.

5.6. Normal Co-ordinate Analysis (General Quadratic Force Field)

The set of frequencies obtained using a Urey-Bradley force field were reasonably close to the experimentally observed frequencies. The assumption of only one type of stretching force constant (Urey-Bradley Force Field) is probably most responsible for the small disagreement between the calculated and observed ν_1' and ν_3' frequencies. The calculated frequencies for ν_1' and ν_3' were 662 cm^{-1} and 683 cm^{-1} while the observed frequencies are

660 cm^{-1} and 686 cm^{-1} respectively. In order to obtain slightly better agreement for these frequencies, a general quadratic force field was assumed rather than a Urey-Bradley force field.

The excited state normal co-ordinates were, therefore, obtained using a general quadratic force field according to the methods outlined by Shimanouchi[77]. A brief description of the method is given below.

According to Shimanouchi, the reason it is often difficult to obtain a convergent set of force constants is the fact that we are trying to adjust force constants for which no information is given by the data on the frequencies. The divergence also occurs when the number of force constants to be adjusted is larger than the number of physical observables.

To avoid the divergence problem Shimanouchi suggests that the force constants to be determined be separated into two sets, k_A and k_B; the k_A set being those force constants for which the frequencies give information and which can be freely adjusted. The k_B set contains those force constants which cannot be estimated for which the frequencies contain little information. In the present work the diagonal force constants were classified in the k_A set while the off-diagonal force constants constituted the k_B set.

A trial set of k_A force constants was then adjusted from the normal equation[77];

$$\tilde{J}_A W J_A \Delta k_A = \tilde{J}_A W \Delta \nu^o \qquad (5.21)$$

the values of the elements of k_B being assumed to be zero. J_A is the Jacobian matrix for the k_A set and is of the form:

$$J = \partial(\nu_1, \nu_2, \nu_3)/\partial(f_{ii}) \qquad (5.22)$$

W is a diagonal weighting matrix, the elements of which are given by

$$W_{ii} = \frac{1}{\lambda_i^2} \qquad (5.23)$$

where $\lambda_i = 4\pi^2c^2\nu_i^2$ and $\Delta\nu^o$ is the frequency-deviation vector

$$\Delta\nu^o = \nu^{obs} - \nu^o$$

and ν^o is the value calculated from the trial set of force constants k^o.

When the final converged set of k_A force constants is determined, we calculate the p_{AB} matrix defined by

$$\Delta k_A^B = p_{AB}\Delta k_B \tag{5.24}$$

where Δk_A^B is the correction which must be made to the converged k_A set when the k_B is varied by Δk_B.

In the present work it was possible to obtain the three excited state frequencies with the inclusion of only diagonal force constants; the off-diagonal force constants being zero or very small. This, therefore, suggests that in the excited state the motion along one normal co-ordinate is largely independent of the motion along the other two normal co-ordinates. Since no correction to the convergent set of diagonal force constants was required, a discussion of the procedures involved will not be given. The methods are, however, clearly outlined by Shimanouchi[77].

For the Franck-Condon calculations (Coon's Method[35]), it is necessary to have the normal co-ordinates for only the totally symmetric vibrations ν_1 and ν_2. Therefore it is convenient to use symmetry co-ordinates s_i given by (see Figure 5.1)

$$s_1 = (\Delta r_1 + \Delta r_2)/\sqrt{2} \qquad (A_1) \tag{5.25}$$

$$s_2 = r_o\Delta\phi \qquad (A_1) \tag{5.26}$$

$$s_3 = (\Delta r_1 - \Delta r_2)/\sqrt{2} \qquad (B_2) \tag{5.27}$$

The potential energy in symmetry co-ordinates then becomes

$$V = \tfrac{1}{2}(f_{11}+f_{12})s_1^2 + \tfrac{1}{2}f_{33}s_2^2 + \tfrac{1}{2}(f_{11}-f_{12})s_3^2 + \sqrt{2}\,f_{13}s_1s_2 \tag{5.28}$$

and we now have the four independent force constants $f_{11}+f_{12}$, f_{33}, $f_{11}-f_{12}$, and f_{13} in place of the four force constants f_{11}, f_{33}, f_{12} and f_{13} associated with internal displacement co-ordinates.

The G matrix in symmetry co-ordinates is shown in Table 5.3 after Shimanouchi[77].

Table 5.3

G Matrix for SeO_2 in Symmetry Co-ordinates

(after Shimanouchi[77])

		$(\Delta r_1 + \Delta r_2)/2$	$(r_o \Delta\phi)$	$(\Delta r_1 - \Delta r_2)/2$
A_1:	$(\Delta r_1 + \Delta r_2)/2$	$2t^2\mu_{Se} + \mu_O$	$-2\sqrt{2}\ ts\mu_{Se}$	
	$r_o\Delta\phi$	$-2\sqrt{2}\ ts\mu_{Se}$	$4s^2\mu_{Se} + 2\mu_O$	
B_2:	$(\Delta r_1 - \Delta r_2)/2$			$2s^2\mu_{Se} + \mu_O$

The ground and excited state G and F matrix are given in Tables 5.4 and 5.5 for internal co-ordinates and Tables 5.6 and 5.7 for symmetry co-ordinates respectively.

The Urey-Bradley force constants for the ground and excited electronic state are shown in Table 5.8 and the L matrix (symmetry co-ordinates) is shown in Table 5.9.

Cartesian and mass-weighted cartesian displacement co-ordinates were also calculated using a computer program obtained from the "Quantum Chemistry Programme Exchange" at Indiana University.° Since an arbitrary co-ordinate system was used in the program, the original cartesian co-ordinates of the atoms are tabulated in Table 5.10. The normal co-ordinates in terms of mass-

---

° I would like to thank Dr. D. C. Moule for providing me with a copy of this program.

Table 5.4

G Matrix for the $^1A_1$ Ground and $^1B_2$ Excited Electronic State of $Se^{78}O_2^{16}$ for Internal Co-ordinates (units are a.m.u.$^{-1}$)

		Δr_1	Δr_2	$r_o\Delta\phi$
Ground State	Δr_1	0.07535	-0.00517	-0.01174
	Δr_2	-0.00517	0.07535	-0.01174
	$r_o\Delta\phi$	-0.01174	-0.01174	0.16106
Excited State	Δr_1	0.07535	-0.00244	-0.01259
	Δr_2	-0.00244	0.07535	-0.01259
	$r_o\Delta\phi$	-0.01259	-0.01259	0.15560

Table 5.5

F Matrix for the $^1A_1$ Ground and $^1B_2$ Excited Electronic State of $Se^{78}O_2^{16}$ for Internal Co-ordinates (units are m dynes/Å)

		Δr_1	Δr_2	$r_o\Delta\phi$
Ground State	Δr_1	7.1738	0.20811	0.05593
	Δr_2	0.20811	6.83191	0.05616
	$r_o\Delta\phi$	0.05593	0.05616	0.52191
Excited State	Δr_1	3.499	0.0	0.0
	Δr_2	0.0	0.2648	0.0
	$r_o\Delta\phi$	0.0	0.0	3.5632

Table 5.6

G Matrix for the $^1A_1$ Ground State and $^1B_2$ Excited Electronic State of $Se^{78}O_2^{16}$ for Symmetry Co-ordinates (units are $a.m.u.^{-1}$)

		$(\Delta r_1+\Delta r_2)/2$	$r_o\Delta\phi$	$(\Delta r_1-\Delta r_2)/2$
Ground State	$(\Delta r_1+\Delta r_2)/2$	0.070175	-0.01660	0.0
	$r_o\Delta\phi$	-0.01660	0.161065	0.0
	$(\Delta r_1-\Delta r_2)/2$	0.0	0.0	0.080532
Excited State	$(\Delta r_1+\Delta r_2)/2$	0.072906	-0.017817	0.0
	$r_o\Delta\phi$	-0.017817	0.155604	0.0
	$(\Delta r_1-\Delta r_2)/2$	0.0	0.0	0.077802

Table 5.7

F Matrix for the $^1A_1$ Ground State and $^1B_2$ Excited Electronic State of $Se^{78}O_2^{16}$ for Symmetry Co-ordinates (units are m dynes/Å)

		$(\Delta r_1+\Delta r_2)/2$	$r_o\Delta\phi$	$(\Delta r_1-\Delta r_2)/2$
Ground State	$(\Delta r_1+\Delta r_2)/2$	7.109786	-0.011575	0.0
	$r_o\Delta\phi$	-0.011575	0.524665	0.0
	$(\Delta r_1-\Delta r_2)/2$	0.0	0.0	6.84006
Excited State	$(\Delta r_1+\Delta r_2)/2$	3.49973	-0.00208	0.0
	$r_o\Delta\phi$	-0.00208	0.26479	0.0
	$(\Delta r_1-\Delta r_2)/2$	0.0	0.0	3.56316

Table 5.8

Urey-Bradley Force Constants for $Se^{78}O_2^{16}$ in the Ground and Excited Electronic State

	K	H	F+F'
Ground State	6.852	0.439	0.17
Excited State	3.590	0.328	-0.080

Table 5.9

L and L^{-1} Matrix for the Ground and Excited State of $Se^{78}O_2^{16}$ using Symmetry Co-ordinates (units are a.m.u.$^{-1/2}$)

	L* Matrix			L^{-1} Matrix		
Ground State	0.26472	0.008998	0.0	3.75248	-0.085687	0.0
	-0.076114	0.394045	0.0	0.724837	2.521233	0.0
	0.0	0.0	0.283782	0.0	0.0	3.523829
Excited State	0.269869	0.008741	0.0	3.681271	-0.083240	0.0
	-0.078539	0.386568	0.0	0.747926	2.56995	0.0
	0.0	0.0	0.278930	0.0	0.0	3.585130

*The L Matrix has been normalized in the sense $LL^t = G$ and gives the symmetry co-ordinates in terms of the normal co-ordinates ($S = LQ$), while L^{-1} is related to the reverse transformation ($Q = L^{-1}S$).

Table 5.10

Original Cartesian Co-ordinates for $Se^{78}O_2^{16}$ in the Ground and Excited Electronic State

Atom	Ground State			Excited State		
	x	y	z	x	y	z
O_1	-1.4676	0.0	-0.2139	-1.535	0.0	-0.2485
Se	0.1393	0.0	-0.2139	0.2049	0.0	-0.2485
O_2	0.7887	0.0	1.2560	0.5369	0.0	1.4594

Table 5.11

Calculated and Observed Frequencies for the $^1A_1$ Ground and $^1B_2$ Excited Electronic State of $Se^{78}O_2^{16}$

	Frequency	Urey-Bradley Force Field	General Quadratic Force Field	Observed
Ground State	ν_1	966.8 cm^{-1}	923 cm^{-1}	923 cm^{-1}
	ν_2	922.5 cm^{-1}	373 cm^{-1}	373 cm^{-1}
	ν_3	374.0 cm^{-1}	967 cm^{-1}	967 cm^{-1}
Excited State	ν_1	659 cm^{-1}	660 cm^{-1}	660 cm^{-1}
	ν_2	260 cm^{-1}	260 cm^{-1}	260 cm^{-1}
	ν_3	689.5 cm^{-1}	686 cm^{-1}	686 cm^{-1}

weighted cartesian and cartesian displacement co-ordinates are given in Table 5.12.

The agreement between the observed and calculated frequencies for the Urey-Bradley and general quadratic force field are given in Table 5.11 for both the ground and excited state.

The normal co-ordinates for SeO_2 are shown in Figure 5.2 in terms of the mass-weighted cartesian displacement co-ordinates given above in Table 5.12.

5.7. Franck-Condon Calculations (Coon's Method[71])

The present interest in carrying out Franck-Condon calculations was to elucidate the geometric structure of selenium dioxide in the $^1B_2$ excited electronic state. The transition probability for an electronic transition from the ground electronic state ϕ_o to an excited electronic state ϕ_i is given by the square of the transition moment $M_{oo}^{i\mu}$ as

$$M_{oo}^{i\mu} = \langle\phi_o|r|\phi_i\rangle\langle\phi_o|\phi_\mu\rangle \qquad (5.29)$$

where ϕ_o is the vibrationless level of the ground electronic state and ϕ_μ the μth vibrational level of the excited electronic state. The intensity of a particular vibronic band in the electronic transition is, therefore, given by the Franck-Condon overlap integral $\langle\phi_o|\phi_\mu\rangle$ between the ground and excited state vibrational wavefunctions. The magnitude of this integral is accordingly related to the change in structure of the molecule going from the ground to excited electronic state. It should, therefore, be possible to relate the intensity distribution within a vibrational progression to the change in the molecular geometry accompanying the electronic transition. This is the basis of the Coon method.

In order to carry out the above Franck-Condon calculation it was, therefore, necessary to have completed a vibrational analyses and measured

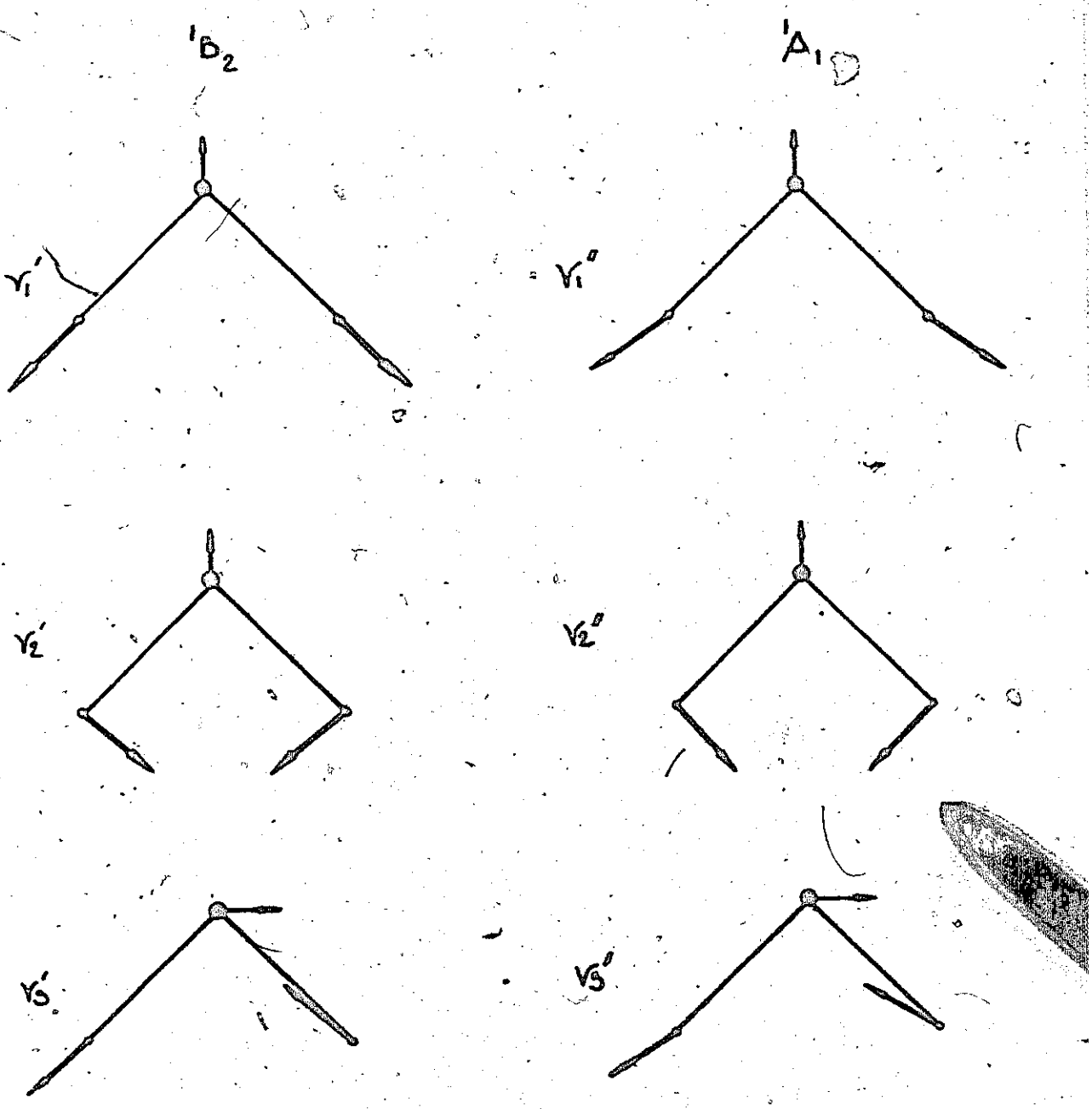

FIGURE 5.2 NORMAL CO-ORDINATES OF $Se^{78}O_2^{16}$ IN TERMS OF MASS WEIGHTED CARTESIAN DISPLACEMENT CO-ORDINATES.

Table 5.12

Normal Co-ordinates for $Se^{78}O_2^{16}$ in the $^1A_1$ Ground and $^1B_2$ Excited Electronic State in Terms of Cartesian and Mass-Weighted Cartesian Co-ordinates. The upper numbers refer to the mass-weighted co-ordinates. The displacements are given along the three principle axes of the molecule.

	(Oxygen)$_1$			Selenium			(Oxygen)$_2$		
Ground State	Δ_a	Δ_b	Δ_c	Δ_a	Δ_b	Δ_c	Δ_a	Δ_b	Δ_c
ν_1	-0.5457	0.3786	0.0	0.0	-0.3430	0.0	0.5457	0.3786	0.0
	-0.1364	0.0946	0.0	0.0	-0.0388	0.0	0.1364	0.0946	0.0
ν_2	0.4496	0.4594	0.0	0.0	-0.4163	0.0	-0.4496	0.4594	0.0
	0.1124	0.1148	0.0	0.0	-0.0471	0.0	-0.1124	0.1148	0.0
ν_3	0.5219	-0.3400	0.0	-0.4730	0.0	0.0	0.5219	0.3400	0.0
	0.1305	-0.0805	0.0	-0.0535	0.0	0.0	0.1305	0.0850	0.0
Excited State									
ν_1	-0.02896	0.04306	0.0	-0.30015	-0.28644	0.0	0.69143	0.58915	0.0
	-0.00724	0.01077	0.0	-0.03400	-0.03245	0.0	0.17288	0.14731	0.0
ν_2	0.50162	0.41945	0.0	0.00405	-0.37675	0.0	-0.51056	0.41208	0.0
	0.12543	0.10488	0.0	0.00046	-0.04268	0.0	-0.12766	0.10304	0.0
ν_3	0.69769	-0.58244	0.0	-0.32608	0.0	0.0	0.02201	0.01083	0.0
	0.17445	-0.14563	0.0	-0.03694	0.0	0.0	0.00550	0.00271	0.0

the relative intensity of several vibronic bands. In order to evaluate the overlap integrals of Equation (5.29) the ground state L matrix is required and thus the necessity for doing the normal co-ordinate analysis.

The vibrational wavefunctions ϕ_v in Equation (5.29) are assumed to be of the form

$$\phi_v = \prod_{i=1}^{3} \phi_i(Q_i) \tag{5.30}$$

where the product is taken over the 3N-6 = 3 normal co-ordinates Q_i. The transition moment of Equation (5.29) upon substitution of (5.30) is

$$M_{oo}^{i\mu} = R_e \int [\prod_{i=1}^{3} \phi_i''(Q_i'')][\prod_{\mu=1}^{3} \phi_\mu'(Q_\mu')] dQ_1' dQ_2' dQ_3' \tag{5.31}$$

In order to evaluate this integral it is necessary to specify the transformation between the ground and excited state normal co-ordinates. Duschinsky[79] has shown what the required transformation is of the form

$$Q_k'' = \sum_j (a_{kj} Q_j' + d_i) \tag{5.32}$$

That is, the ground state co-ordinates Q'' are related to the excited state co-ordinates Q' by means of a rotation plus a translation.

Coon[71], however, assumes the above transformation can be effected in the following way:

$$Q'' = Q' + D \tag{5.33}$$

Since the internal displacement co-ordinates of the molecule are related to the normal co-ordinates by

$$R'' = L'' Q'' \tag{5.34}$$

Substitution of Equation (5.33) into (5.34) with $Q' = 0$ for the equilibrium

excited state configuration gives, as a first approximation to the excited state structure,

$$R'' = L''D$$

The elements of the D matrix are related to the experimentally measured intensities, and are obtained in the following way

$$\frac{R(1,0)}{R(0,0)} = \frac{\sqrt{2}\,\beta^2\gamma}{(1+\beta^2)} = 8\pi^2 c\nu_i' \frac{(\nu_i'')^2 d_i^2}{(\nu_i' + \nu_i'')^2} \qquad (5.36)$$

$$\frac{R(2,0)}{R(0,0)} = \frac{1}{\sqrt{2}(1+\beta^2)}\left[\frac{2\beta^4\gamma^2}{(1+\beta^2)} + (1-\beta^2)\right] \qquad (5.37)$$

where

$$\beta_i = \alpha_i''/\alpha_i', \quad \gamma_i = -\alpha_i' d_i \text{ and } \alpha_i^2 = 4\pi^2 c\nu_i/h \qquad (5.38)$$

Since in the present work, the excited state L matrix was available, the change in the internal co-ordinates could be obtained directly from the relationship

$$R' = L'D \qquad (5.39)$$

which is equivalent to Coon's second approximation to the excited state structure.

Since the spectrum contained progressions in both the upper state totally symmetric stretching frequency ν_1', and angle bending frequency ν_2', it was possible to obtain changes in both the bond length and bond angle. The calculated values for α, β for specific vibronic bands are given in Table 5.13.

Since the sign of the individual d_i is undetermined in Equation (5.39), there are 2^n possible upper state geometries consistent with the observed intensities where n is the number of totally symmetric upper state normal co-

ordinates. Since a rotational analysis was performed on the 1_0^3 band, the upper state geometry was known and thus the proper choice of sign for d_1 and d_2 determined.

The calculate values of d_1 and d_{2_1} along with the vibronic band used, are given in Table 5.14.

In the Franck-Condon calculations the units of d are $g.^{1/2}cm$. The L matrix must have the units $g.^{-1/2}$ It is therefore necessary to convert the L matrix given in Table 5.9 from a.m.u. to g. Since $LL^t = G$, and G has the units $(a.m.u.)^{-1}$, the required units for $L(g^{-1/2})$ are obtained by multiplying each element of the L matrix by $1.0/(1.66024)^{1/2} = 0.77609$. The L matrix with units $g^{-1/2}$ used in the Franck-Condon calculation is shown in Table 5.15.

5.8. Conclusions and Discussion

The fundamental frequencies for selenium dioxide may be accounted for easily using a general quadratic force field and slightly less accurately with the assumption of a Urey-Bradley force field (see Table 5.11).

The geometry determined by means of the Franck-Condon principle, gives r(Se—O) as 1.71 Å and θ(O—Se—O) as 98.48°. This is in reasonable agreement with r = 1.74 Å and θ = 101.0° determined by rotational analysis of the 1_0^3 vibronic band. The geometry determined from rotational analysis is probably most reliable since the former requires an estimate of the intensity of several bands involving ν_1' and ν_2'. The intensities were measured from an expanded trace obtained photo-electrically from a Cary 14 spectrophotometer. The discrepancy between the geometry calculated by means of the Franck-Condon Principle and that determined from rotational analysis probably lies in the estimate of intensities used in the former calculation.

Table 5.13

Vibrational Frequencies and Parameters used in Franck-Condon Calculations for SeO_2

	Ground State	Excited State
ν_1	923 cm^{-1}	660 cm^{-1}
ν_2	373 cm^{-1}	260 cm^{-1}
α_1*	40.618×10^{19}	34.349×10^{19}
α_2	25.718×10^{19}	21.559×10^{19}
	$\beta_1 = 1.1825$	$\beta_2 = 1.197$

*Units of α are $cm/sec^3.org.$

Table 5.14

Calculate Values of d_1 and d_2 for the $^1B_2$ Electronic State of SeO_2

Band (a) (ν_1', ν_2')	Band (b) (ν_1', ν_2')	$d \times 10^{20}$ $g^{1/2}cm$
(1,0)	(2,0)	$d_1 = 0.5032$
(2,1)	(2,0)	$d_1 = 0.645$
(3,1)	(3,0)	$d_1 = 0.645$

Table 5.15

L Matrix Used in Franck-Condon Calculation

(units are $g^{-1/2}$)

	$(\Delta r_1+\Delta r_2)/2$	$r_o\Delta\phi$
$(\Delta r_1+\Delta r_2)/2$	0.20944	0.006784
$r_o\Delta\phi$	-0.06093	0.300011

CHAPTER SIX

CONCLUSIONS

The B-System of selenium dioxide has been analysed in detail. The extensive absorption system extending from 3400 Å - 2400 Å has been shown to result from a $^1B_2 \leftarrow X, ^1A_1$ electronic transition. A vibrational analysis of the electronic transition has successfully account for all the vibronic bands (>100) and yielded the three excited state fundamental frequencies. In addition gas phase values for the ground state totally symmetric stretching and bending frequencies were determined for the first time. The spectrum has been extended $\sim$2000 cm^{-1} to the red of previous investigations.

A rotational analysis of the 1_0^3 vibronic band has been carried out using the band contour method, and the excited state geometry completely determined. A normal co-ordinate analysis of the ground and excited state was performed and Franck-Condon calculations were carried out to further confirm the excited state geometry determined by rotational analysis.

Perhaps the most interesting aspect of the present work is the suggestion of a double-minimum potential well along Q_3' in the excited $^1B_2$ electronic state of SeO_2. The 3_0^1 and 5_0^3 bands have been assigned. To the author's knowledge selenium dioxide is the only symmetric triatomic molecule in which transitions to excited state double-minimum levels have been observed. It is felt this observation is the only existing confirmation for the possible presence of a double-minimum along the asymmetric stretching co-ordinate in certain excited electronic states of symmetric bent AB_2 type molecules.

BIBLIOGRAPHY

1. M. Born and R. Oppenheimer, Ann. Physik, 87, 457 (1927).
2. N. Bohr, Phil. Mag., 26, 1 (1913).
3. A. Einstein, Z. Physik., 18, 121 (1917).
4. G. W. King, "Spectroscopy and Molecular Structure", New York: Holt, Rinehart and Winston, Inc. (1964).
5. F. A. Cotton, "Chemical Applications of Group Theory", New York: Interscience Publishers (1965).
6. R. H. Hochstrasser, "Molecular Aspects of Symmetry", New York: W. A. Benjamin Co. Inc. (1966).
7. J. Duchesne and B. Rosen, J. Chem. Phys. 15, 631 (1947).
8. J. Duchesne and B. Rosen, Physica (Utrecht) 8, 540 (1941).
9. Choong-Shin Piaw, Ann. Phys. (Paris) 10, 191 (1938).
10. R. K. Asundi, M. Jahn-Khan, and R. Samuel, Trans. Faraday Soc. 27, 378 (1937).
11. S. F. Evans, Nature (London) 125, 528 (1930).
12. P. B. V. Haranath and V. Sivaramamurty, Indian J. Phys. 35, 599 (1961).
13. E. M. Voigt, B. Meyer, A. Morelle and J. Smith, J. Mol. Spectry. 34, 179 (1970).
14. S. N. Cesaro, M. Spoliti, A. J. Hinchcliffe and S. J. Ogden, J. Chem. Phys., to appear.
15. J. W. Hastie, R. Hauge and J. L. Margrave, J. Inorg. Nucl. Chem. 31, 281 (1969).
16. J. W. Rabalais, J. M. McDonald, V. Scherr, and S. P. McGlynn, Chemical Rev. 71, 73 (1971).
17. G. Herzberg and E. Teller, Zeits für physik. Chemie, B21, 410 (1933).
18. A. Giguère and M. Falk, Spectrochim Acta. 16, 1 (1960).
19. G. W. King, J. Sci. Instru. 35, 11 (1958).
20. Bengt Edlén, J. Optical Soc. Am. 43, 339 (1953).

21. "Handbook of Chemistry and Physics" (48th Edition), The Chemical Rubber Co. D-116 (1968).

22. H. J. Maria, D. Larson, M. McGarville and S. P. McGlynn, Accounts of Chemical Research 3, 368 (1970).

23. E. F. Hayes and G. V. Pfeiffer, J. Am. Chem. Soc. 90, 4773 (1968).

24. K. F. Greenough and A. B. F. Duncan, J. Am. Chem. Soc. 83, 555 (1961).

25. R. B. Canton and A. B. F. Duncan, J. Am. Chem. Soc. 90, 1945 (1968).

26. M. Keeton and D. P. Santry, Chemical Physics Letters, 7, 105 (1970).

27. R. S. Mulliken, Rev. Mod. Phys., 14, 204 (1942).

28. A. D. Walsh, J. Chem. Soc., 2266 (1953).

29. J. W. Rabalais, J. M. McDonald, V. Scherr and S. P. McGlynn, Chem. Rev. 71, 73 (1971).

30. G. Herzberg, "Electronic Spectra and Electronic Structure of Polyatomic Molecules", Princeton, New Jersey: D. Van Nostrand Co., Inc. (1966).

31. D. A. Ramsay, "Determination of Organic Structures by Physical Methods", Vol. 2, Chapter 4, New York: Academic Press (1962).

32. G. Herzberg and E. Teller, Z. physik. Chem. B21, 410 (1933).

33. R. Renner, Zeit. Phys. 92, 172 (1934).

34. W. R. Thorson and I. Nakagawa, J. Chem. Phys. 33, 994 (1960).

35. J. B. Coon, N. W. Naugle and R. D. McKenzie, J. Mol. Spectry. 20, 107 (1966).

36. J. B. Coon and E. Ortiz, J. Mol. Spectry. 1, 81 (1957).

37. J. B. Coon, P. M. Elliott, J. W. Riggs and S. U. Kim, Bull. Am. Phys. Soc. 12, 182 (1967).

38. J. B. Coon, F. A. Cesani and F. P. Huberman, J. Chem. Phys. 52, 1647 (1970).

39. D. G. Carroll, A. T. Armstrong, and S. P. McGlynn, J. Chem. Phys. 44, 1865 (1966).

40. J. C. Brand and K. Srikameswaran, Private Communication.

41. J. C. Brand, V. T. Jones and C. Di Lauro, J. Mol. Spectry. 40, 616 (1971).

42. A. J. Meyer, Disc. Faraday Soc. 35, 127 (1963).

43. E. C. Y. Inn and Y. Tanaka, J. Opt. Soc. Amer. 43, 870 (1953); Advan. Chem. Ser., No. 21, 263 (1959).

44. A. D. Kirshenbaum and A. G. Streng, J. Chem. Phys. 35, 1440 (1961).

45. B. T. Darling and Chung-Wang Lui, J. Mol. Spectry., 21, 146 (1966).

46. A. E. Douglas, Can. J. Phys., 36, 147 (1958).

47. P. J. Gardner, Chem. Phys. Letters, 4, 167 (1969).

48. S. J. Strickler and D. B. Howell, J. Chem. Phys., 49, 1947 (1968).

49. I. Dubois and B. Rosen, Disc. Faraday Soc., 35, 124 (1963).

50. H. J. Maria, A. Wahlborg and S. P. McGlynn, J. Chem. Phys., 49, 4925 (1968).

51. R. M. Hochstrasser and H. P. Marchetti, J. Chem. Phys. 50, 1727 (1969).

52. W. C. Allen and R. N. Dixon, Trans. Far. Soc., 65, 1168 (1969).

53. J. W. Sidman, J. Am. Chem. Soc., 79, 2669 (1957).

54. L. E. Lewis, H. J. Maria and S. P. McGlynn, Czech. J. Phys., B20, No. 9 (1970).

55. L. E. Harris and S. P. McGlynn, unpublished work.

56. W. G. Trawick and W. H. Eberhardt, J. Chem. Phys., 22, 1462 (1954).

57. H. Takeo, E. Kiroto and Y. Morino, J. Mol. Spectry. 34, 370 (1970).

58. C. Shin-Piaw, Ann. de Phys. (11) 10, 173 (1938).

59. J. Franck, Trans. Faraday Soc. 21, part 3 (1925).

60. H. Sponer and E. Teller, Rev. Mod. Phys. 13, 75 (1941).

61. J. B. Coon, F. A. Cesani and C. W. Loyd, Disc. Faraday Soc. 35, 118 (1963).

62. P. M. Elliott, thesis, Texas A. and M. University, 1964; P. M. Elliott and J. B. Coon, Bull. Am. Phys. Soc. 9, 145 (1964).

63. K. Shrikameswaran, Private Communication.

64. R. S. Mulliken, Can. J. Chem. 36, 10 (1958).

65. S. L. Altmann, Proc. Roy. Soc. A298, 184 (1967).

66. H. C. Longuet-Higgins, Molec. Phys. 6, 445 (1963).

67. W. R. Thorson and I. Nakagawa, J. Chem. Phys. 33, 994 (1960).

68. R. N. Dixon, Trans. Far. Soc. 60, 1363 (1964).

69. J. W. C. Johns, Can. J. Phys. 45, 2639 (1967).

70. H. A. Jahn, Phys. Rev., 56, 680 (1939).

71. J. B. Coon, R. E. De Wames and C. N. Loyd, J. Mol. Spectry. 8, 285 (1962).

72. H. C. Urey and C. A. Bradley, Phys. Rev. 38, 1969 (1931).

73. T. Shimanouchi, J. Chem. Phys. 17, 245 (1949).

74. J. Overend and J. R. Scherer, J. Chem. Phys. 32, 1289 (1960).

75. E. B. Wilson, J. C. Decius and P. C. Cross, Molecular Vibrations, New York: McGraw-Hill Book Company, Inc. (1955).

76. H. C. Urey, Nature 181, 1458 (1958).

77. T. Shimanouchi, Physical Chemistry, Volume IV, New York: Academic Press (1970).

78. C. R. Subramanian, M.Sc. Thesis, Brock University, St. Catharines, Ontario (1968).

79. F. Duschinski, Acta Physiochim. U.R.S.S. VII, 551 (1937).

80. J. Hirschfelder, J. Chem. Phys. 8, 431 (1940).

81. R. C. Johnson, "An Introduction to Molecular Spectra", London: Methuen and Co. Ltd. (1949).

82. G. Herzberg, "Infrared and Raman Spectra of Polyatomic Molecules", New York: D. Van Nostrand Co. Inc. (1945).

83. N. Metropolis, Phys. Rev. 60, 283 (1941).

84. A. Mani and J. R. Lombardi, J. Mol. Spectry. 31, 308 (1969).

85. K. G. Kidd and G. W. King, J. Mol. Spectry. 40, 458 (1971).

86. Miu Yung Chan, L. Wilardjo and P. N. Parker, J. Mol. Spectry. 40, 473 (1971).

87. H. M. Foley and H. M. Randall, Phys. Rev. 59, 171 (1941).

88. D. M. Dennison, Rev. Mod. Phys. 3, 280 (1931).

89. E. Teller, Hand-und Jahrb. d. Chem. Phys. Vol. 9, II, 43 (1934).

90. P. C. Cross, R. M. Hainer and G. W. King, J. Chem. Phys. 12, 210 (1944).

91. Jon T. Hougen, J. Chem. Phys. 39, 358 (1963).

92. J. C. Brand and K. Shrikameswaran, Private Communication.

APPENDIX I

Frequencies of the Observed Band Heads in the $^1B_2 \leftarrow {}^1A_1$ Electronic Transition of $Se^{78}O_2^{16}$, $Se^{78}O_2^{18}$ and $Se^{80}O_2^{16}$ Grouped into Progressions

Legend

The frequencies of the observed band heads of $Se^{78}O_2^{16}$, $Se^{78}O_2^{18}$ and $Se^{80}O_2^{16}$ are given in cm^{-1}. All bands listed are observed at pressures which varied between 0.01 Torr and 10 Torr in a 50 cm quartz cell.

The relative intensities given are only rough visual estimates relative to neighbouring bands. The abbreviations used in the Table are:

v = very

w = weak

s = strong

$Se^{78}O_2^{16}$ (cm^{-1} vac.)	$Se^{78}O_2^{18}$ (cm^{-1} vac.)	$Se^{80}O_2^{16}$ (cm^{-1} vac.)	Assignment	Intensity
31955.0	31963.9	31957.4	0_0^0	vw
32606.9	32588.4	32610.5	1_0^1	w
33249.4	33196.1	33247.6	1_0^2	s
33900.9	33812.7	33906.2	1_0^3	s
34566.1	34448.5	34569.1	1_0^4	vs
35223.8	35075.2	35217.6	1_0^5	vs
35870.0	35683.9*	35863.9	1_0^6	vvs
36537.6	36326.0	36528.5	1_0^7	s
37174.3	36933.0	37173.4	1_0^8	s
37823.3	37553.0	37813.2	1_0^9	w
38471.5	38166.6	38454.9	1_0^{10}	w
39114.2	38787.3	39098.3	1_0^{11}	vw
39757.4	39404.5	39742.5	1_0^{12}	vvw
40402.7	40020.3	-	1_0^{13}	vvw
32033.8	32042.3	32035.3	3_0^1	w
32277.1	32296.9	32271*	$1_4^4 3_0^2$	vvw
32539.1	32519.8	32533.6	$1_3^3 3_0^2$	vw
32801.3	32776.0	32801.5	$1_2^2 3_0^2$	w
33066.2	33024.5	33064.4	$1_1^1 3_0^2$	w
33327.5	33273.4	33326.1	3_0^2	w
33594.5	33488.2	33591.9	$2_0^1 3_0^2$	w
34026.5	33902.1	34024.5	3_0^3	w
34681.2	34532.8	-	$1_0^2 3_0^2$	s
35320.7	35167.3	35314.8	$1_0^3 3_0^2$	s

* overlapped

$Se^{78}O_2^{16}$ (cm^{-1} vac.)	$Se^{78}O_2^{18}$ (cm^{-1} vac.)	$Se^{80}O_2^{16}$ (cm^{-1} vac.)	Assignment	Intensity
35981.0	35794.9	35973.0	$1_0^4 3_0^2$	s
36643.8	36428.4	36629.1	$1_0^5 3_0^2$	vs
37294.5	37054.5	37283.9	$1_0^6 3_0^2$	vs
37950.1	37667.7	37933.3	$1_0^7 3_0^2$	s
38593.4	38287.7	38571.9	$1_0^8 3_0^2$	w
39241.1	38905.5	39227.1	$1_0^9 3_0^2$	vw
39985.2	39523.4	39876.7	$1_0^{10} 3_0^2$	vvw
35583.1	35372.8	-	$1_0^3 2_0^1 3_0^2$	s
36233.4	36002.2	36221.0	$1_0^4 2_0^1 3_0^2$	s
36884.8	36655.1	36874.9	$1_0^5 2_0^1 3_0^2$	vs
37537.7	37280.6	37526.9	$1_0^6 2_0^1 3_0^2$	vs
38186.9	37898.0	38175.9	$1_0^7 2_0^1 3_0^2$	s
38833.1	38496.6	38808.8	$1_0^8 2_0^1 3_0^2$	w
39477.6	39134.6	39463.2	$1_0^9 2_0^1 3_0^2$	vw
40121.9	39747.2	40102.9	$1_0^{10} 2_0^1 3_0^2$	vvw
38056.1	37781.5	38046.0	$1_0^6 3_0^3$	w
38706.6	38396.3	38692.3	$1_0^7 3_0^3$	w
39396.1	39012.1	39370.7	$1_0^8 3_0^3$	vw
39989.5	39625.8	39974.3	$1_0^9 3_0^3$	vw
40629.7	40251.6	-	$1_0^{10} 3_0^3$	vvw
41271.6	40855.4	-	$1_0^{11} 3_0^3$	vvw
32856.0	32816.3	32854.0	$1_0^1 2_0^1$	w
33507.9	33440.8	33505.0	$1_0^2 2_0^1$	s
34158.6	34058.3	34153.2	$1_0^3 2_0^1$	s
34822.5	34693.9	34818.3	$1_0^4 2_0^1$	vs

$Se^{78}O_2^{16}$ (cm^{-1} vac.)	$Se^{78}O_2^{18}$ (cm^{-1} vac.)	$Se^{80}O_2^{16}$ (cm^{-1} vac.)	Assignment	Intensity
35479.9	35317.2	35472.6	$1_0^5 2_0^1$	vs
36139.5	35946.9	36131.3	$1_0^6 2_0^1$	vvs
36801.7	36576.2	36791.8	$1_0^7 2_0^1$	vs
37455.3	37213.4	37445.4	$1_0^8 2_0^1$	s
38105.7	37825.9	38095.0	$1_0^9 2_0^1$	s
38752.1	38437.9	38741.*	$1_0^{10} 2_0^1$	w
39396.1	39046.2	39370.7	$1_0^{11} 2_0^1$	w
40034.0	39650.6	-	$1_0^{12} 2_0^1$	vw
33116.1	33071.0	33113.*	$1_0^1 2_0^2$	w
33765.2	33691.8	33763.6	$1_0^2 2_0^2$	s
34412.2	34308.5	34408.2	$1_0^3 2_0^2$	s
35069.8	34947.7	35070.8	$1_0^4 2_0^2$	vs
35731.1	35557.0	35723.7	$1_0^5 2_0^2$	vs
36390.2	36185.6	36381.1	$1_0^6 2_0^2$	vvs
37049.2	36814.4	37038.7	$1_0^7 2_0^2$	vs
37701.3	37444.8	37689.0	$1_0^8 2_0^2$	vs
38351.6	38053.8	38339.7	$1_0^9 2_0^2$	w
38999.8	38675.8	38981.1	$1_0^{10} 2_0^2$	w
39647.4	39297.0	39633.0	$1_0^{11} 2_0^2$	vw
40294.1	39907.9	40272.8	$1_0^{12} 2_0^2$	vvw
31032.0	31085.9	31039.6	1_1^0	vw
30115.3	30215.9	30118.7	1_2^0	vvw
29201.0	29349.9	-	1_3^0	vvvw
31110.7	31164.4	31112.4	$1_1^0 3_0^1$	vw

*overlapped

$Se^{78}O_2^{16}$ (cm^{-1} vac.)	$Se^{78}O_2^{18}$ (cm^{-1} vac.)	$Se^{80}O_2^{16}$ (cm^{-1} vac.)	Assignment	Intensity
30192.4	30291.6	30195.3	$1_2^0 3_0^1$	vvw
29280.4	29427.9	-	$1_3^0 3_0^1$	vvvw
31687.3	31710.3	31689.8	1_1^1	w
32330.0	32325.6	32324.5	1_1^2	w
32980.1	32948.1	32974.9	1_1^3	s
33640.7	33560.6	33634.5	1_1^4	s
34306.5	34202.6	34305.6	1_1^5	vs
35010.3	34872.6	35004.7	1_1^6	vs
31582.0	31605.	31585.*	2_1^0	vw
31208.2	31252.	-	2_2^0	vw
30665.8*	30732.	30675.*	$1_1^0 2_1^0$	vvw
30285.*	30379.	30295.*	$1_1^0 2_2^0$	vvw
29753.4	-	29758.1	$1_2^0 2_1^0$	vvw
29380.1	-	-	$1_2^0 2_2^0$	vvw
31378.5	-	31379.9	$1_1^0 2_0^1 3_0^1$	vw
31616.2	-	31611.9*	$1_4^3 3_0^2$	vvw
31877.8	- *	31878.3	$1_3^2 3_0^2$	vvw
32142.5	32146.*	32142.8	$1_2^1 3_0^2$	vvw
32404.6	32394.6	32403.*	$1_1^0 3_0^2$	w
32302.4	32296.9	32302.1	$2_0^1 3_0^1$	w
30748.3			$1_2^1 + 1_1^0 2_1^0 3_0^1$	vvw

APPENDIX II

Double-Minimum Potential Calculations for the $^1B_2$ Excited State of SeO_2

In order to explain the abnormally high intensity of the $2\nu_3'$ band in the electronic spectrum resulting from the $^1B_2 \leftarrow {}^1A_1$ transition of SeO_2, it was necessary to suggest the presence of a double minimum in the potential well along the excited state asymmetrical stretching co-ordinate Q_3'.

The methods used are those outlined by Coon and his co-workers[35]. The double-minimum potential function is of the "Gaussian barrier type" and can be written

$$V(Q) = \frac{1}{2}\lambda Q^2 + A \exp(-a^2Q^2) \qquad (a.1)$$

where Q is a mass weighted co-ordinate defined by $2T = \dot{Q}^2$.

The minima of the potential function are determined by differentiating a.1 with respect to Q and equating the result to zero. The two minima $\pm Q_m$ are given by

$$Q_m^2 = (1/a^2)\ln(2a^2A/\lambda) \qquad (a.2)$$

A shape function ρ, which determines the anharmonicity of the outer walls of the well relative to the walls of the barrier is defined by

$$a^2 = e^{\rho}\lambda/2A \qquad (a.3)$$

Coon[35] then defines a frequency ν_o given by the relation

$$\lambda = (2\pi c\nu_o) \qquad (a.4)$$

A dimensionless parameter B is then defined so that the barrier height is $Bhc\nu_o$

which with the aid of Equations (a.1), (a.2) and (a.3) give the barrier height b in cm^{-1} as

$$b = B\nu_o \qquad (a.5)$$

The actual determination of the energy levels in the double-minimum potential well was done in the following way for $\rho = 0.6$. From the spectrum, using the experimentally observed levels 0_0^0, 3_0^1 and 3_0^2 the following ratio was determined

$$\frac{G(1^+) - G(0^+)}{G(0^-) - G(0^+)} = \frac{1372.6}{78.9} = 17.3967 \qquad (a.6)$$

From the tables of energy levels G/ν_o as a function of B provided by Coon, the above ratio is plotted against B as shown in Figure A.1. The value of B = 1.0637 was found to correspond to the above ratio of 17.3967.

A plot of $G(1^+)/\nu_o - G(0^+)/\nu_o$ against B, then yields the correct value for $G(1^+)/\nu_o - G(0^+)/\nu_o$ corresponding to the value of $B_{calc.}$ determined above. This plot is shown in Figure A.2. From Figures A.1. and A.2., $B_{calc.} = 1.0637$ and $G(1^+)/\nu_o - G(0^+)/\nu_o = 0.735076$.

The value of ν_o is then calculated from the identity

$$\nu_o = \frac{G(1^+) - G(0^+)}{\frac{G(1^+)}{\nu_o} - \frac{G(0^+)}{\nu_o}} = \frac{1372.6}{0.735076} = 1867.6 \qquad (a.7)$$

With the aid of ν_o previously determined, the barrier height b is given by

$$b = B\nu_o = 1.0637 \times 1867.6 = 1986.57\ cm^{-1} \qquad (a.8)$$

The energy levels may then be calculated using the tables provided by Coon. The resulting double-minimum potential well with the first four calculated levels is given in Figure A.3.

The two minima of the potential well are located[1] at $\pm Q_m$ where

$$Q_m^2 = \frac{2\rho}{e^\rho - \rho - 1} \frac{h}{4\pi^2 c} \frac{B}{\nu_o} \qquad (a.9)$$

Substituting $\rho = 0.6$, $B = 1.0637$ and $\nu_o = 1867.6\ cm^{-1}$ into (a.9) gives $Q_m^2 = 0.1722 \times 10^{-40}\ g.cm^2$.

For small displacements the kinetic energy is given by $2T = \mu\dot{r}^2$ where

$$\mu = \frac{2nM}{2n \sin^2\alpha + M} \qquad (a.10)$$

and n and M are the mass of the oxygen and selenium atom respectively. α is the O-Se-O bond angle in the excited state (101.0°). Substitution of $n = 15.99491$ gm, $M = 77.9173$ and $\sin 101° = 0.7716$ into Equation gives $\mu = 25.706$ gm.

Therefore, using $2T = \dot{Q}^2$ and setting $Q = Q_m$ we have

$$Q_m^2 = \mu r_m^2 \qquad (a.11)$$

Insertion of $Q_m = 0.1722 \times 10^{-40}\ g.cm^2$ and $\mu = 25.706$ g into (a.11) gives $r_m = 0.0818$ Å.

Therefore in certain vibronic levels involving ν_3', the equilibrium geometry of SeO_2 is asymmetric with bond lengths $r_{sym.} \pm 0.0818$ Å where r_{sym} is the equilibrium bond lengths of the symmetric structure.

From a rotational band contour analysis of the 1_0^3 vibronic band, assuming a symmetric structure, the equilibrium bond length of SeO_2 in this vibronic level was found to be 1.74 Å. Therefore at the potential minima along Q_3' of the excited $^1B_2$ electronic state of SeO_2 the bond lengths are approximately 1.74 ± 0.082 Å.

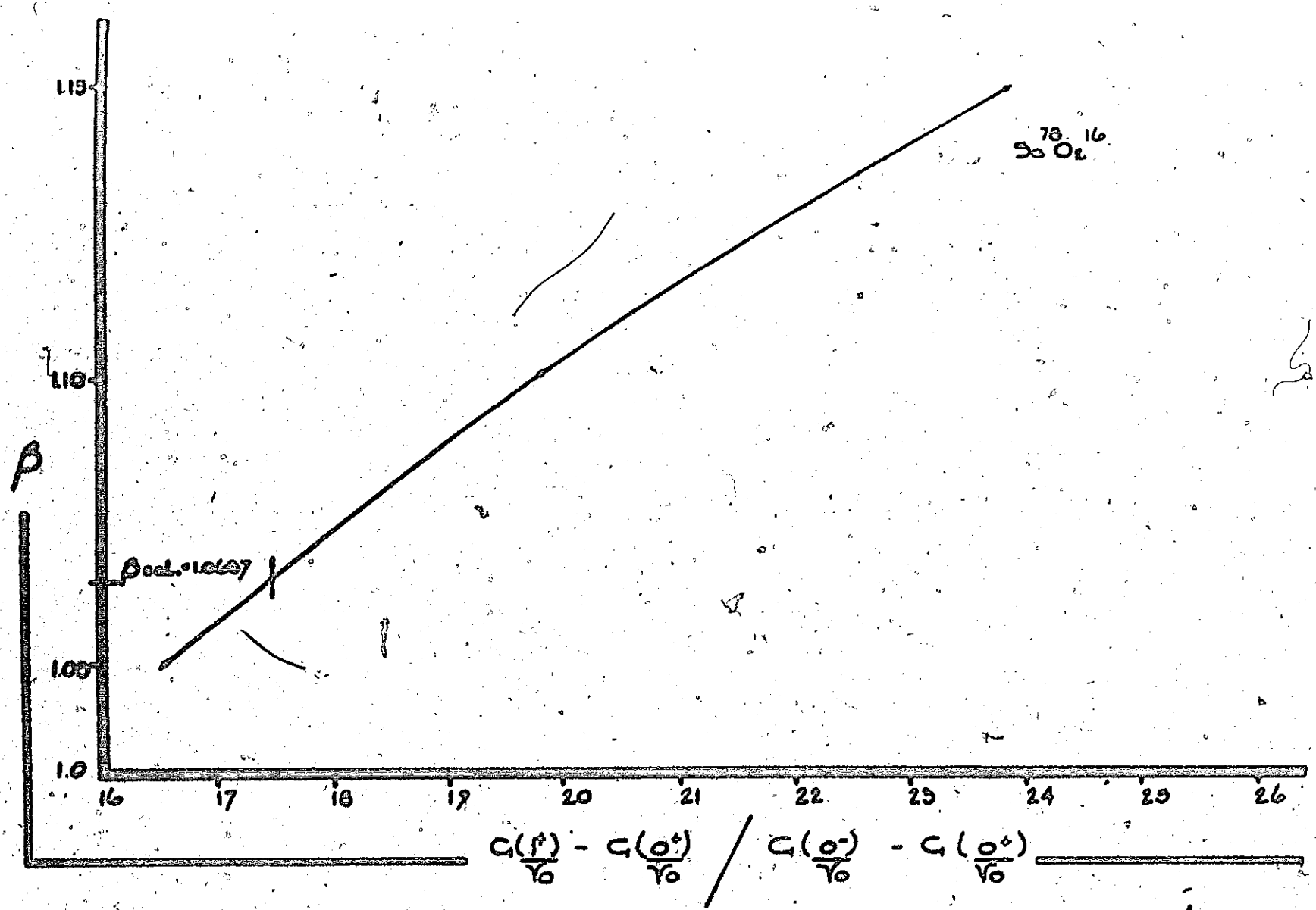

FIGURE 8.2.1 DETERMINATION OF β FOR ρ = 0.6 CORRESPONDING TO $[G(1^+)/V_0 - G(0^+)/V_0] / [G(0^-)/V_0 - G(0^+)/V_0] = 17.997$ USING THE DOUBLE-MINIMUM POTENTIAL LEVELS PROVIDED BY COON[95]

ATH.4

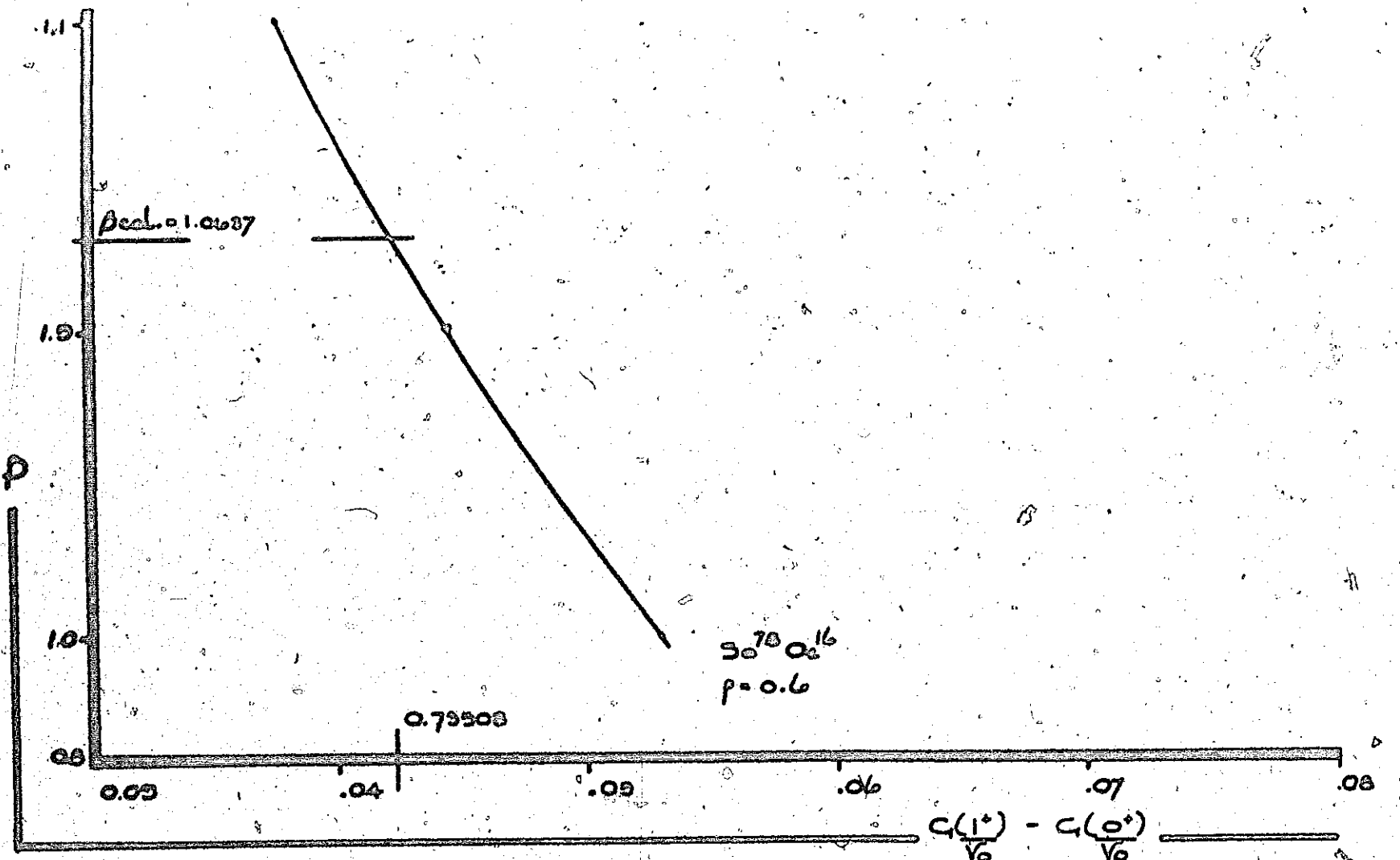

FIGURE B.2.2 DETERMINATION OF THE VALUE OF $G(1^+)/V_0 - G(0^+)/V_0$ CORRESPONDING TO $\beta_{cal} = 1.064$ WITH THE AID OF THE ENERGY LEVELS BY COON[33]

ALL.3

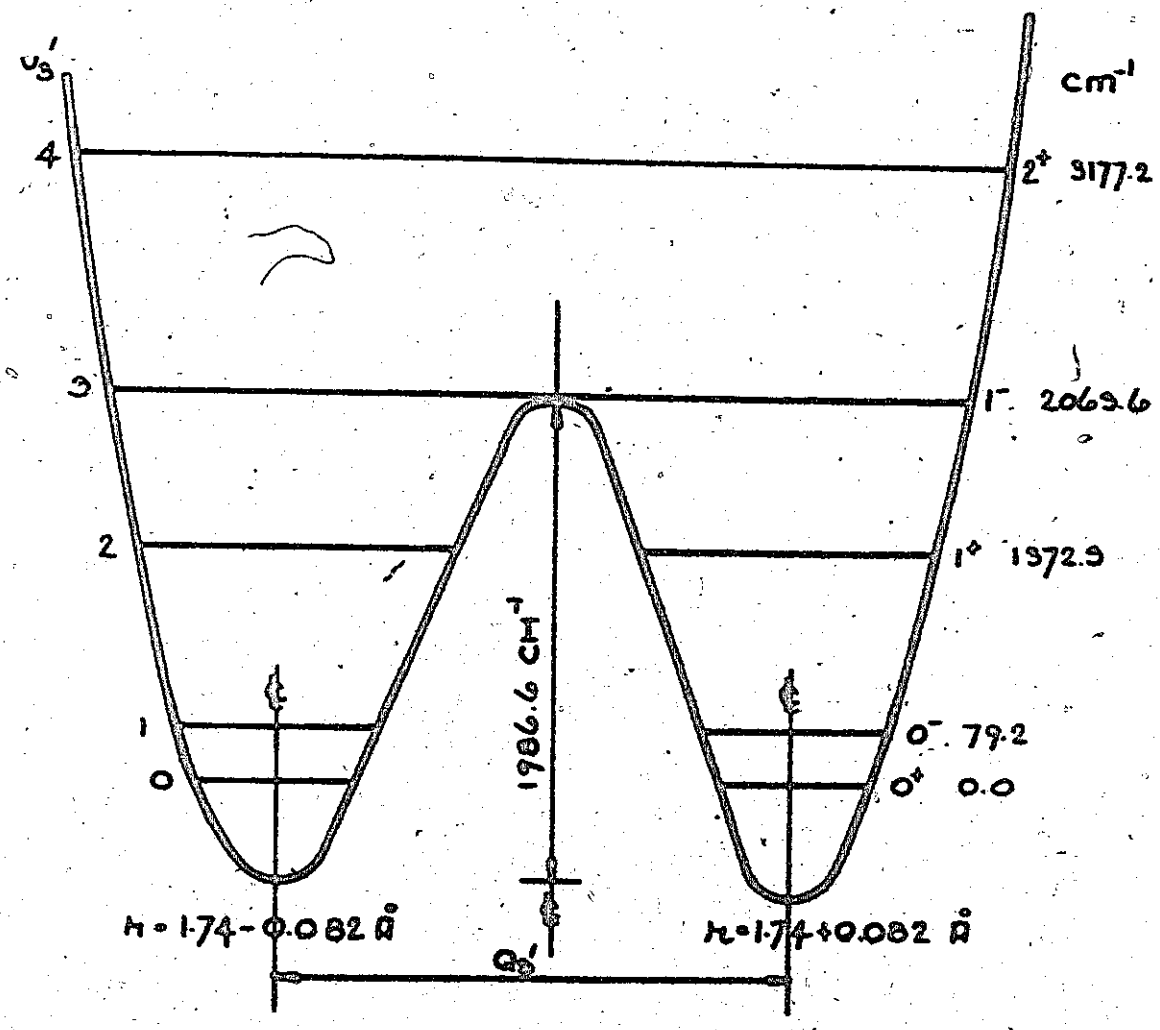

FIGURE A-2-3 THE DOUBLE-MINIMUM POTENTIAL IN THE ANTISYMMETRIC STRETCHING CO-ORDINATE OF THE $^1B_2$ EXCITED STATE OF $Se^{78}O_2^{16}$. THE VALUE OF $G(0^+)$ = 897.0 cm^{-1}.

APPENDIX III

Energy of Sub-Band Origins and $\Delta\nu$ Verses K_p Plots for $Se^{78}O_2^{18}$ and $Se^{80}O_2^{16}$ Molecules

Table A.3.1

K numbering for sub-band origins of the 1_0^3 vibronic band of $Se^{78}O_2^{18}$, assuming the transition is polarized parallel to the top axis.

K''	ν (Experimental) cm^{-1}	ν (Calculated) cm^{-1}	Deviation (cm^{-1})
8	33798.813	33798.768	-0.044
9	33793.710	33793.708	-0.001
10	33788.042	33788.055	0.013
11	33781.729	33781.807	0.078
12	33774.866	33774.966	0.100
13	33767.594	33767.531	-0.062
14	33759.631	33759.502	-0.128
15	33750.948	33750.880	-0.067
16	33741.553	33741.664	0.111

Table A.3.2

K numbering for sub-band origins of the 1_0^3 vibronic band of $Se^{80}O_2^{16}$, assuming the transition is polarized parallel to the top axis

K"	ν (Experimental) cm^{-1}	ν (Calculated) cm^{-1}	Deviation (cm^{-1})
8	33885.483	33885.096	-0.386
9	33880.133	33880.059	-0.073
10	33874.380	33874.457	0.077
11	33867.560	33868.290	0.730
12	33861.088	33861.559	0.471
13	33854.388	33854.263	-0.124
14	33846.801	33846.403	-0.397
15	33838.258	33837.978	-0.279
16	33829.315	33828.988	-0.326
17	33819.502	33819.434	-0.067
18	33809.199	33809.316	0.117
19	33798.374	33798.633	0.259

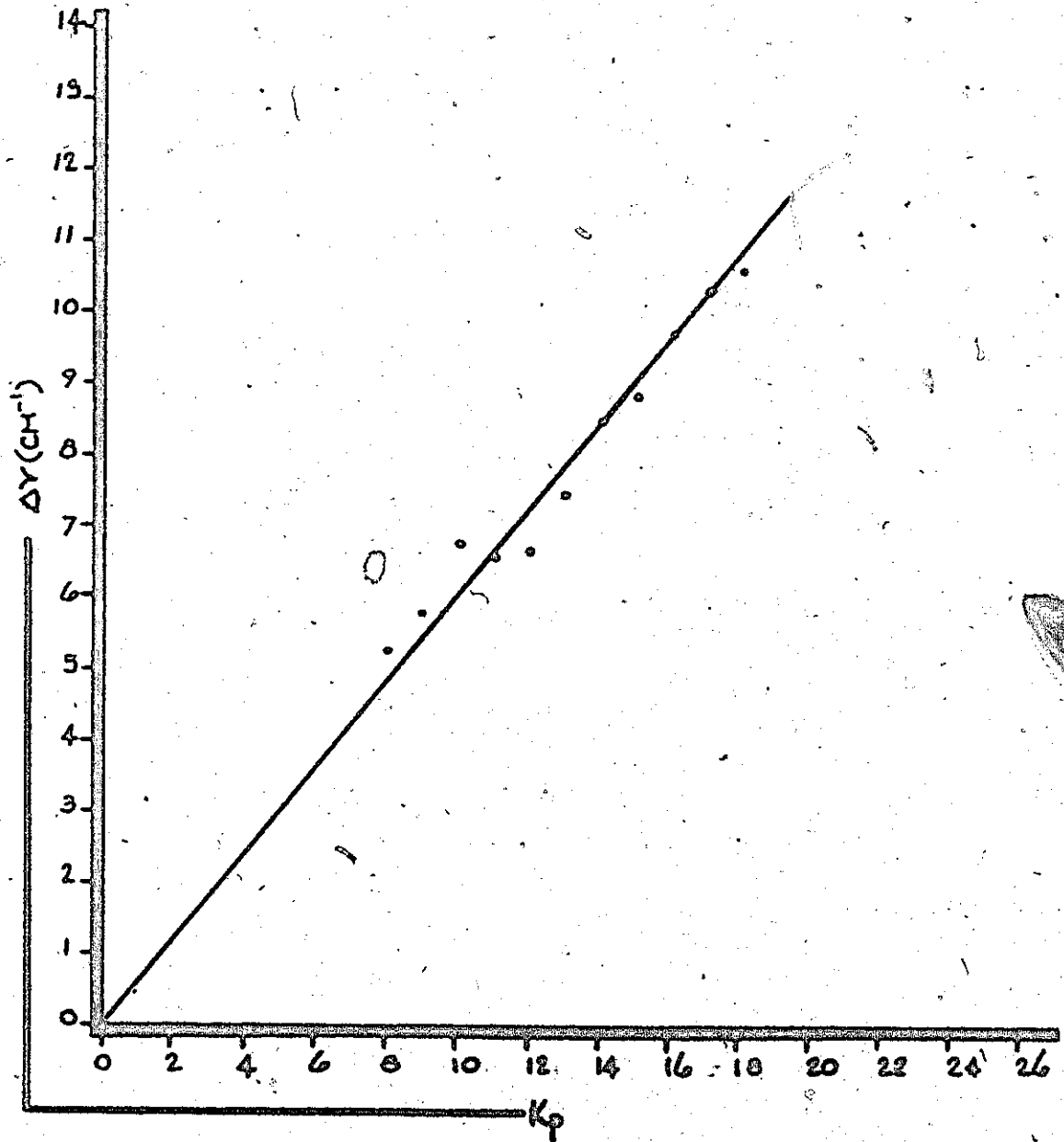

FIGURE A.3.1 PLOT OF THE P BRANCH HEAD SEPARATION ($\Delta\nu$) AGAINST K_p FOR THE 1$^{0}_{0}$ VIBRONIC BAND OF $^{32}S^{16}O_2$. FROM A LEAST SQUARE FIT OF THE ABOVE POINTS THE INTERCEPT IS FOUND TO BE 0.040.

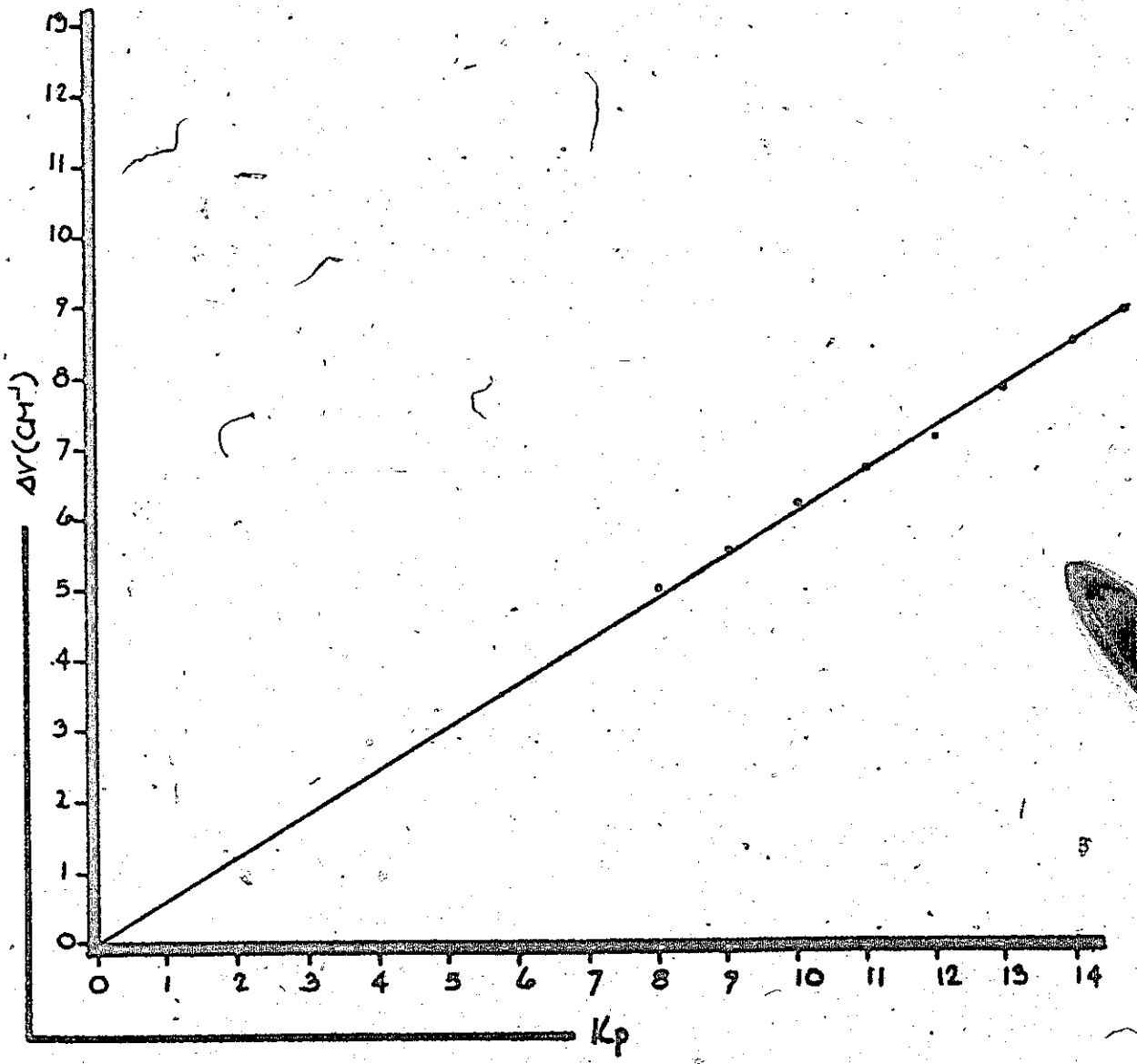

FIGURE A.3-2. PLOT OF R BRANCH HEAD SEPERATION (ΔV) AGAINST Kp FOR THE 1^3_0 VIBRONIC BAND OF $Se^{78}O_2^{16}$. FROM A LEAST SQUARE FIT OF THE ABOVE POINTS THE INTERCEPT IS FOUND TO BE 0.284.